EPFL

POLITECNICO MILANO 1863

GR MeC Composite Mechanics Group

Selected topics on advanced composites in engineering structures

Lecture III – Fracture

Prof. Anastasios P. Vassilopoulos

Dr. Angelo Savio Calabrese

Beyond imagination!

https://sumrwind.com/

How are they made?

https://www.youtube.com/watch?v=jpRudTUIyfM

Paradox!

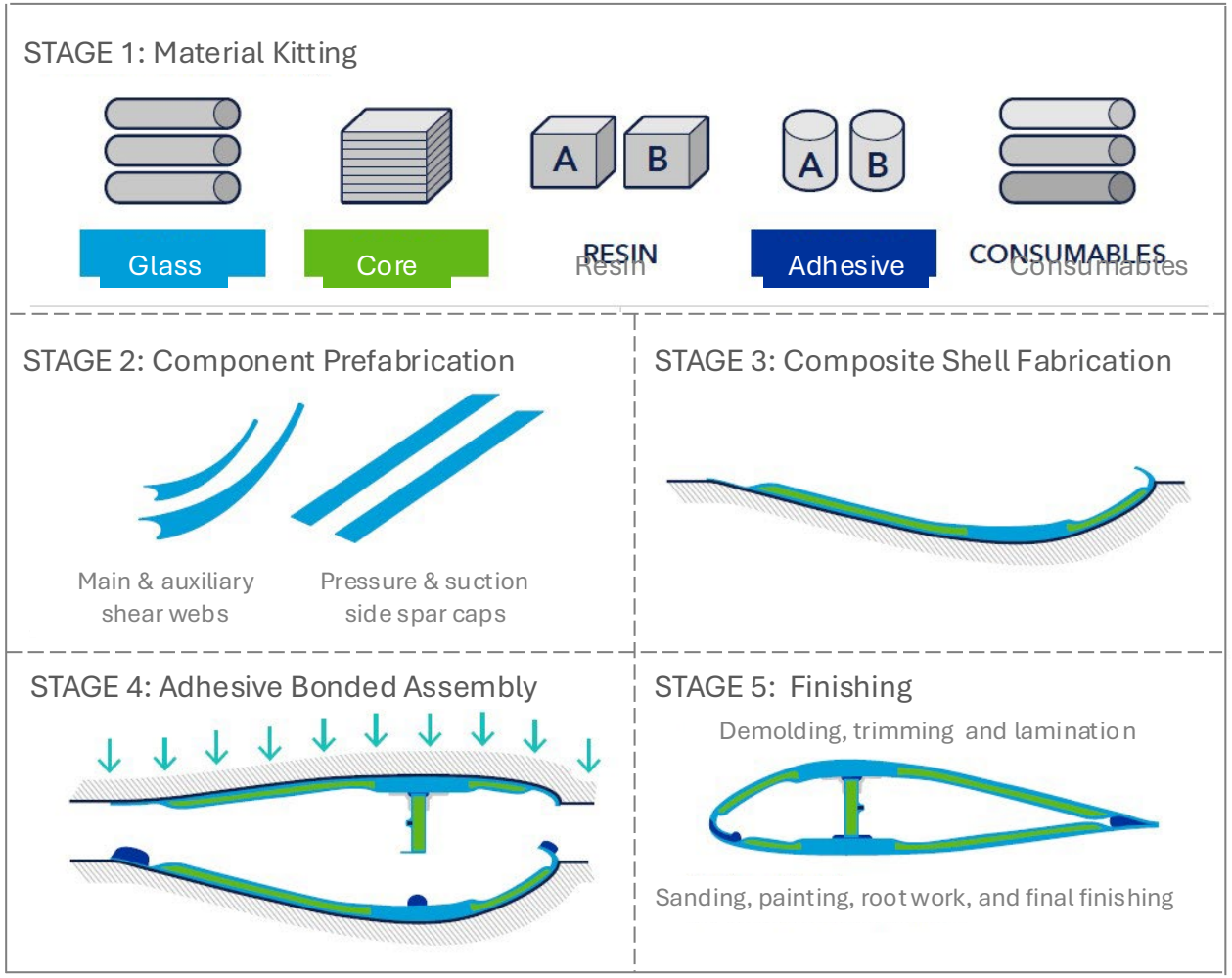

Typical manufacturing process of rotor blades

> "Blades have grown, but manufacturing processes have largely remained the same.
>
> - DNV report 2023

Many adhesive joints

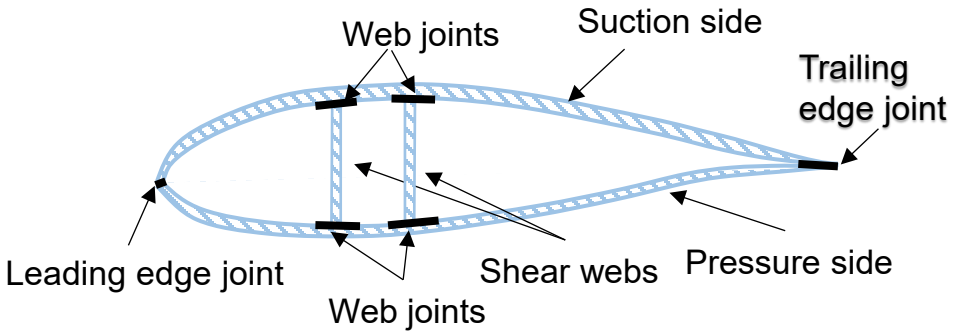

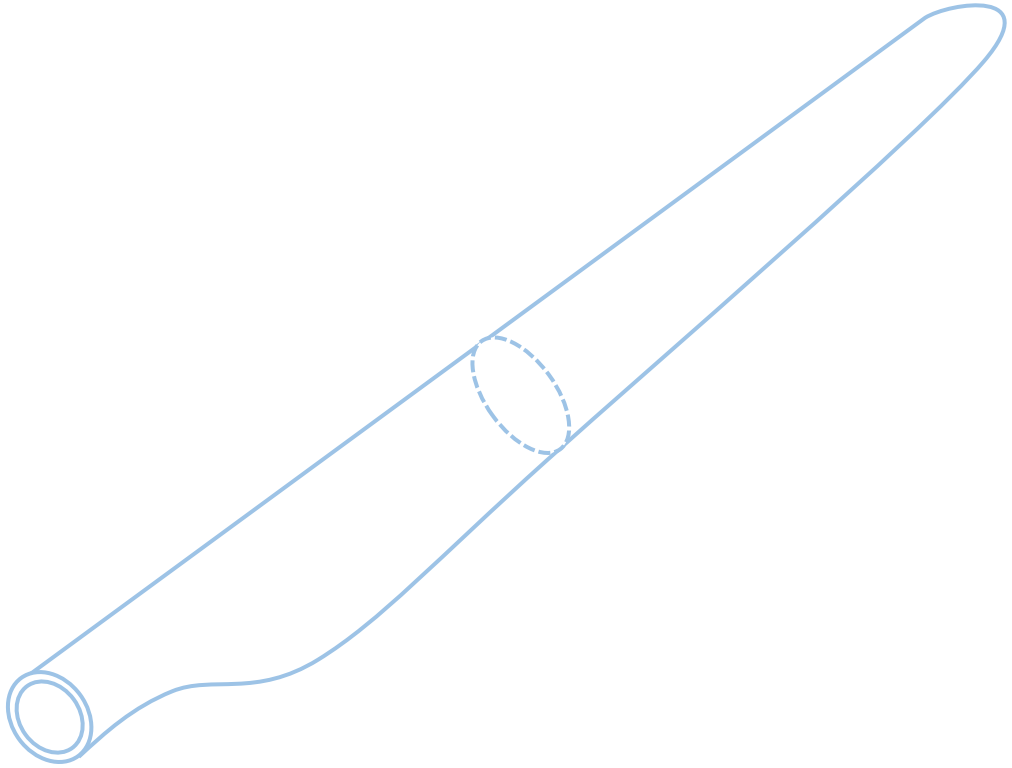

Thick adhesive joint

01 **Adhesive assembly**

Fiber reinforced epoxy

composite + epoxy adhesive

Several adhesive joints

02 **Size**

>100m

Electric production efficiency

Thick adhesive layer

(1-25 mm)

1 **Thickness**

Design

Compensate the variations

2 **Long lifetime**

20-25 years

Fracture / fatigue behavior

3 **Low cost**

Materials

Manufacturing process

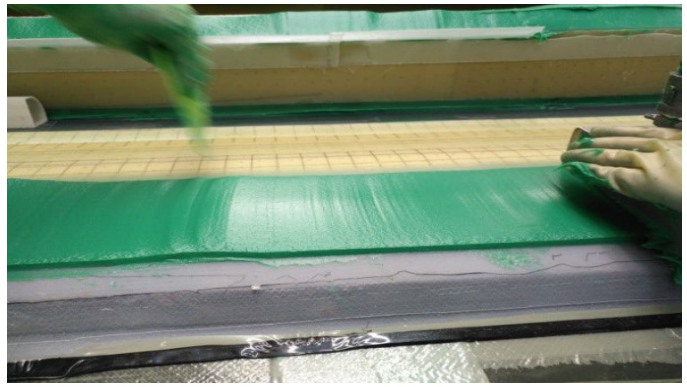

Griffin D, Malkin M. Lessons Learned from Recent Blade Failures: Primary Causes and Risk-Reducing Technologies
https://www.kd-supplychain.com/wind-turbine-blade-epoxy-structural-adhesive-wd3135dwd3137d-product

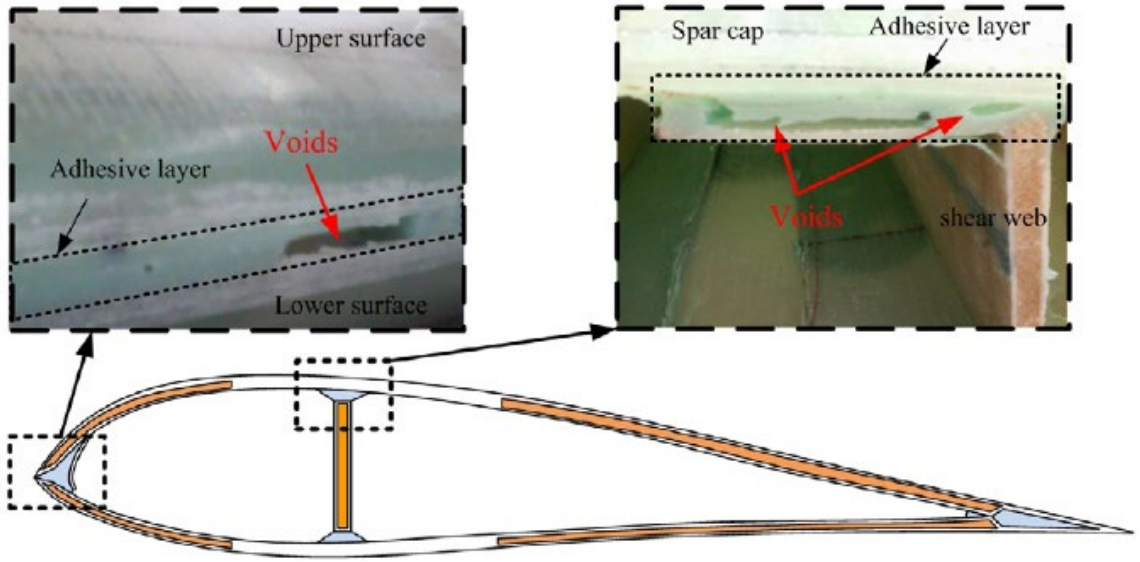

Fracture and fatigue behavior

01

Thickness

Cohesive / adhesive failure

Voids

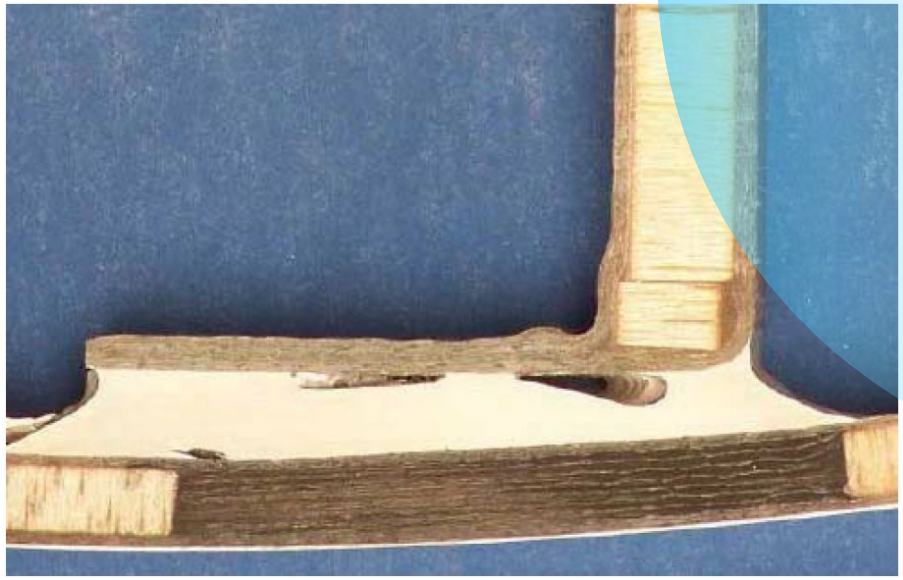

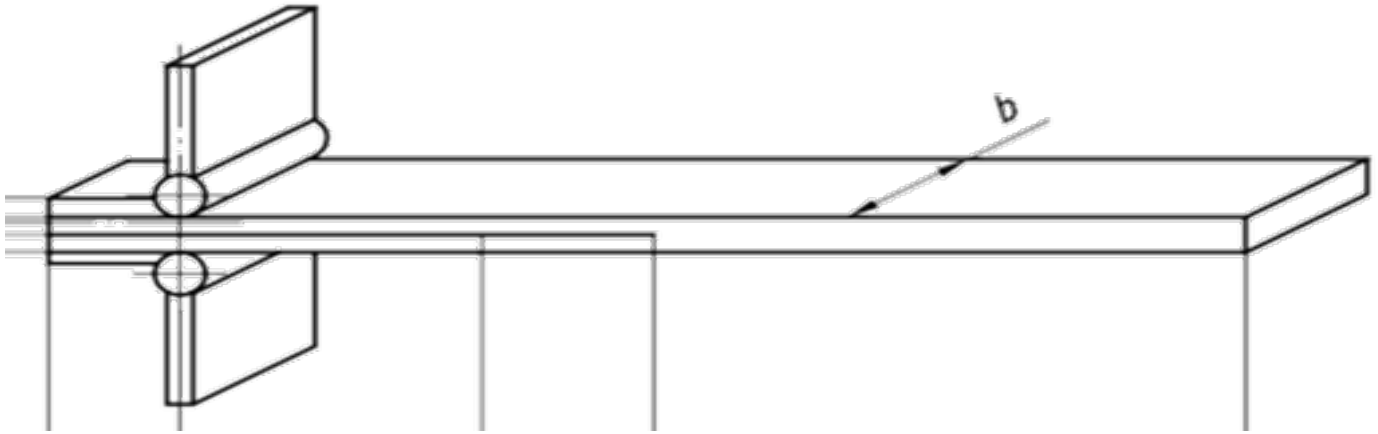

Mode I: DCB

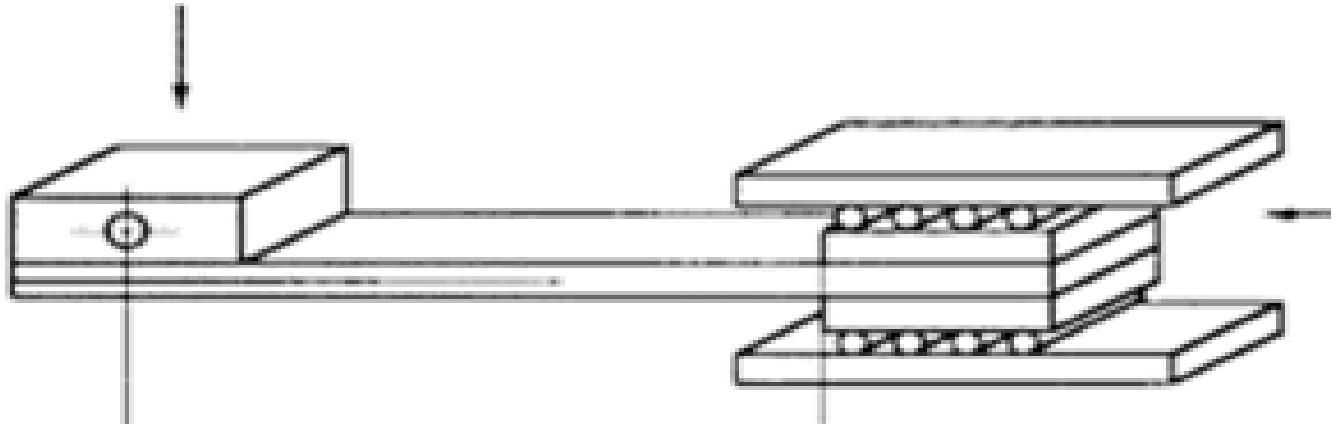

Mode II: ELS

Standardized tests

- Limited information
- Certain areas of application

The ALOHA Airlines flight 243 (1988)

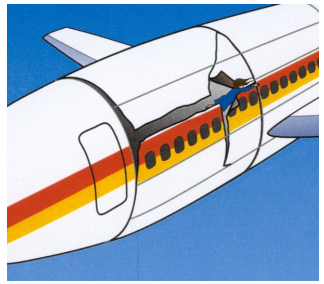

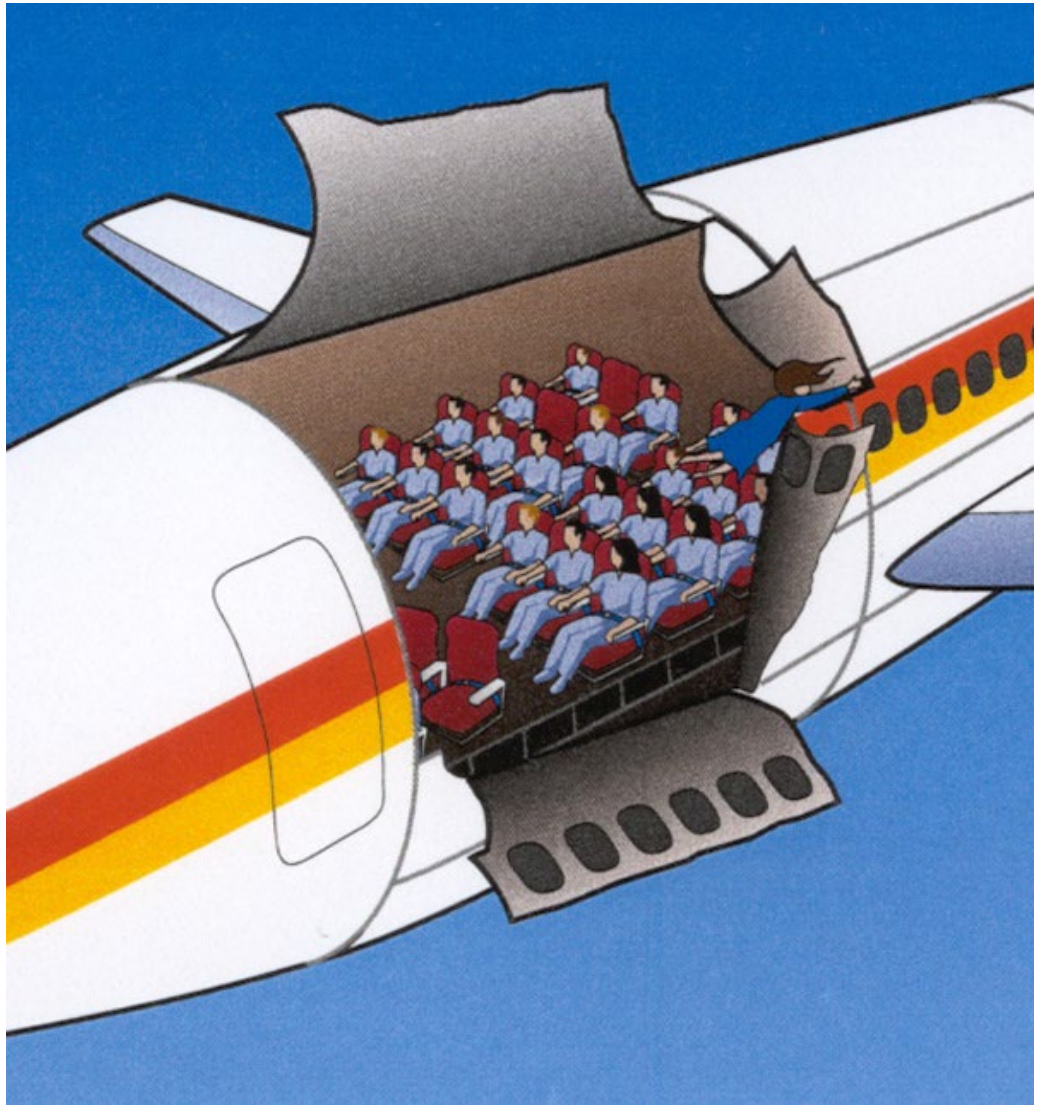

The ALOHA Airlines flight 243 (1988)

https://www.youtube.com/watch?v=YYa7Fq5Ec6c

Composite constructions in Europe

Pont y Ddraig
2013, UK

- Fast and energy-efficient lifting cycles

Avançon bridge
2012, Switzerland

- Lane widening while maintaining the old abutment walls

Novartis Campus entrance building,
2006, Switzerland

- Composite roof integrating structural, building physical and architectural functions

Delamination in composites – 1D/2D/3D

Initiation

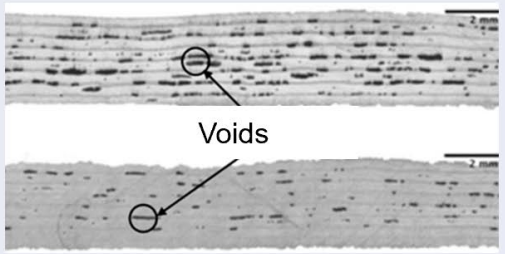

(Mehdikhani et al. 2019)

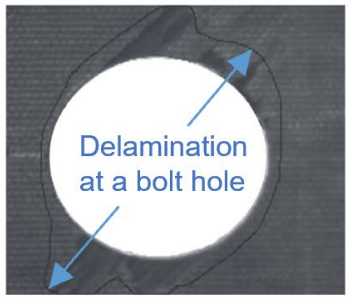

(Krishnamoorthy et al. 2009)

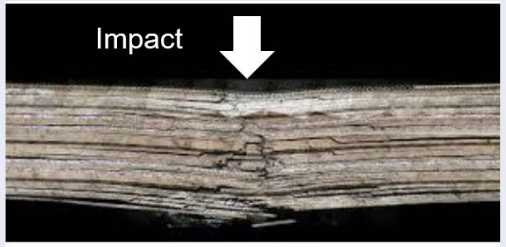

(Cook 2009)

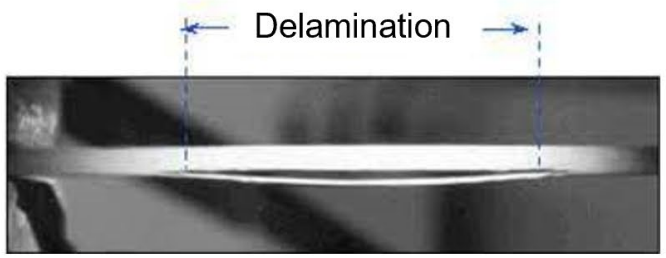

(Nimje 2016)

Delamination

Separation of interlaminar layers or plies

Propagation

Delamination buckling

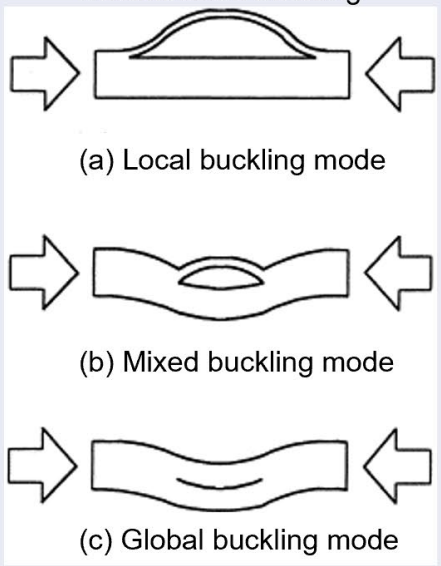

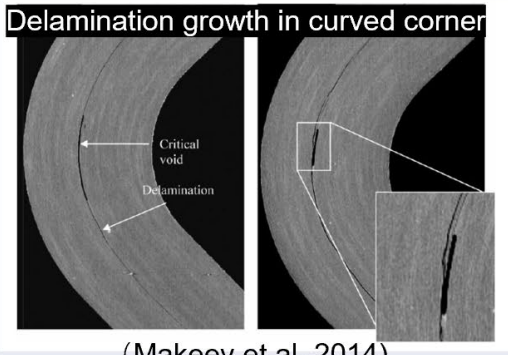

(Makeev et al. 2014)

Joints in FRP composite (civil eng.) structures

- **FRP bridge deck panels**

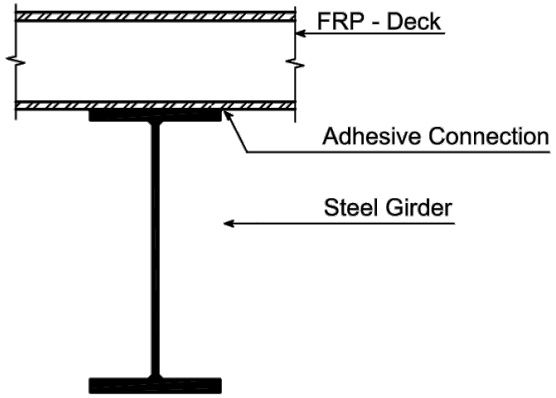

Overview of the experimental set-up

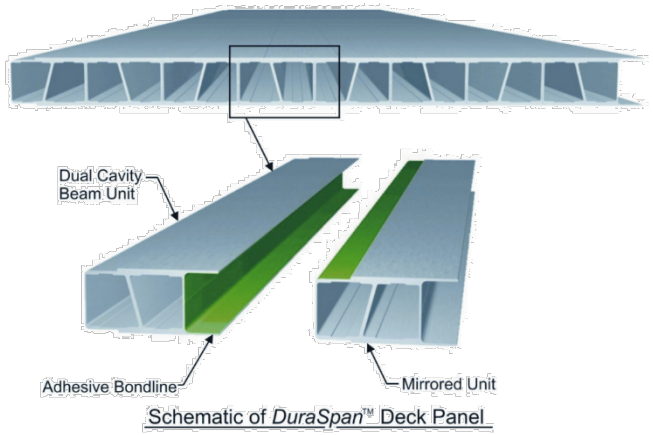

Schematic of *DuraSpan*™ Deck Panel

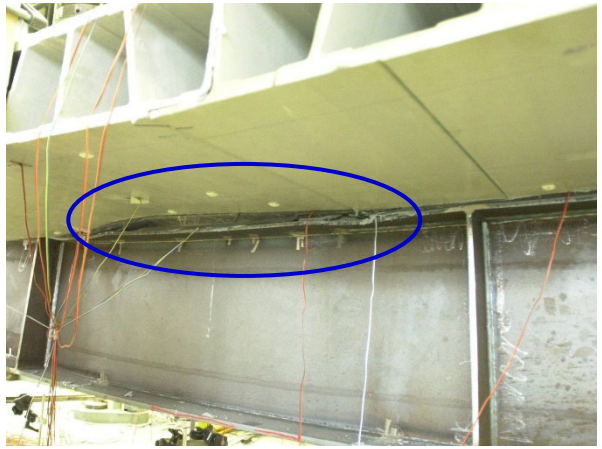

Failure of adhesive bond

Crack front is (almost) never straight (?)

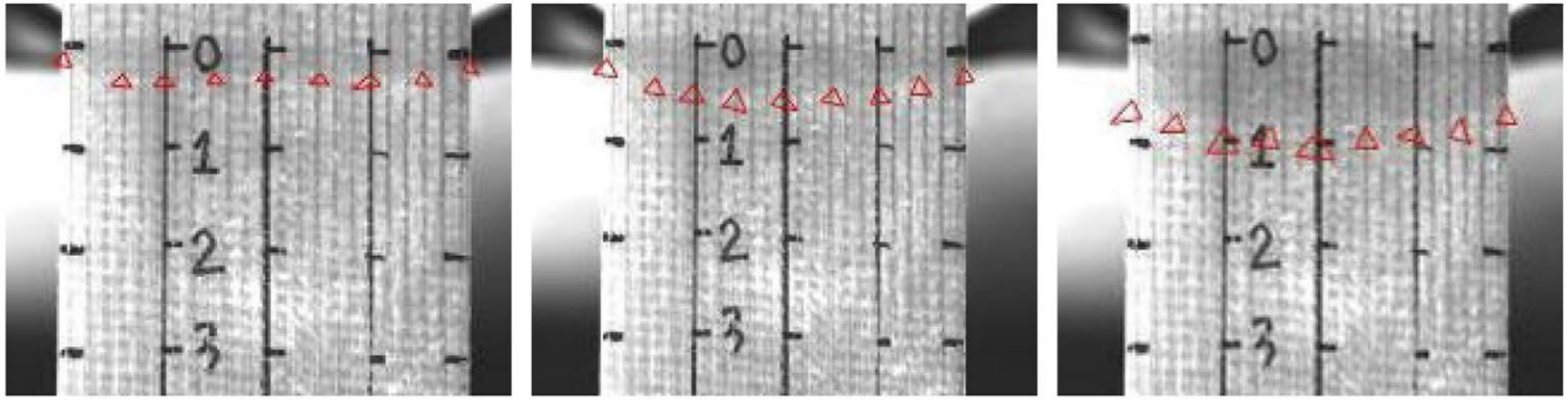

(a) (b) (c)

Curved crack front for conventional specimen DCB-0-2: (a) C105 (b) VIS (c) Propagation.

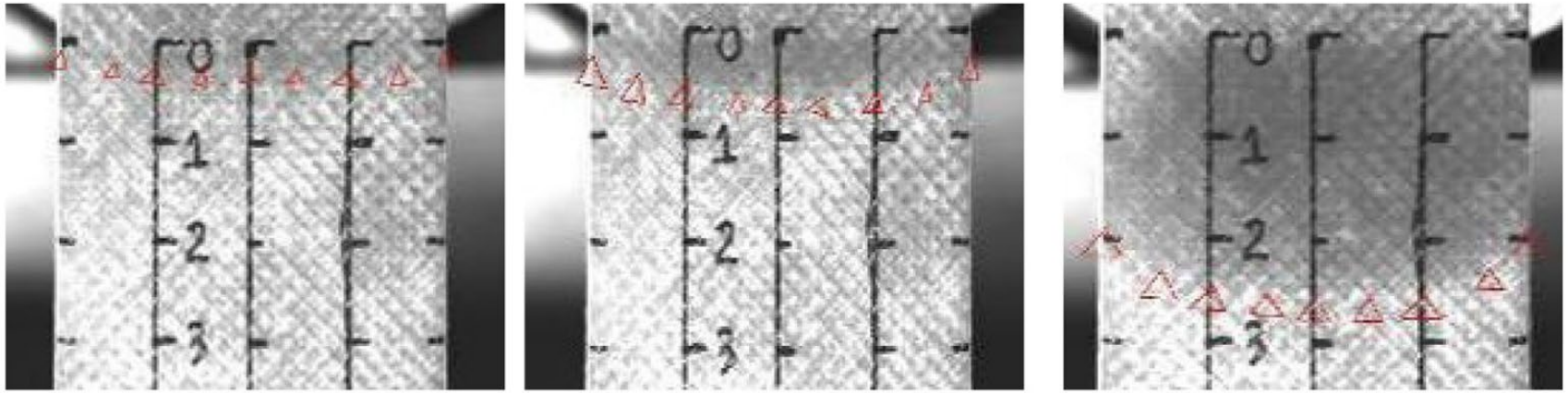

(a) (b) (c)

Curved crack front for conventional specimen DCB-45-2: (a) C105 (b) VIS (c) Propagation.

Composite Structures 227 (2019) 111311

Contents lists available at ScienceDirect

Composite Structures

journal homepage: www.elsevier.com/locate/compstruct

Influence of curved delamination front on R-curve of DCB specimen

Zhengwen Jiang[a], Shui Wan[b], Thomas Keller[c], Zhi Fang[d], Anastasios P. Vassilopoulos[c,*]

Composites’ fracture

- **Delamination/debonding**
  - Laminates
  - Sandwich panels
- **Joint fracture**
  - Fracture mechanics joints
  - Structural joints
- **Planar delamination/debonding**
  - Laminate 2D cracks
  - 2D Delamination in sandwich panels

1D fracture

Fracture mechanics

- It was Alan Arnold Griffith (**1920**) who published* the results of his theoretical calculations an experiments on **brittle fracture** using glass.
  Griffith developed the basis for fracture mechanics – he thus became the ”early father” of fracture mechanics

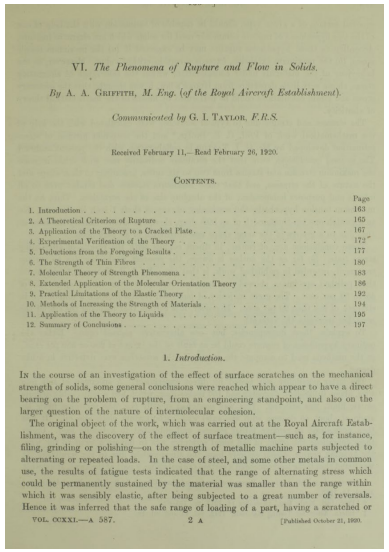

VI. *The Phenomena of Rupture and Flow in Solids.*

By A. A. Griffith, *M. Eng. (of the Royal Aircraft Establishment).*

Communicated by G. I. Taylor, *F.R.S.*

Received February 11,—Read February 26, 1920.

Contents.

1. *Introduction.*

In the course of an investigation of the effect of surface scratches on the mechanical strength of solids, some general conclusions were reached which appear to have a direct bearing on the problem of rupture, from an engineering standpoint, and also on the larger question of the nature of intermolecular cohesion.

The original object of the work, which was carried out at the Royal Aircraft Establishment, was the discovery of the effect of surface treatment—such as, for instance, filing, grinding or polishing—on the strength of metallic machine parts subjected to alternating or repeated loads. In the case of steel, and some other metals in common use, the results of fatigue tests indicated that the range of alternating stress which could be permanently sustained by the material was smaller than the range within which it was sensibly elastic, after being subjected to a great number of reversals. Hence it was inferred that the safe range of loading of a part, having a scratched or

Vol. CCXXI.—A 587. 2 A [Published October 21, 1920.

He introduced the “Griffiths criterion”

$$\sigma\sqrt{\alpha} = const$$

To explain this behavior with thermodynamics theory introduced the “strain energy release rate” known as “*G*” which can physically be understood as: the rate at which energy is absorbed by growth of the crack:

$$G = \frac{\pi\sigma^2\alpha}{\mathrm{E}} \qquad \text{critical } G, or\ G_c = \frac{\pi\sigma_c^2\alpha}{\mathrm{E}}$$

*Griffith, A. A. (1921). "The Phenomena of Rupture and Flow in Solids". Philosophical Transactions of the Royal Society A: Mathematical, Physical and Engineering Sciences. 221 (582–593): 163–198. doi:10.1098/rsta.1921.0006 (open access).

Fracture mechanics

- In **1957** Irwin introduced* the concept of the stress intensity factor (K_I) setting the basis for the linear elastic fracture mechanics.
  Irwin invented the term “fracture mechanics” and is assumed as the modern “father of fracture mechanics”

Most engineering materials show some nonlinear elastic and inelastic behavior

He introduced the “Stress intensity factor” to estimate the energy in linear elastic media:

$$\sigma\sqrt{\pi a} = K_I$$

$$K_c = \begin{cases} \sqrt{EG_c} & \text{for plane stress} \\ \sqrt{\dfrac{EG_c}{1-\nu^2}} & \text{for plane strain} \end{cases}$$

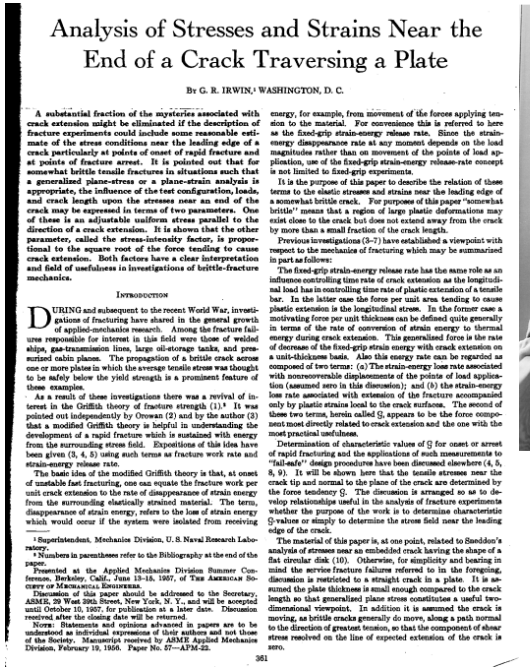

Analysis of Stresses and Strains Near the End of a Crack Traversing a Plate

By G. R. IRWIN,[1] WASHINGTON, D. C.

A substantial fraction of the mysteries associated with crack extension might be eliminated if the description of fracture experiments could include some reasonable estimate of the stress conditions near the leading edge of a crack particularly at points of onset of rapid fracture and at points of fracture arrest. It is pointed out that for somewhat brittle tensalle fractures in situations such that a generalized plane-stress or a plane-strain analysis is appropriate, the influence of the test configuration, loads, and crack length upon the stresses near an end of the crack may be expressed in terms of two parameters. One of these is an adjustable uniform stress parallel to the direction of a crack extension. It is shown that the other parameter, called the stress-intensity factor, is proportional to the square root of the force tending to cause crack extension. Both factors have a clear interpretation and field of usefulness in investigations of brittle-fracture mechanics.

Introduction

DURING and subsequent to the recent World War, investigations of fracturing have shared in the general growth of applied-mechanics research. Among the fracture failures responsible for interest in this field were those of welded ships, gas-transmission lines, large oil-storage tanks, and pressurized cabin planes. The propagation of a brittle crack across one or more plates in which the average tensile stress was thought to be safely below the yield strength is a prominent feature of these examples.

As a result of these investigations there was a revival of interest in the Griffith theory of fracture strength (1).[2] It was pointed out independently by Orowan (2) and by the author (3) that a modified Griffith theory is helpful in understanding the development of a rapid fracture which is sustained with energy from the surrounding stress field. Expositions of this idea have been given (3, 4, 5) using such terms as fracture work rate and strain-energy release rate.

The basic idea of the modified Griffith theory is that, at onset of unstable fast fracturing, one can equate the fracture work per unit crack extension to the rate of disappearance of strain energy from the surrounding elastically strained material. The term, disappearance of strain energy, refers to the loss of strain energy which would occur if the system were isolated from receiving energy, for example, from movement of the forces applying tension to the material. For convenience this is referred to here as the fixed-grip strain-energy release rate. Since the strain-energy disappearance rate at any moment depends on the load magnitudes rather than on movement of the points of load application, use of the fixed-grip strain-energy release-rate concept is not limited to fixed-grip experiments.

It is the purpose of this paper to describe the relation of these terms to the elastic stresses and strains near the leading edge of a somewhat brittle crack. For purposes of this paper “somewhat brittle” means that a region of large plastic deformations may exist close to the crack but does not extend away from the crack by more than a small fraction of the crack length.

Previous investigations (3–7) have established a viewpoint with respect to the mechanics of fracturing which may be summarized in part as follows:

The fixed-grip strain-energy release rate has the same role as an influence controlling time rate of crack extension as the longitudinal load has in controlling time rate of plastic extension of a tensile bar. In the latter case the force per unit area tending to cause plastic extension is the longitudinal stress. In the former case a motivating force per unit thickness can be defined quite generally in terms of the rate of conversion of strain energy to thermal energy during crack extension. This generalized force is the rate of decrease of the fixed-grip strain energy with crack extension on a unit-thickness basis. Also this energy rate can be regarded as composed of two terms: (a) The strain-energy loss rate associated with nonrecoverable displacements of the points of load application (assumed zero in this discussion); and (b) the strain-energy loss rate associated with extension of the fracture accompanied only by plastic strains local to the crack surfaces. The second of these two terms, herein called $\mathcal{G}$, appears to be the force component most directly related to crack extension and the one with the most practical usefulness.

Determination of characteristic values of $\mathcal{G}$ for onset or arrest of rapid fracturing and the applications of such measurements to “fail-safe” design procedures have been discussed elsewhere (4, 5, 8, 9). It will be shown here that the tensile stresses near the crack tip and normal to the plane of the crack are determined by the force tendency $\mathcal{G}$. The discussion is arranged so as to develop relationships useful in the analysis of fracture experiments whether the purpose of the work is to determine characteristic $\mathcal{G}$-values or simply to determine the stress field near the leading edge of the crack.

The material of this paper is, at one point, related to Sneddon’s analysis of stresses near an embedded crack having the shape of a flat circular disk (10). Otherwise, for simplicity and bearing in mind the service fracture failures referred to in the foregoing, discussion is restricted to a straight crack in a plate. It is assumed the plate thickness is small enough compared to the crack length so that generalized plane stress constitutes a useful two-dimensional viewpoint. In addition it is assumed the crack is moving, as brittle cracks generally do move, along a path normal to the direction of greatest tension, so that the component of shear stress resolved on the line of expected extension of the crack is zero.

[1] Superintendent, Mechanics Division, U. S. Naval Research Laboratory.

[2] Numbers in parentheses refer to the Bibliography at the end of the paper.

Presented at the Applied Mechanics Division Summer Conference, Berkeley, Calif., June 13–15, 1957, of The American Society of Mechanical Engineers.

Discussion of this paper should be addressed to the Secretary, ASME, 29 West 39th Street, New York, N. Y., and will be accepted until October 10, 1957, for publication at a later date. Discussion received after the closing date will be returned.

Note: Statements and opinions advanced in papers are to be understood as individual expressions of their authors and not those of the Society. Manuscript received by ARME Applied Mechanics Division, February 19, 1956. Paper No. 57—APM-23.

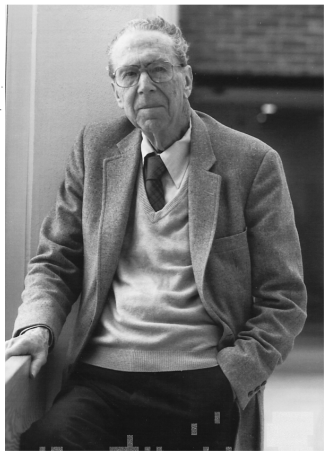

George R. Irwin

*Irwin G (1957), Analysis of stresses and strains near the end of a crack traversing a plate, Journal of Applied Mechanics 24, 361–364 .

Fatigue/Fracture mechanics

- Paris in **1961** showed that the fatigue crack growth rate ($d\alpha/dN$) is a function of the stress intensity factor range ΔK, (describing what is called today a fatigue crack growth curve - FCG)

$$\frac{d\alpha}{dN} = C \cdot \Delta K^m$$

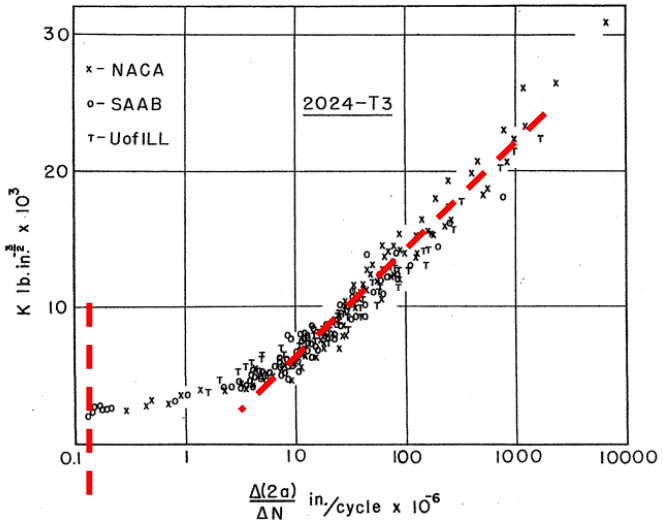

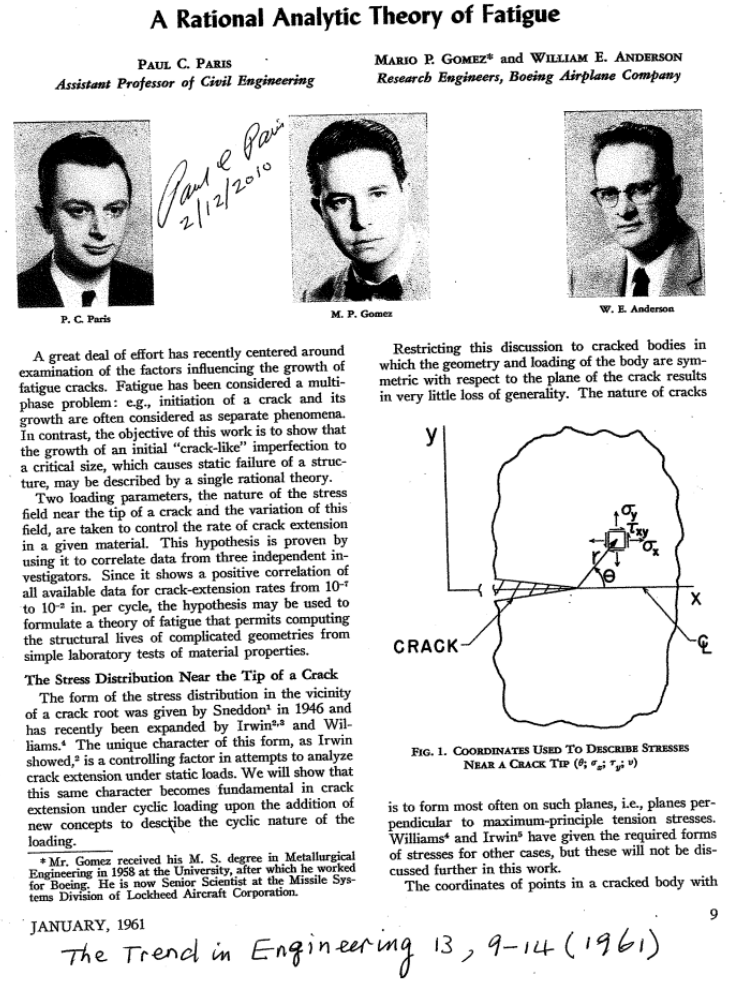

A Rational Analytic Theory of Fatigue

PAUL C. PARIS
Assistant Professor of Civil Engineering

MARIO P. GOMEZ* and WILLIAM E. ANDERSON
Research Engineers, Boeing Airplane Company

P. C. Paris

M. P. Gomez

W. E. Anderson

A great deal of effort has recently centered around examination of the factors influencing the growth of fatigue cracks. Fatigue has been considered a multiphase problem: e.g., initiation of a crack and its growth are often considered as separate phenomena. In contrast, the objective of this work is to show that the growth of an initial "crack-like" imperfection to a critical size, which causes static failure of a structure, may be described by a single rational theory.

Two loading parameters, the nature of the stress field near the tip of a crack and the variation of this field, are taken to control the rate of crack extension in a given material. This hypothesis is proven by using it to correlate data from three independent investigators. Since it shows a positive correlation of all available data for crack-extension rates from 10^{-7} to 10^{-2} in. per cycle, the hypothesis may be used to formulate a theory of fatigue that permits computing the structural lives of complicated geometries from simple laboratory tests of material properties.

The Stress Distribution Near the Tip of a Crack

The form of the stress distribution in the vicinity of a crack root was given by Sneddon[1] in 1946 and has recently been expanded by Irwin[2,3] and Williams.[4] The unique character of this form, as Irwin showed,[2] is a controlling factor in attempts to analyze crack extension under static loads. We will show that this same character becomes fundamental in crack extension under cyclic loading upon the addition of new concepts to describe the cyclic nature of the loading.

* Mr. Gomez received his M. S. degree in Metallurgical Engineering in 1958 at the University, after which he worked for Boeing. He is now Senior Scientist at the Missile Systems Division of Lockheed Aircraft Corporation.

Restricting this discussion to cracked bodies in which the geometry and loading of the body are symmetric with respect to the plane of the crack results in very little loss of generality. The nature of cracks

FIG. 1. COORDINATES USED TO DESCRIBE STRESSES NEAR A CRACK TIP (θ; σ_x; τ_{xy}; v)

is to form most often on such planes, i.e., planes perpendicular to maximum-principle tension stresses. Williams[4] and Irwin[5] have given the required forms of stresses for other cases, but these will not be discussed further in this work.

The coordinates of points in a cracked body with

JANUARY, 1961
The Trend in Engineering 13, 9-14 (1961)

* Paris, P. C.; Gomez, M. P.; Anderson, W. E. (1961). "A rational analytic theory of fatigue". The Trend in Engineering. 13: 9–14

Fatigue/Fracture mechanics

- Jaap Schijve in early **1960s** emphasized **variable amplitude fatigue crack growth** testing in aircraft and pointed out the importance of the tensile overloads that can cause growth retardation.
- In **1970** Elber demonstrated the importance of the crack closure on fatigue crack growth.

2001

2015

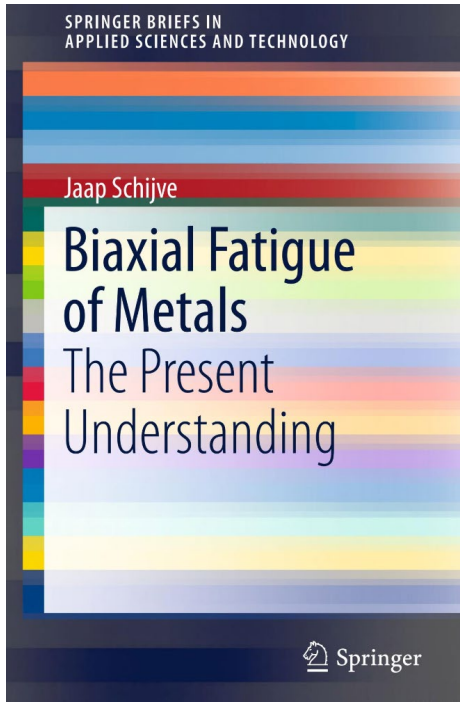

Fracture mechanics – supported by imaging methods

- It was in early **1900s** when Ewin and Humfrey* used the optical microscope to pursue the study of fatigue/fracture mechanisms
- In the **1950**s the scanning electron microscope
- Today DIC/ x-ray tomography

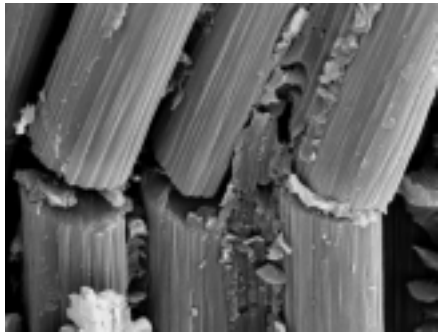

SEM: Fiber kinking due to compression

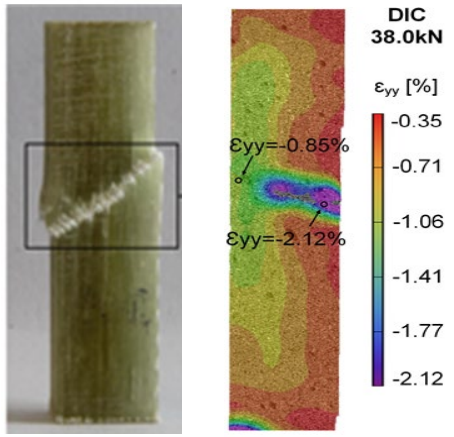

DIC measurement of strain fields

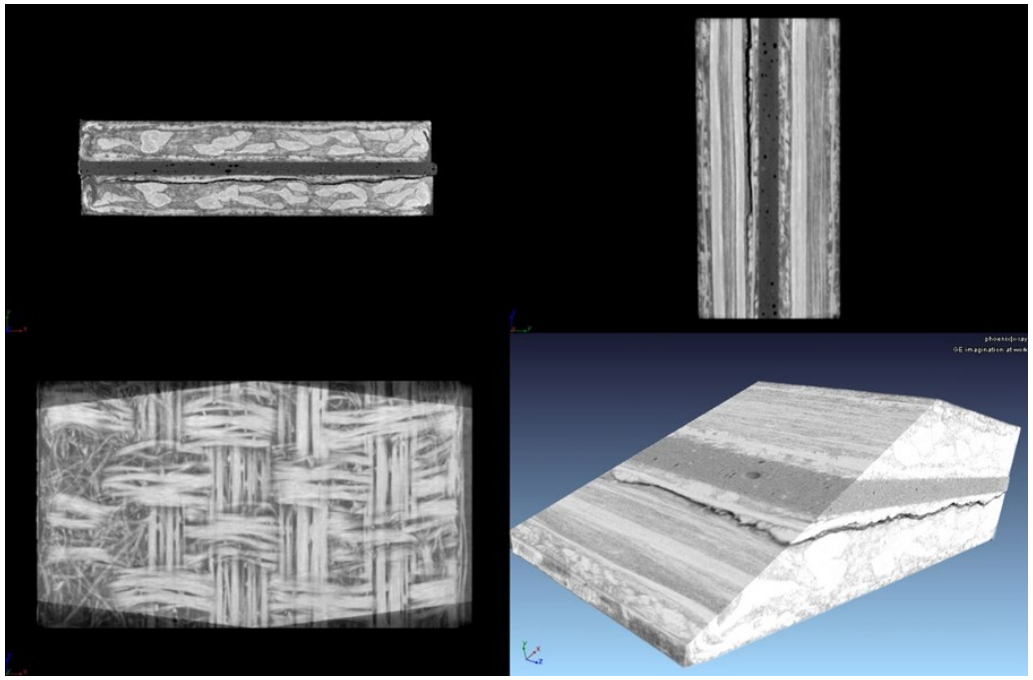

Tomography: Architecture of, and crack in an adhesively bonded

*J. A. Ewin, J. C. W. Humfrey. “The fracture of metals under repeated alternations of stress” Philosophical transactions of the royal society A. Mathematical, physical and engineering sciences, 01 Jan 1903

X-ray digital tomography

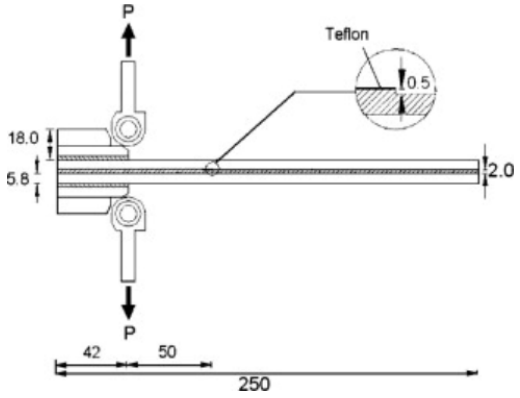

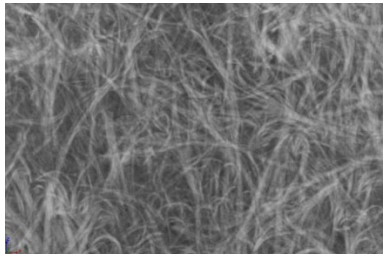

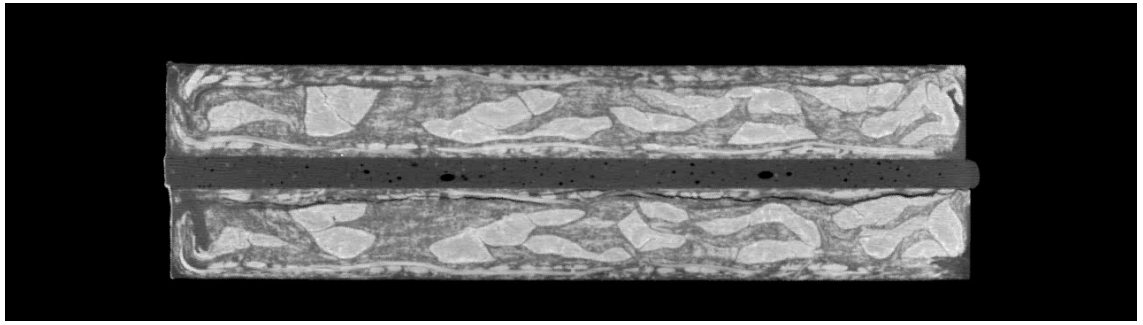

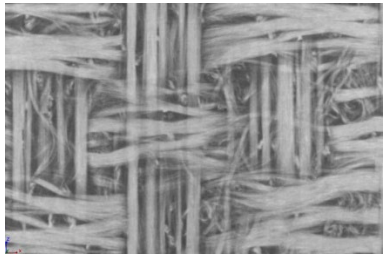

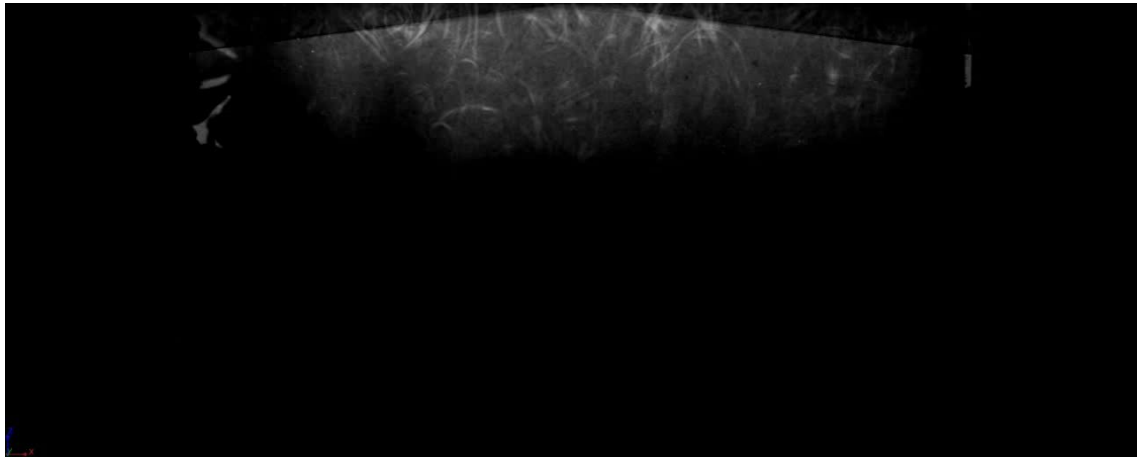

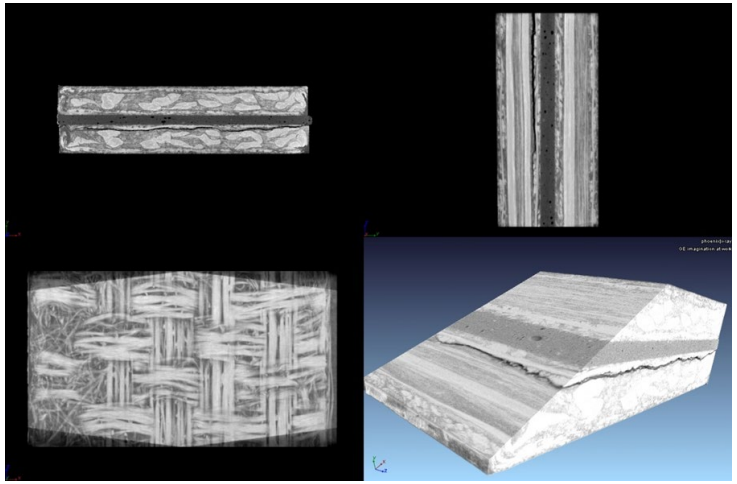

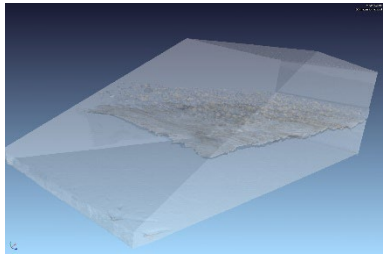

Various needs

"Thin" laminates and this adhesive joints

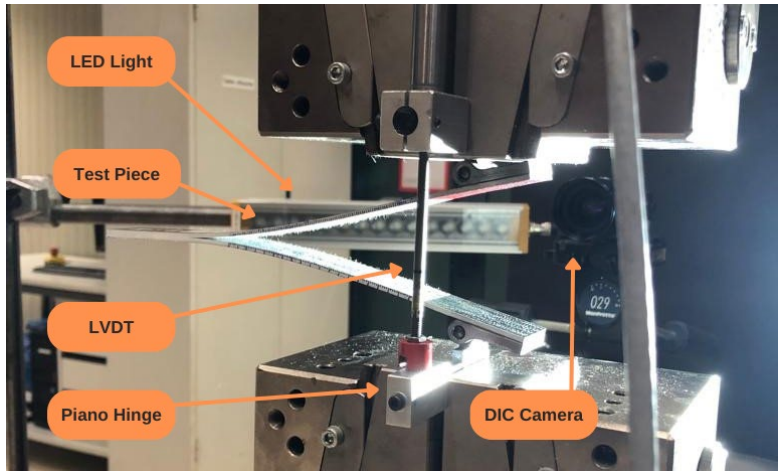

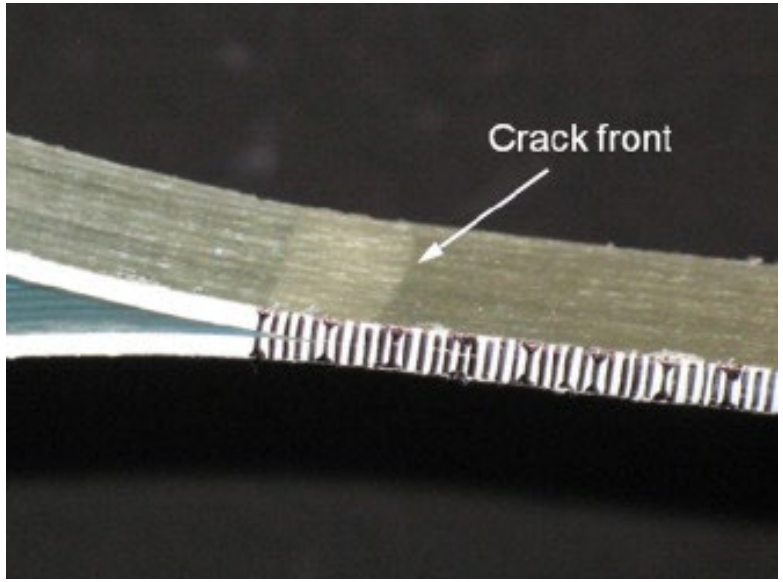

Designation: D 5528 – 01 (Reapproved 2007)$^{\varepsilon 2}$

Standard Test Method for Mode I Interlaminar Fracture Toughness of Unidirectional Fiber-Reinforced Polymer Matrix Composites[1]

This standard is issued under the fixed designation D 5528; the number immediately following the designation indicates the year of original adoption or, in the case of revision, the year of last revision. A number in parentheses indicates the year of last reapproval. A superscript epsilon (ε) indicates an editorial change since the last revision or reapproval.

ε^1 NOTE—Added research report reference to Section 14 editorially in March 2008.
ε^2 NOTE—Corrected Eq. 3 in July 2008.

1. Scope

1.1 This test method describes the determination of the opening Mode I interlaminar fracture toughness, G_{Ic}, of continuous fiber-reinforced composite materials using the double cantilever beam (DCB) specimen (Fig. 1).

1.2 This test method is limited to use with composites consisting of unidirectional carbon fiber and glass fiber tape laminates with brittle and tough single-phase polymer matrices. This limited scope reflects the experience gained in round robin testing. This test method may prove useful for

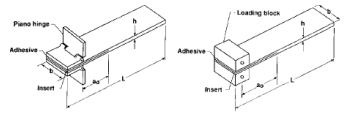

(a) with piano hinges (b) with loading blocks

FIG. 1 Double Cantilever Beam Specimen

INTERNATIONAL STANDARD **ISO 15024**

First edition
2001-12-01

Fibre-reinforced plastic composites — Determination of mode I interlaminar fracture toughness, G_{IC}, for unidirectionally reinforced materials

Composites plastiques renforcés de fibres — Détermination de la ténacité à la rupture interlaminaire en mode I, G_{IC}, de matériaux composites à matrice polymère renforcés de fibres unidirectionnelles

Various needs

"Thin paste" adhesive joints

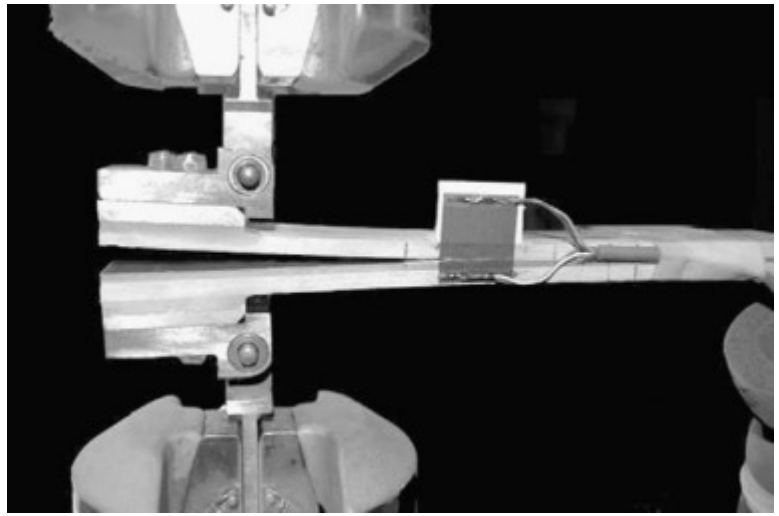

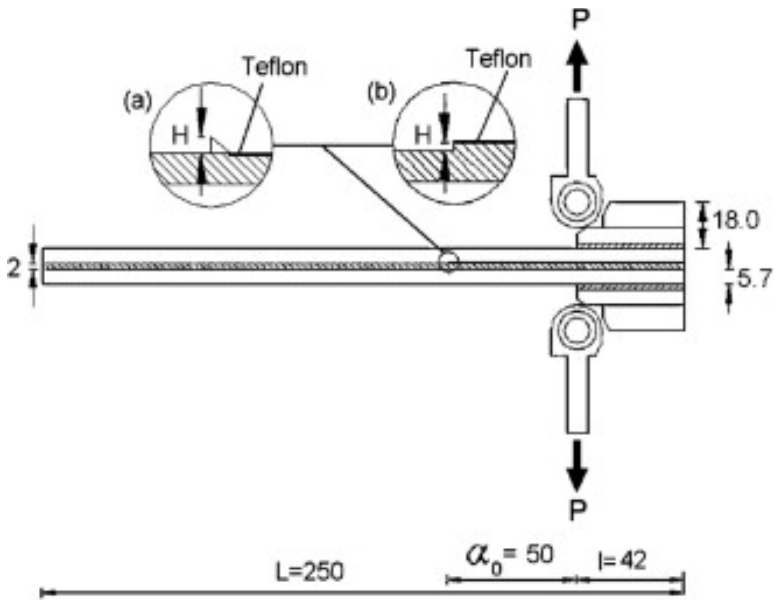

Designation: D 5528 – 01 (Reapproved 2007)$^{\varepsilon 2}$

Standard Test Method for Mode I Interlaminar Fracture Toughness of Unidirectional Fiber-Reinforced Polymer Matrix Composites[1]

This standard is issued under the fixed designation D 5528; the number immediately following the designation indicates the year of original adoption or, in the case of revision, the year of last revision. A number in parentheses indicates the year of last reapproval. A superscript epsilon (ε) indicates an editorial change since the last revision or reapproval.

ε^1 NOTE—Added research report reference to Section 14 editorially in March 2008.
ε^2 NOTE—Corrected Eq. 3 in July 2008.

1. Scope

1.1 This test method describes the determination of the opening Mode I interlaminar fracture toughness, G_{Ic}, of continuous fiber-reinforced composite materials using the double cantilever beam (DCB) specimen (Fig. 1).

1.2 This test method is limited to use with composites consisting of unidirectional carbon fiber and glass fiber tape laminates with brittle and tough polymer matrices. This limited scope

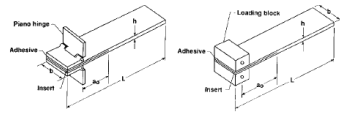

(a) with piano hinges (b) with loading blocks

FIG. 1 Double Cantilever Beam Specimen

?

INTERNATIONAL STANDARD **ISO 15024**

LEFM…

First edition
2001-12-01

Fibre-reinforced plastic composites — Determination of mode I interlaminar fracture toughness, G_{IC}, for unidirectionally reinforced materials

Composites plastiques renforcés de fibres — Détermination de la ténacité à la rupture interlaminaire en mode I, G_{IC}, de matériaux composites à matrice polymère renforcés de fibres unidirectionnelles

Various needs

“Thick paste” adhesive joints

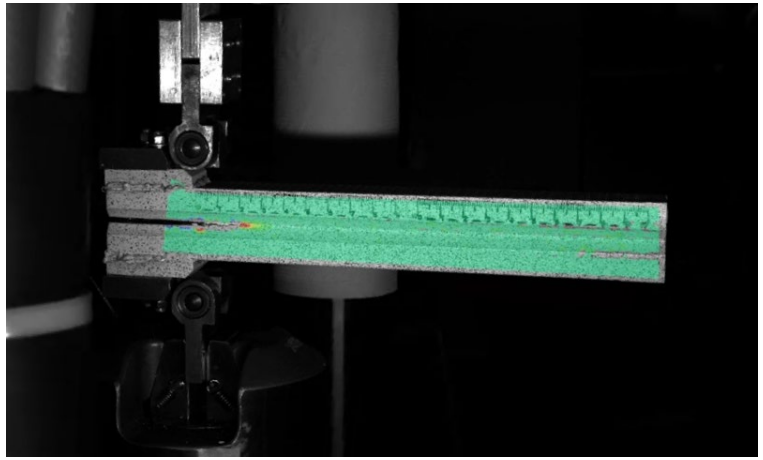

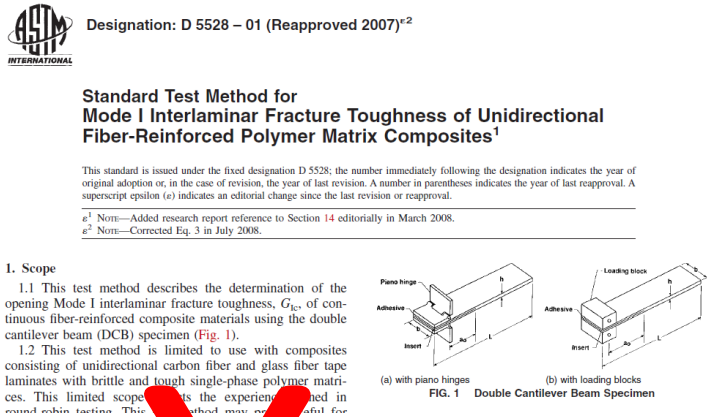

Designation: D 5528 – 01 (Reapproved 2007)ε2

Standard Test Method for
Mode I Interlaminar Fracture Toughness of Unidirectional
Fiber-Reinforced Polymer Matrix Composites[1]

This standard is issued under the fixed designation D 5528; the number immediately following the designation indicates the year of original adoption or, in the case of revision, the year of last revision. A number in parentheses indicates the year of last reapproval. A superscript epsilon (ε) indicates an editorial change since the last revision or reapproval.

ε[1] NOTE—Added research report reference to Section 14 editorially in March 2008.
ε[2] NOTE—Corrected Eq. 3 in July 2008.

1. Scope

1.1 This test method describes the determination of the opening Mode I interlaminar fracture toughness, G_{Ic}, of continuous fiber-reinforced composite materials using the double cantilever beam (DCB) specimen (Fig. 1).

1.2 This test method is limited to use with composites consisting of unidirectional carbon fiber and glass fiber tape laminates with brittle and tough single-phase polymer matrices. This limited scope [illegible] the experience [illegible] in round robin testing. This [illegible] may [illegible] useful for

(a) with piano hinges (b) with loading blocks

FIG. 1 Double Cantilever Beam Specimen

INTERNATIONAL STANDARD

ISO 15024

First edition
2001-12-01

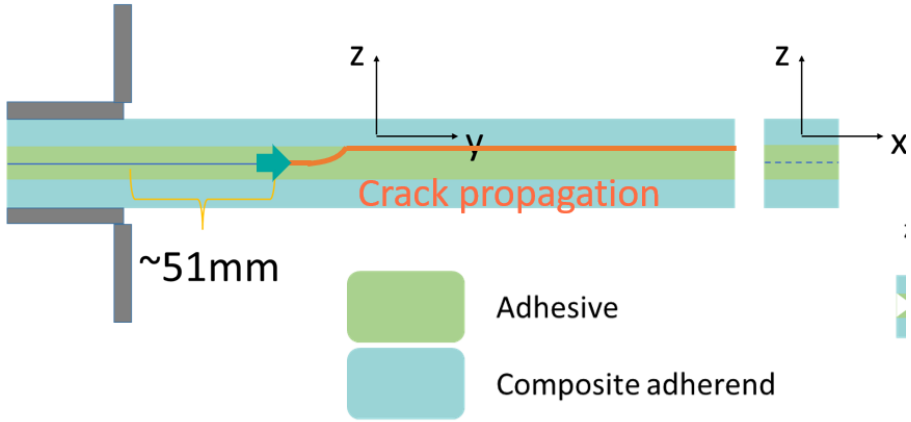

LEFM…

Fibre-reinforced plastic composites — Determination of mode I interlaminar fracture toughness, G_{IC}, for unidirectionally reinforced materials

Composites plastiques renforcés de fibres — Détermination de la ténacité à la rupture interlaminaire en mode I, G_{IC}, de matériaux composites à matrice polymère renforcés de fibres unidirectionnelles

? LEFM…

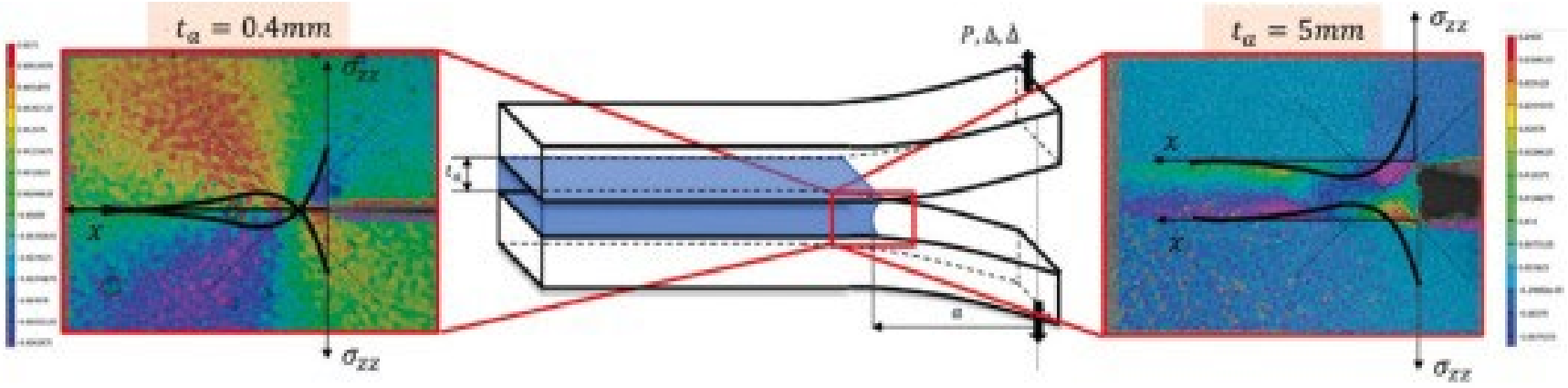

Thin vs. thick joints

The stress field in thin and thick joints is different.

In thicker joints, a plastic zone is introduced ahead of the crack tip and under certain conditions can dominate the fracture process

...A theory used to analyze material failure based on the stress field around a crack tip

Is valid as long as any plastic deformation at the crack tip can be considered as negligible when compared to the overall crack dimensions

LEFM

Therefore, is interesting for materials exhibiting brittle or elastic behavior, such as glass and some polymers.

It involves the linear relationship between the stress-intensity factor and the applied load, critical for understanding crack propagation in materials

$$\sigma\sqrt{\pi\alpha} = K_I$$

Various needs

"Structural joints"

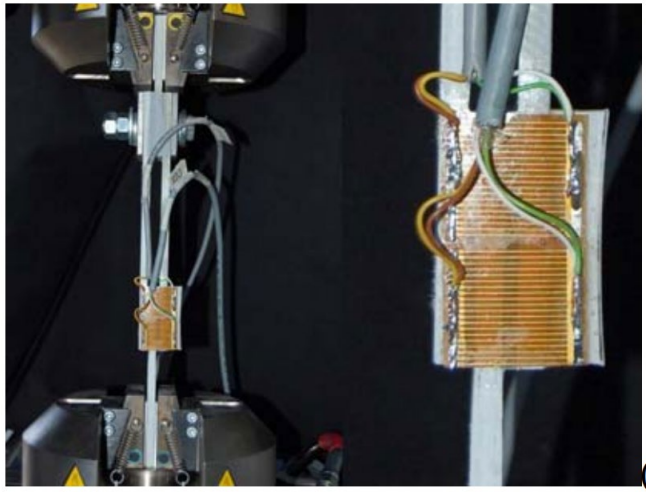

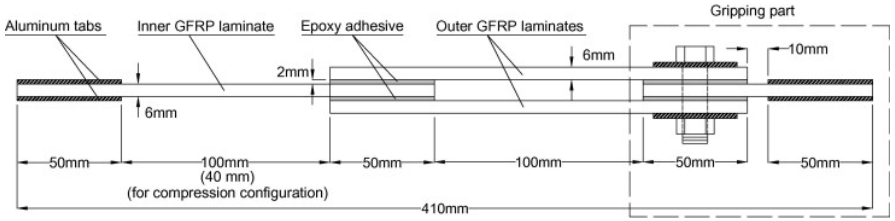

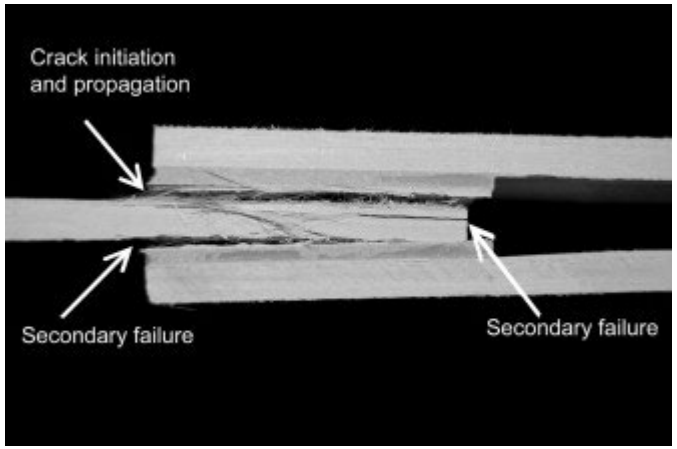

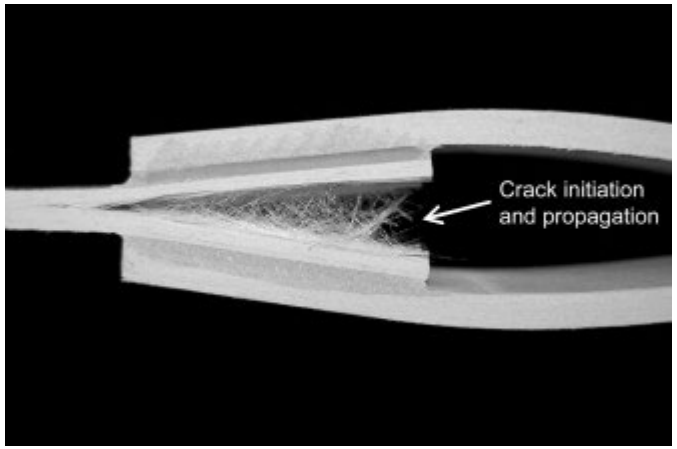

Various needs

"Structural joints"
Sub-component

(a)

(b)

(a) Full scale fatigue experimental set up (b) fiber-tear failure in facesheets and failure in balsa core of adhesively bonded joint [4] © EPFL

Various needs

“Structural joints” Sub-component

Adhesive bond failure between the spar beam and the flange in a wind turbine rotor blade [doi] (b) Henkel-Up Wind-Beam during cyclic test [doi].

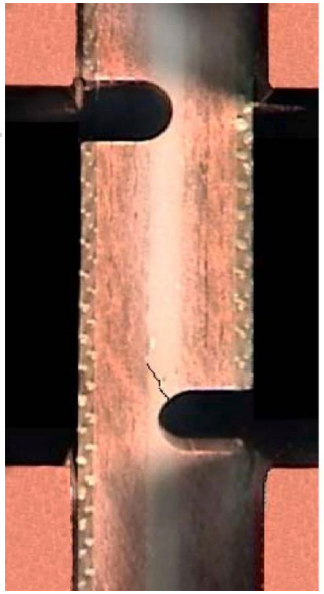

Notched lap shear fatigue specimen A. T. Sears, D. D. Samborsky, P. Agastra, and J. F. Mandell, “Fatigue results and analysis for thick adhesive notched lap shear test,” Collect. Tech. Pap. - AIAA/ASME/ASCE/AHS/ASC Struct. Struct. Dyn. Mater. Conf., no. April, 2010

Objective (quasi-static)

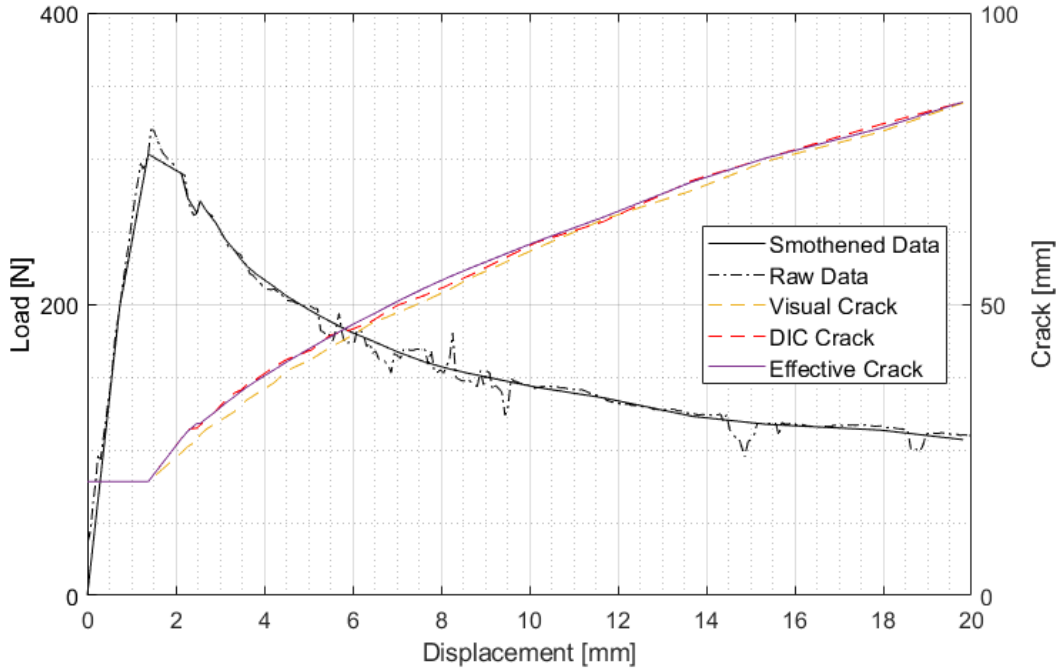

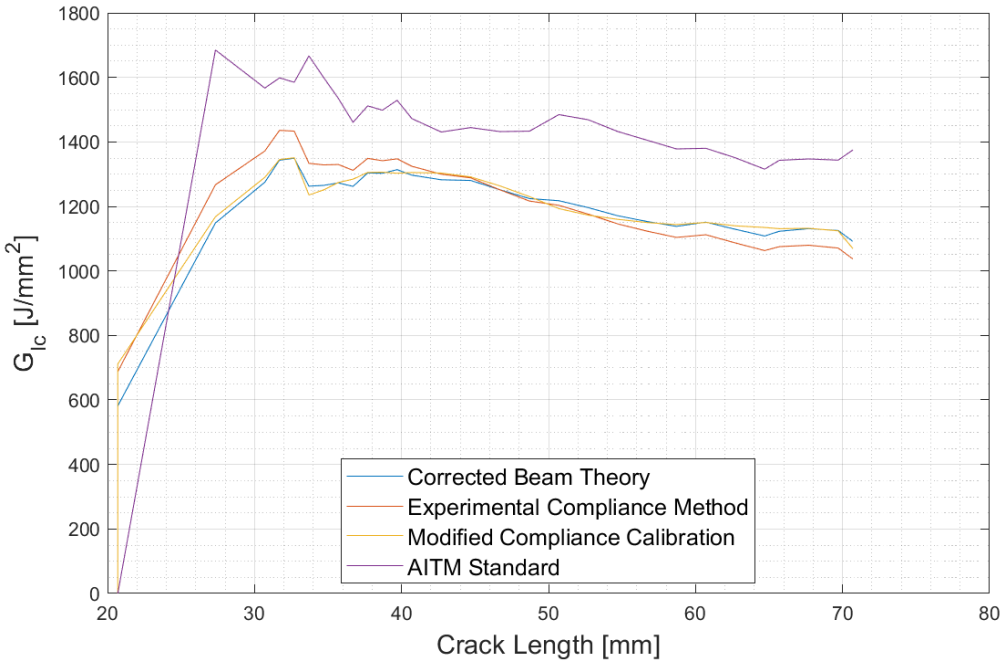

Objective (fatigue)

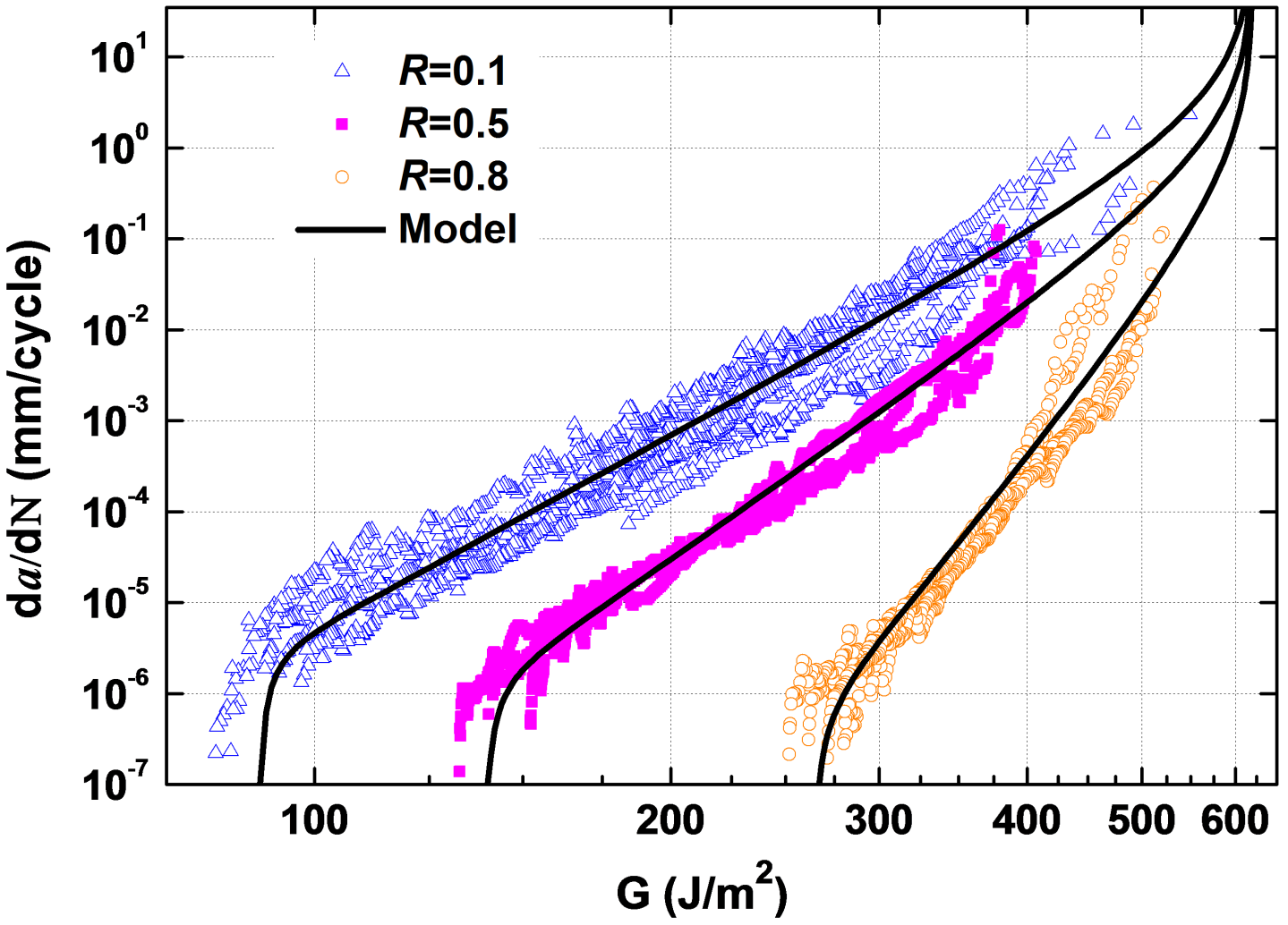

Measures needed (simplified)

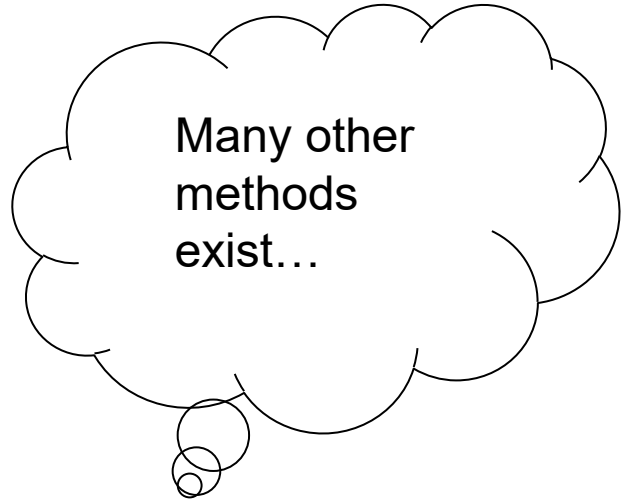

$$\textbf{Modified beam theory}: G_I = \frac{3P\delta F}{2bM(a+|\Delta|)}$$

$$G_I = \frac{3\boldsymbol{P\delta}F}{2bM(\boldsymbol{a}+|\Delta|)}$$

***P**: Applied load*
***δ**: displacement*
***α**: crack length*
F: large displacement correction factor
M: load block correction factor
b: the specimen width and
$\lvert\Delta\rvert$: the effective delamination extension to correct for rotation of DCB arms at delamination front, as recommended in ASTM D5528

Damage monitoring

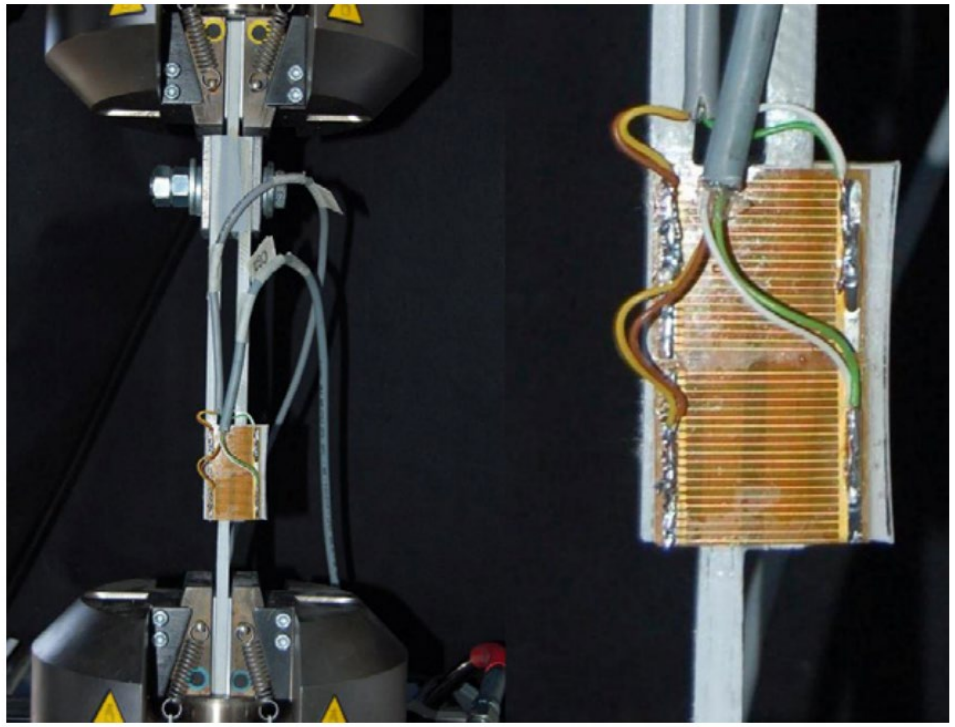

Damage monitoring

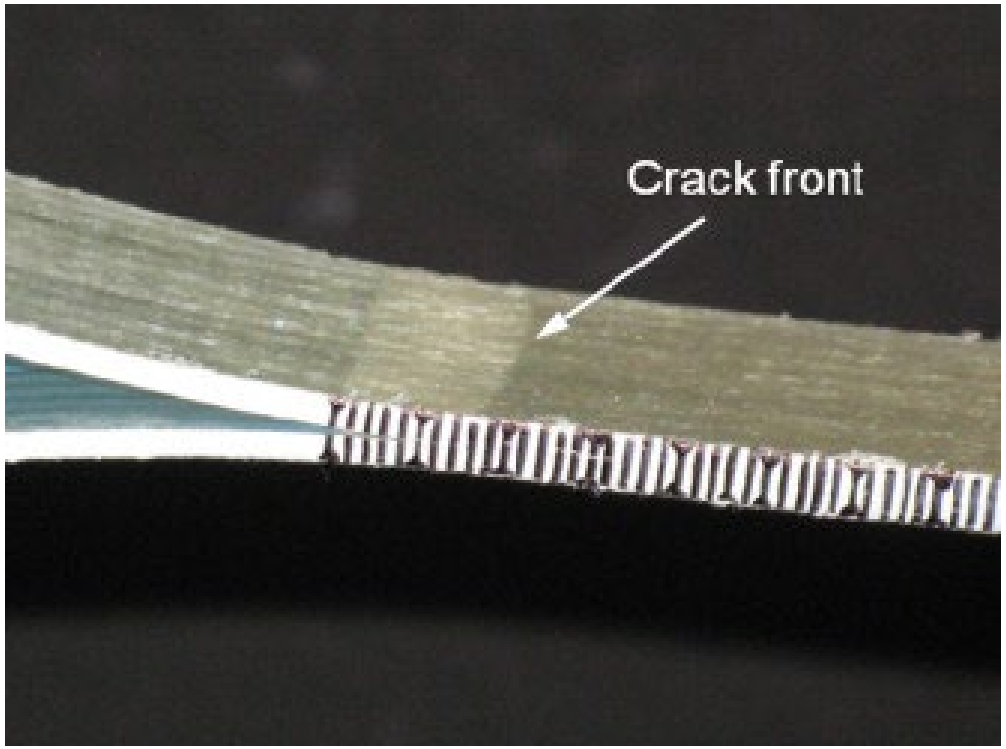

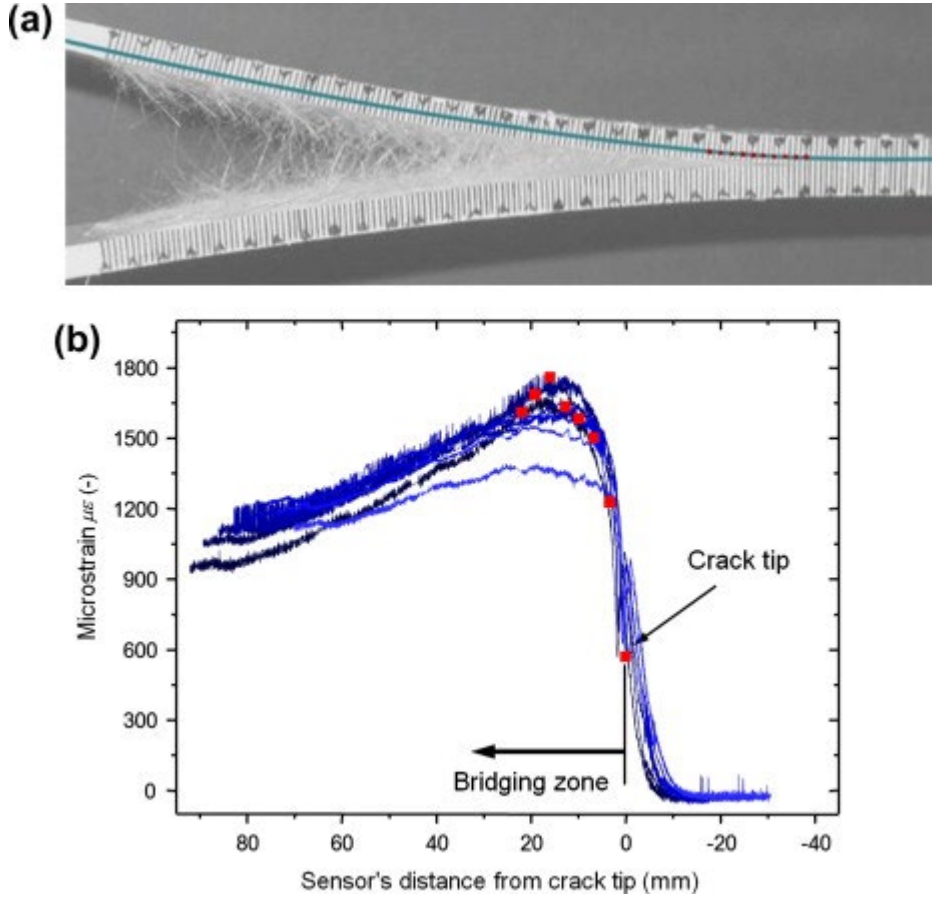

Damage monitoring DIC

DIC = Digital Image Correlation

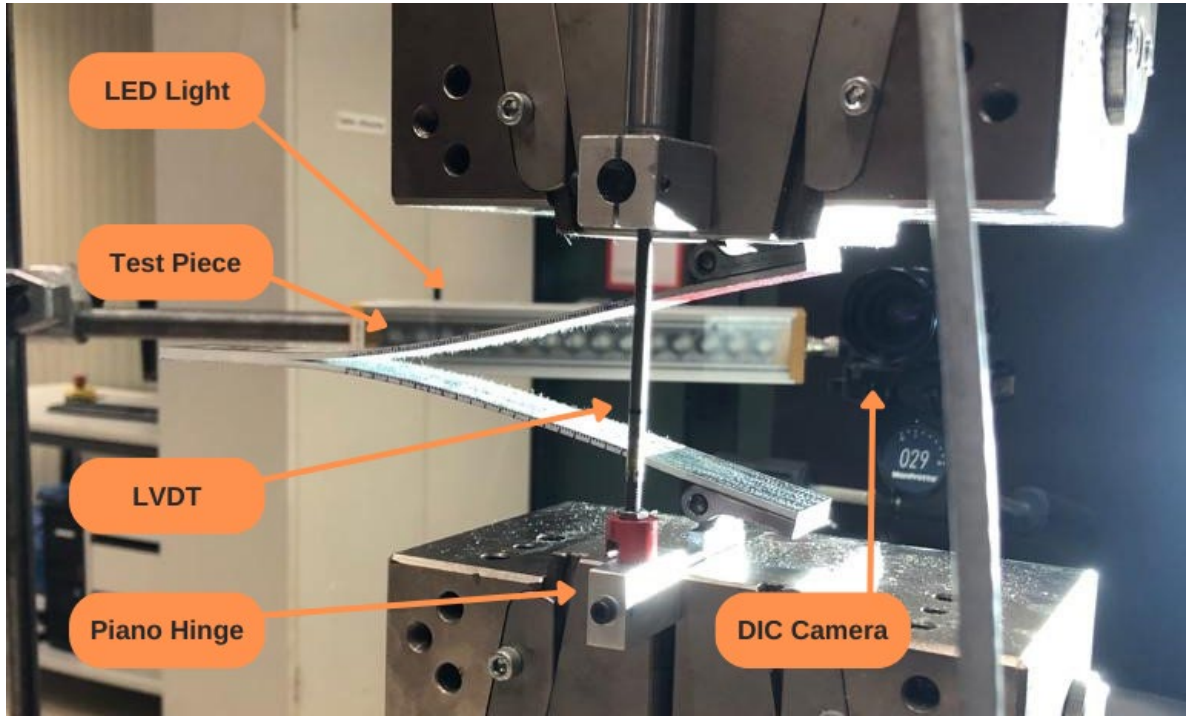

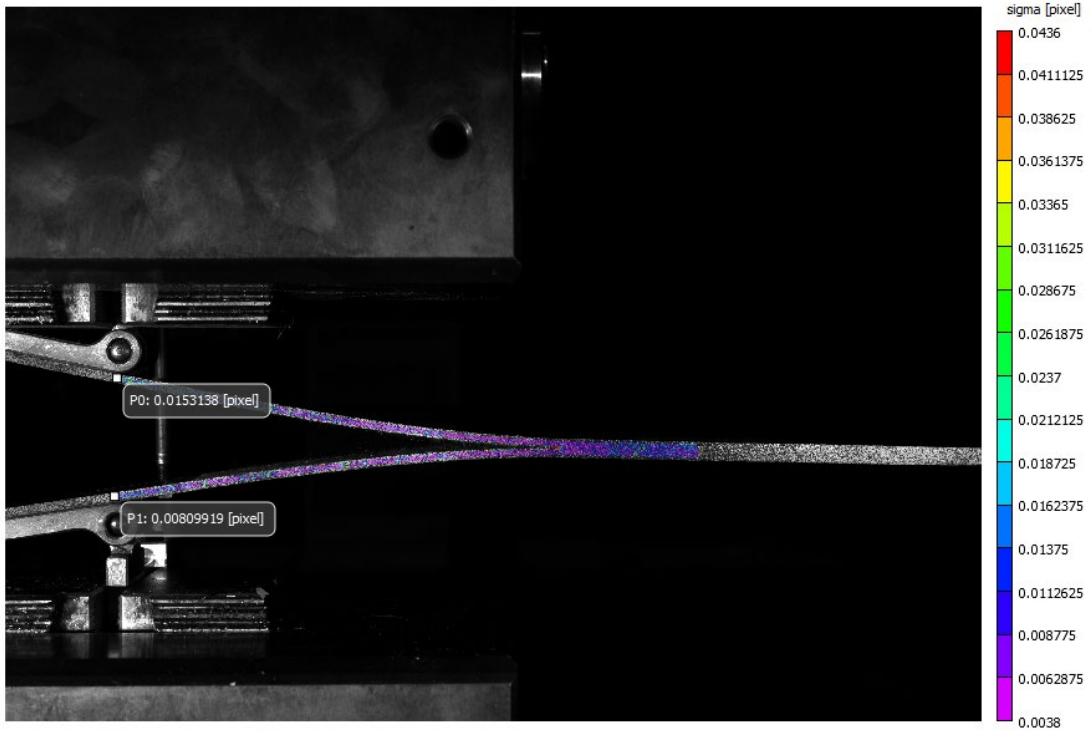

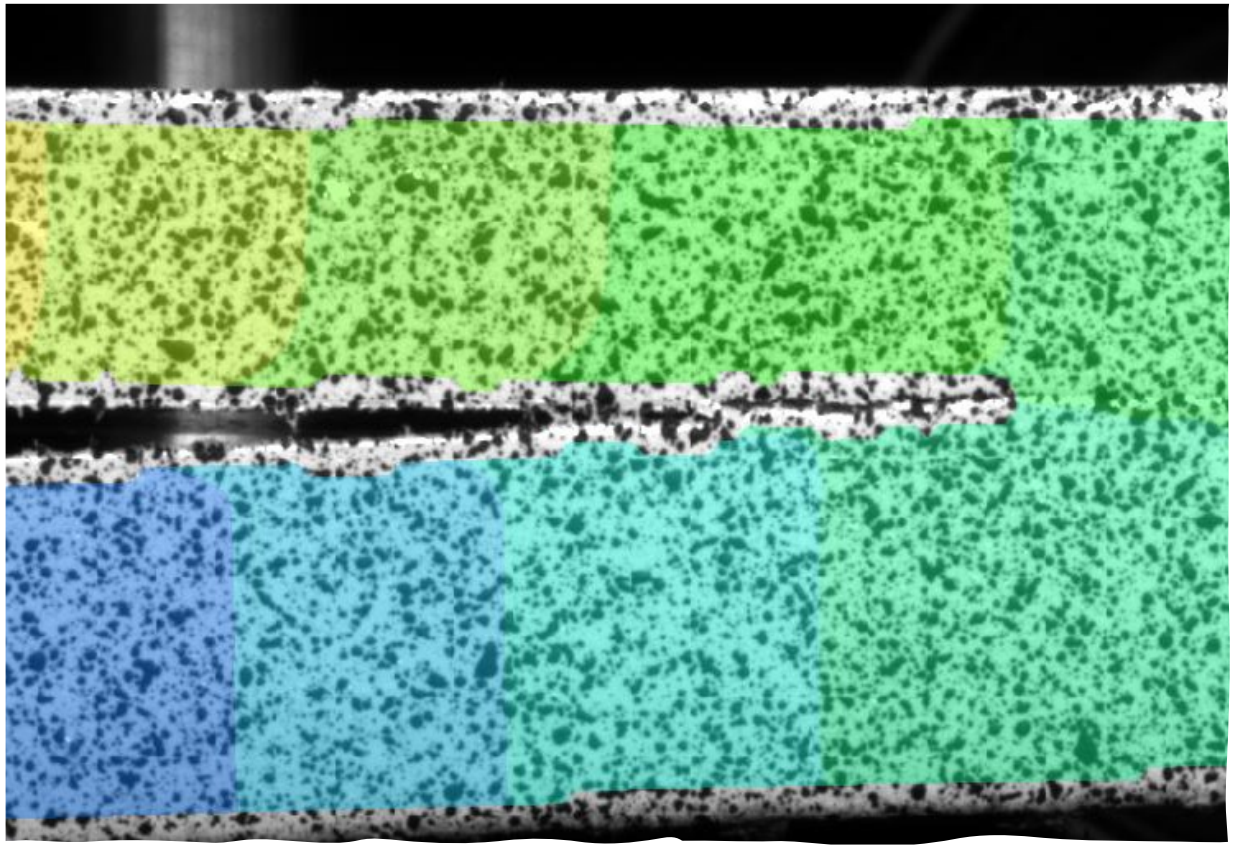

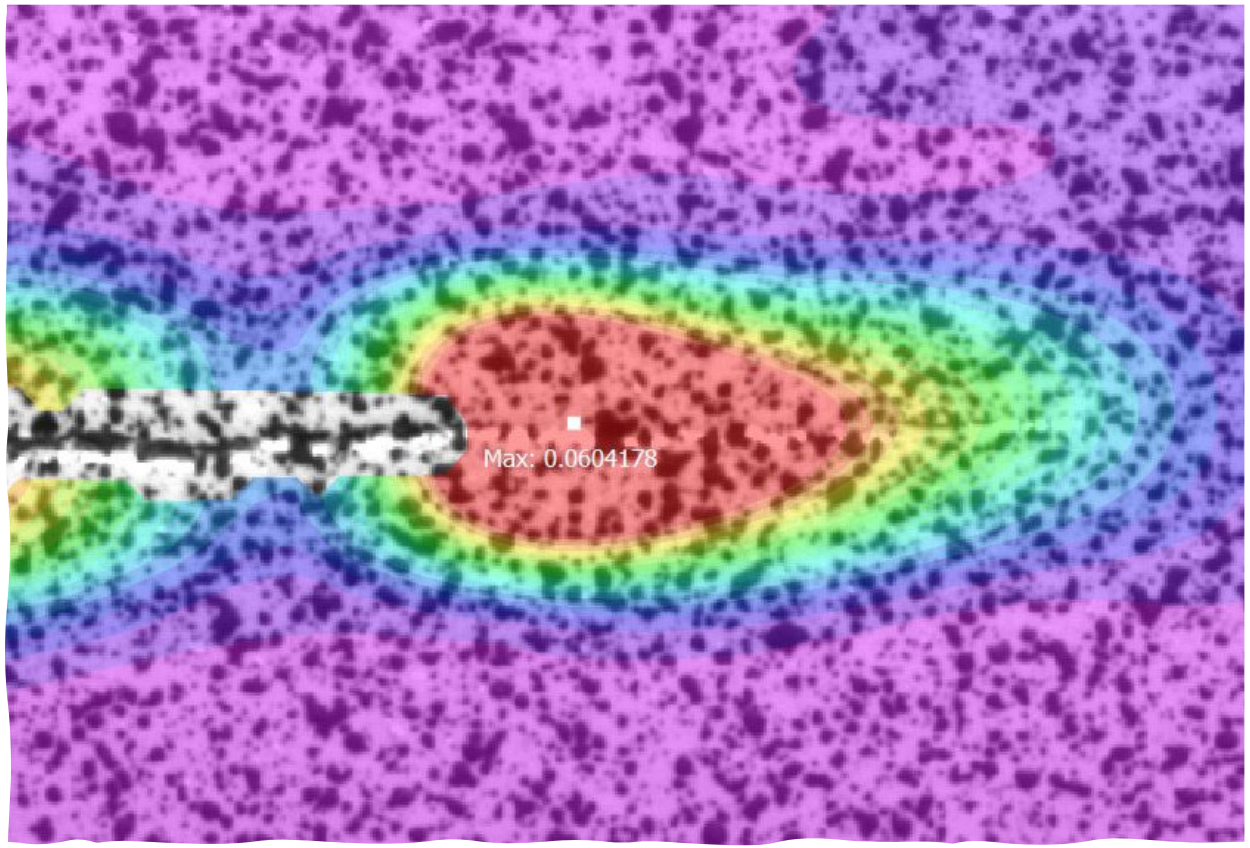

Damage monitoring

Measures needed (when fiber bridging)

$$\textbf{Modified beam theory: } G_I = \frac{3P\delta F}{2bM(a+|\Delta|)}$$

$$\boldsymbol{G_I} = \frac{3P\delta F}{2bM(a+|\Delta|)}$$

What is represented by this value? …

Total SERR!

***P**: Applied load*
***δ**: displacement*
***α**: crack length*
F: large displacement correction factor
M: load block correction factor
b: the specimen width and
$\lvert\Delta\rvert$: the effective delamination extension to correct for rotation of DCB arms at delamination front, as recommended in ASTM D5528

Fiber bridging and CZM

- At the presence of bridging (very common for composites fracture)

- $G_{total} = G_{tip} + G_{br} = G_{total} + \int_0^{\delta_{max}} \hat{\sigma}_b(\delta) d\delta$

- G_{tip} is the fracture toughness at initiation
- G_{br} is the contribution of bridging to G_{total}, expressed by the integral of the traction stresses,
- $\hat{\sigma}_b(\delta)$ on the crack planes with δ_{max} representing the COD at the end of the bridging zone.

J. Rice. A Path Independent Integral and the Approximate Analysis of Strain Concentration by Notches and Cracks J. Appl. Mech., 35 (1968), pp. 379-386

Fiber bridging and CZM

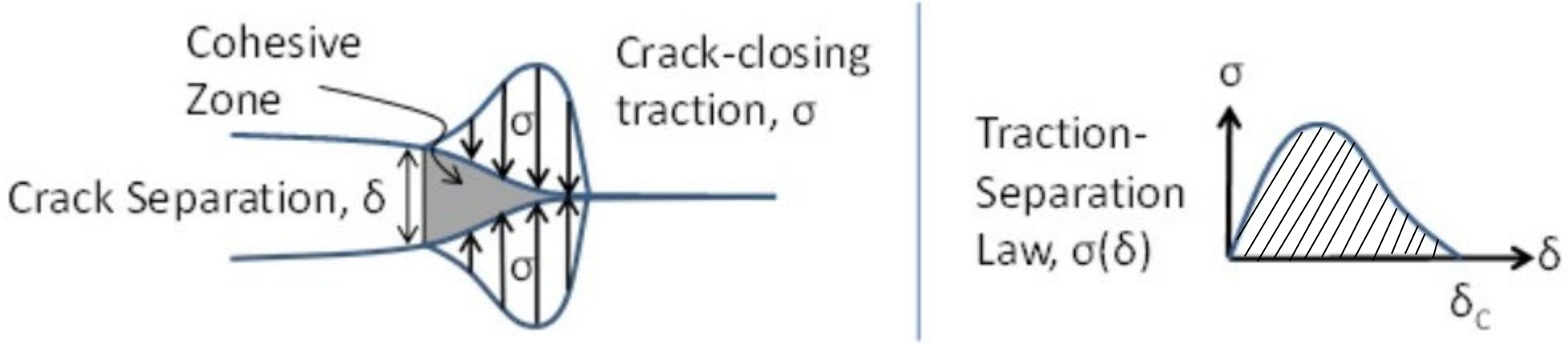

https://www.veryst.com/case-studies/cohesive-zone-model-czm-calibration

$$G_{br} = \int_0^{\delta_{max}} \hat{\sigma}_b(\delta) d\delta$$

Is SERR a material property?

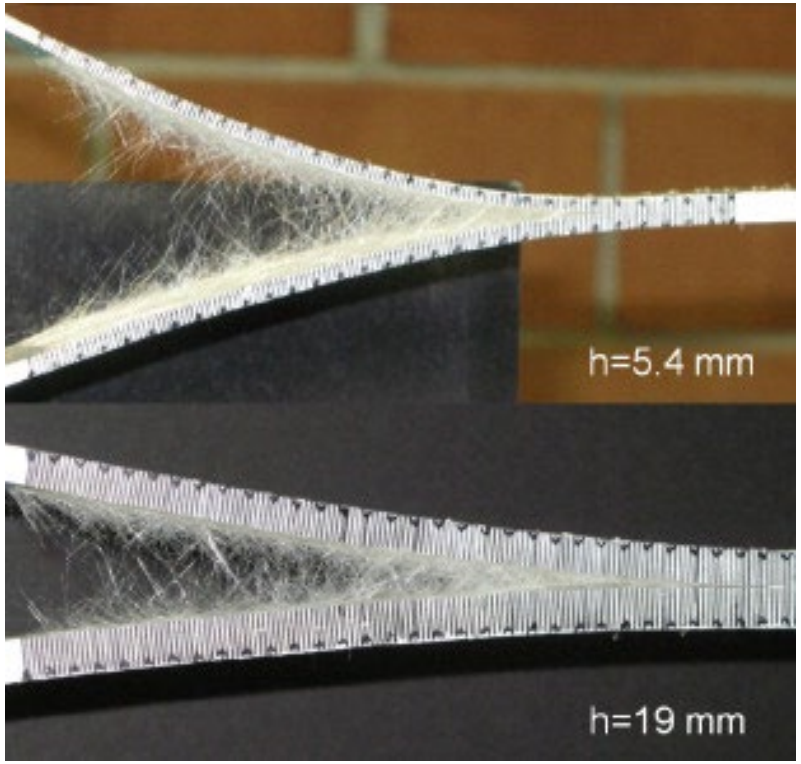

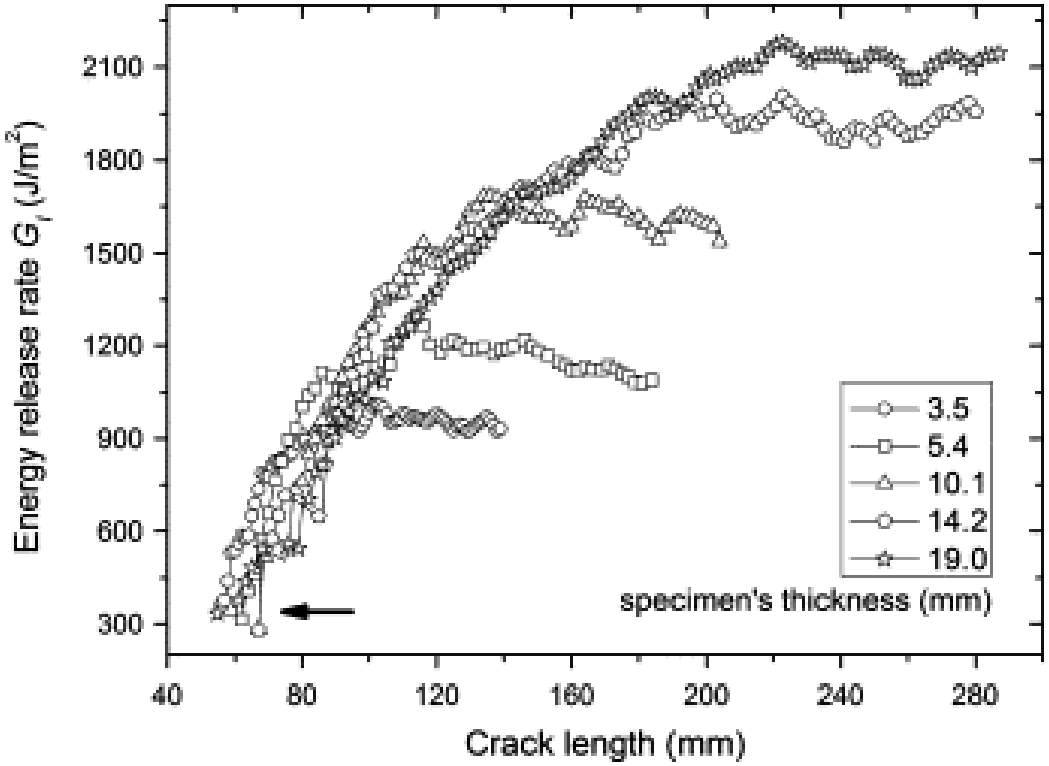

https://doi.org/10.1016/j.compscitech.2013.04.016

Is SERR a material property?

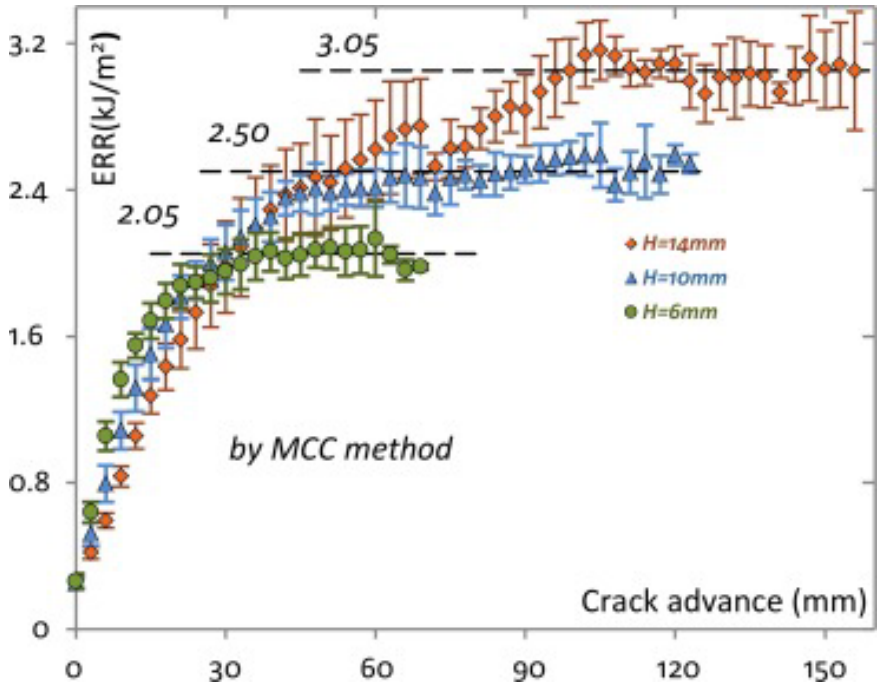

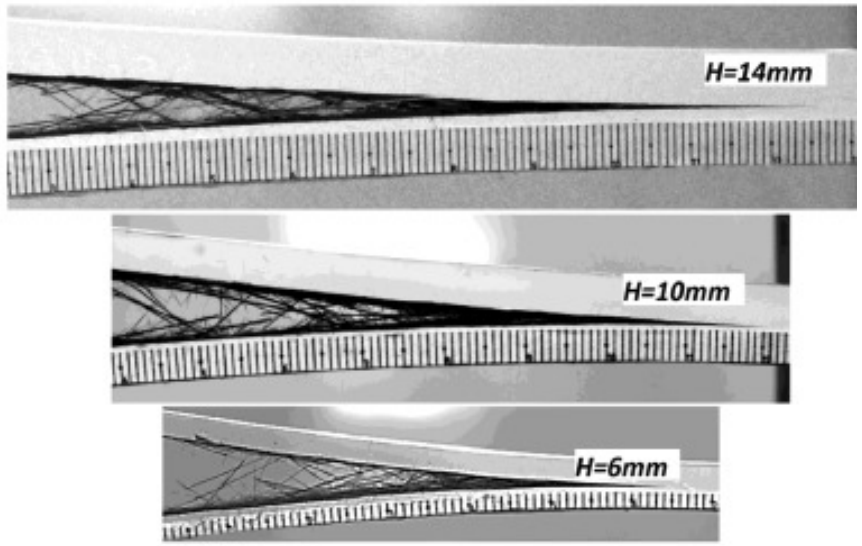

- R-curves depend on specimen thickness
- Steady state bridging zone increases with the thickness

https://doi.org/10.1016/j.ijsolstr.2016.02.007

Other modes of fracture

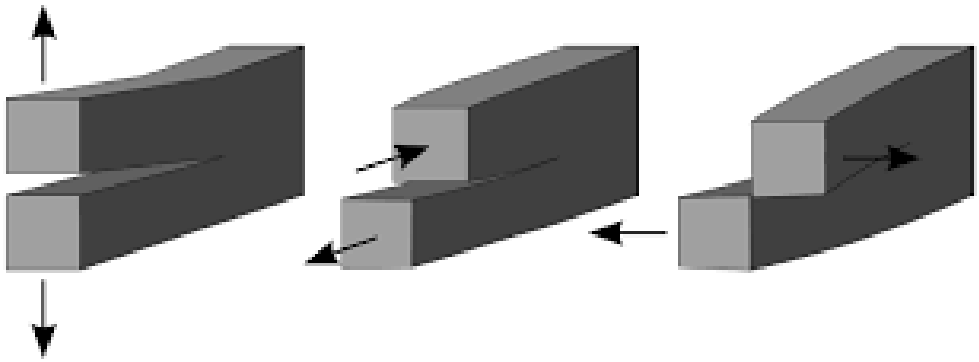

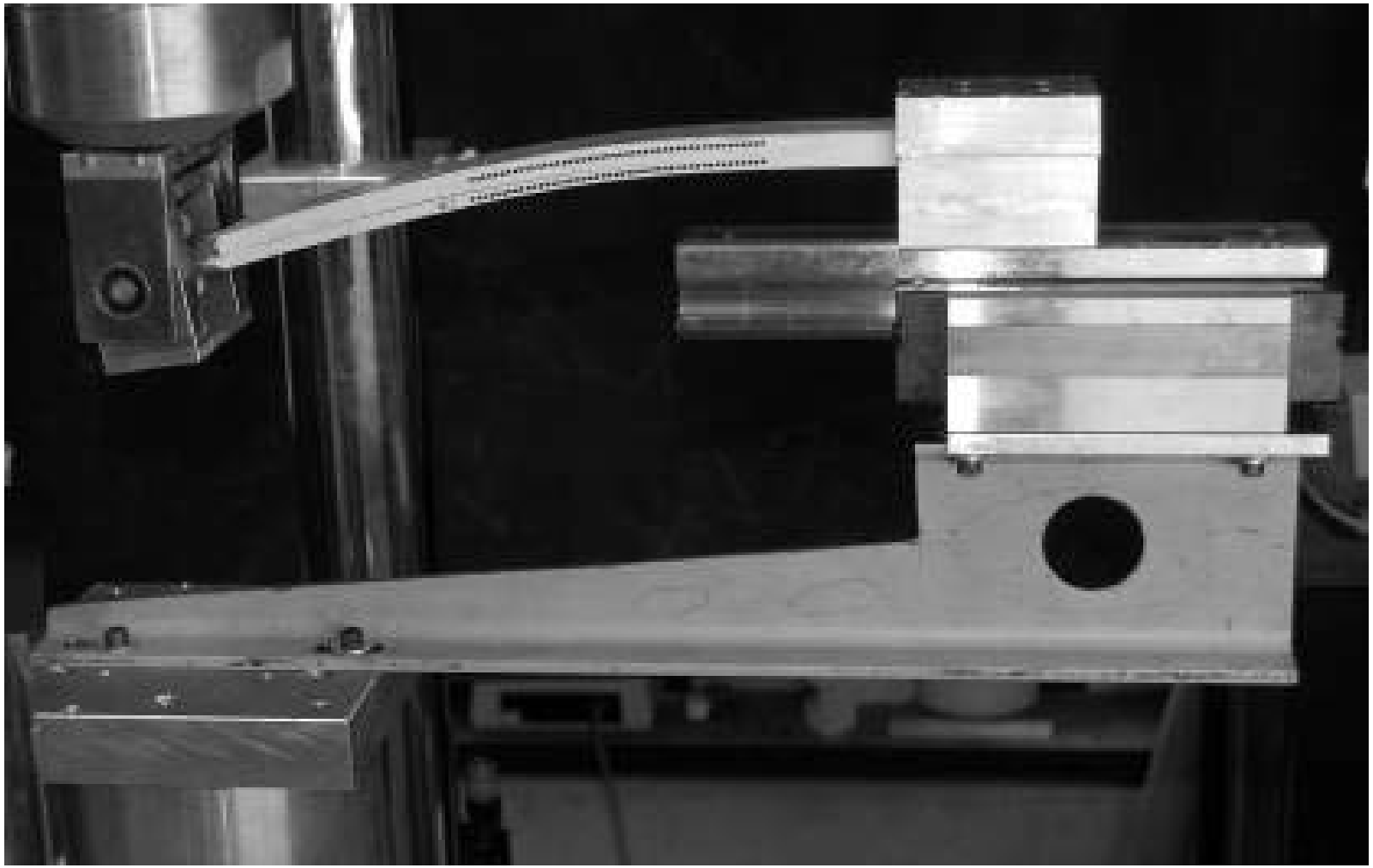

Mode II

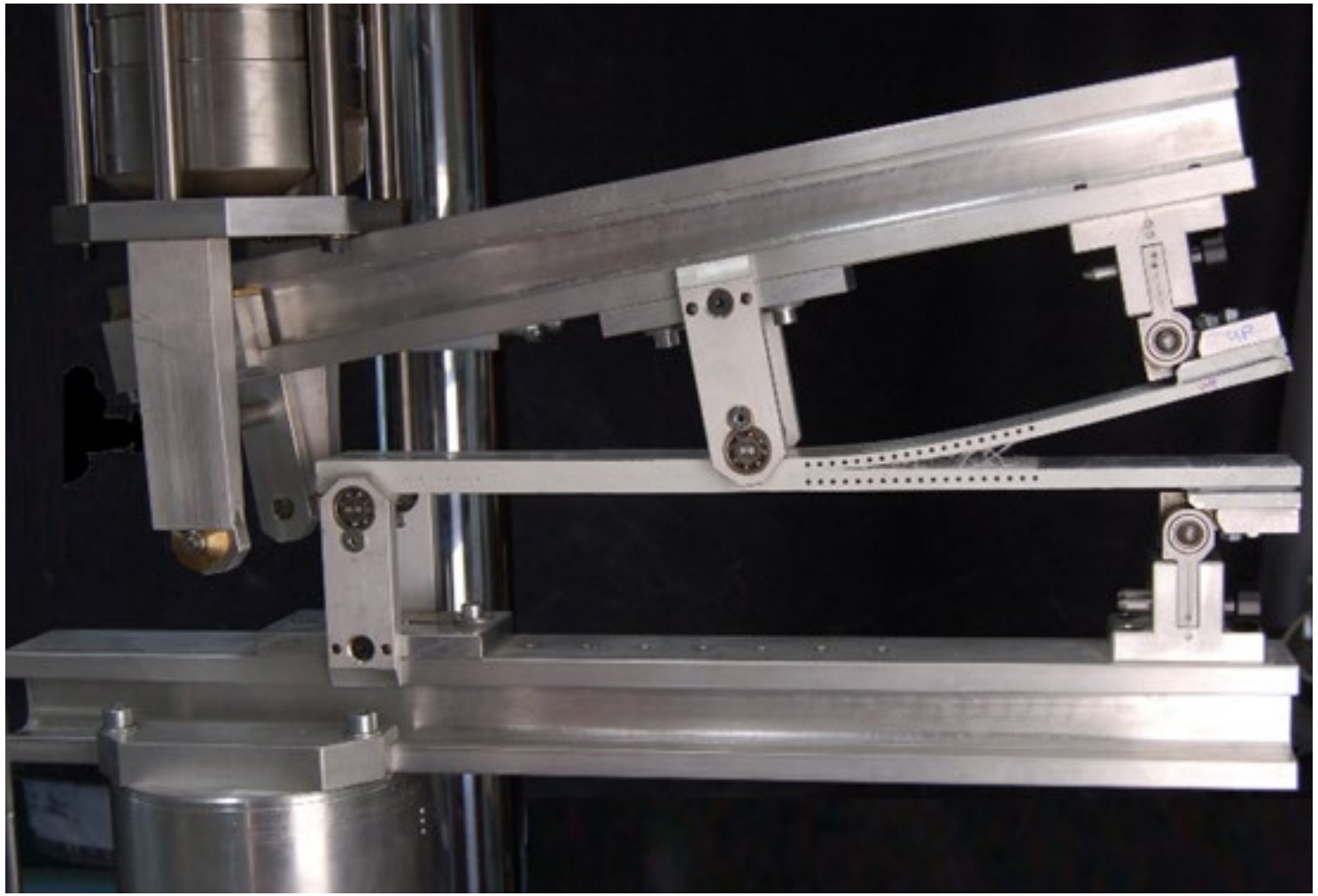

Mixed Mode I-II

Mixed mode set-up

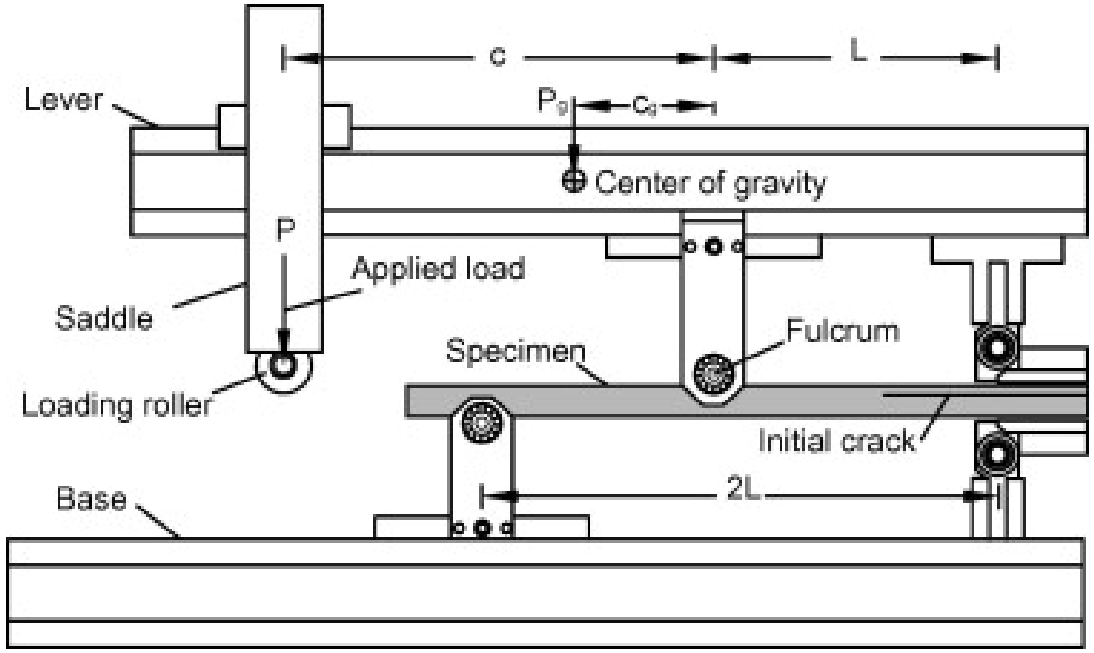

Free body diagram

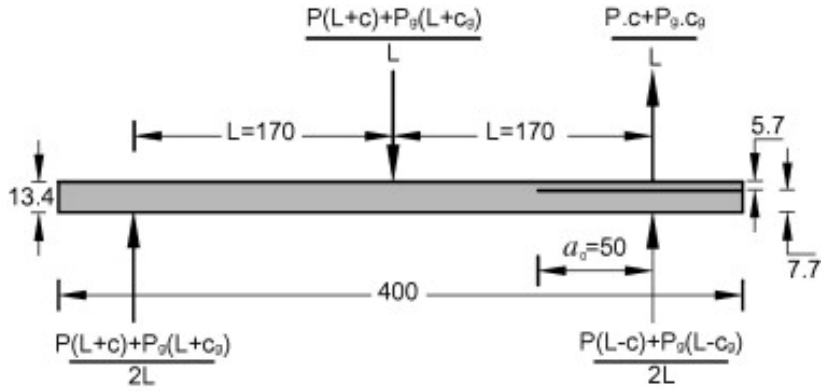

Mixed mode set-up

Free body diagram

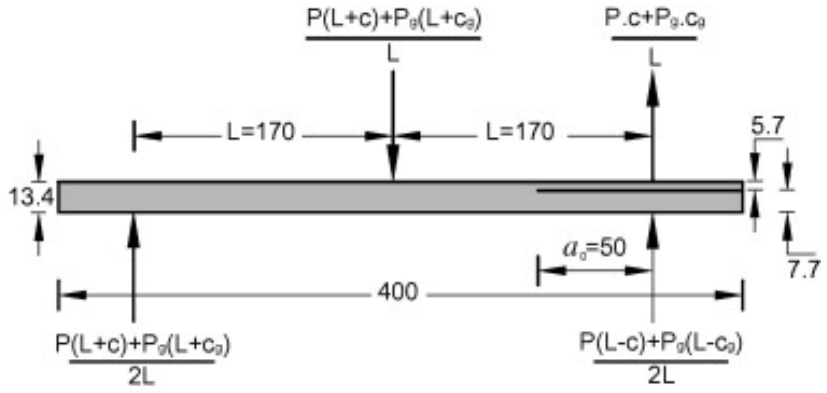

$$G_{\mathrm{I}} = \frac{[(2\psi+1)(Pc+P_{\mathrm{g}}c_{\mathrm{g}})-(P+P_{\mathrm{g}})L]^2}{8\psi\xi(1+\psi)BL^2(EI)_{\mathrm{eq}}}a^2$$

$$G_{\mathrm{II}} = \frac{[P(L+c)+P_{\mathrm{g}}(L+c_{\mathrm{g}})]^2}{8\xi(1+\psi)^2BL^2(EI)_{\mathrm{eq}}}(1+\psi-\xi(1+\psi)^2)a^2$$

With: $\psi = \frac{(EI)_{\mathrm{eq2}}}{(EI)_{\mathrm{eq1}}}, \xi = \frac{(EI)_{\mathrm{eq1}}}{(EI)_{\mathrm{eq}}}$

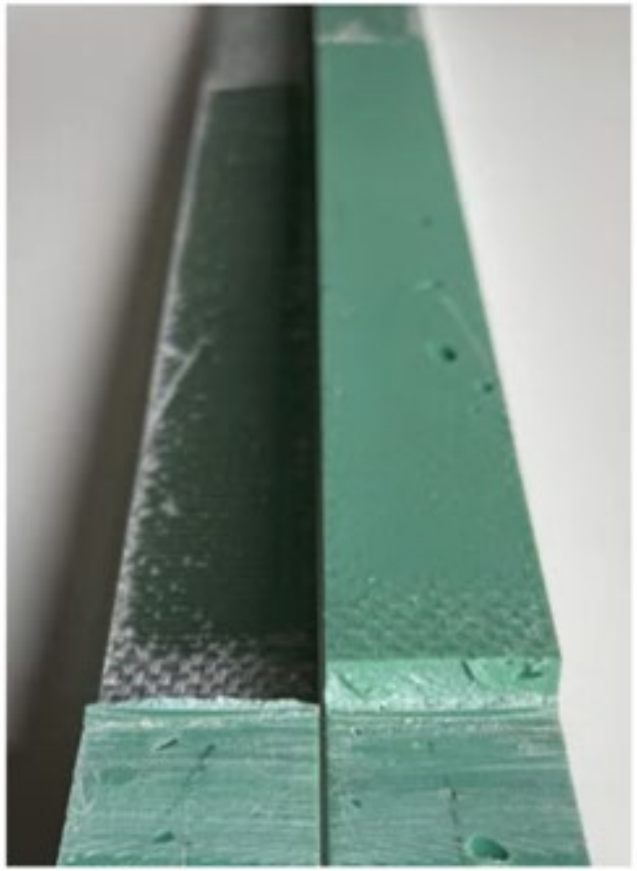

Mode I

Mode III

Mode III

PhD Thesis, Ali Shivaie Kojouri, VUB, 2025

Micromechanics

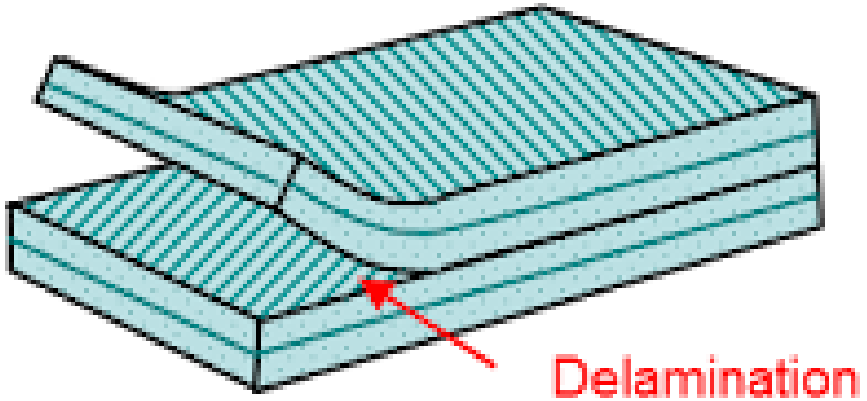

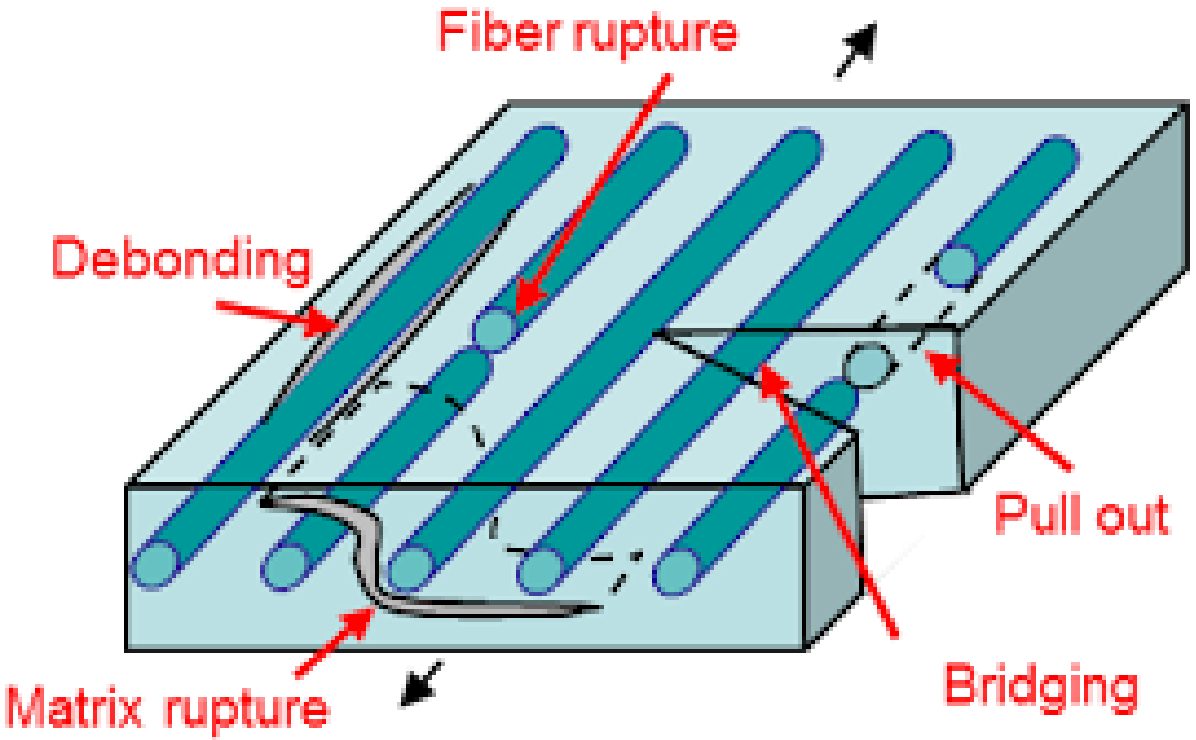

http://www.ltas-cm3.ulg.ac.be/FractureMechanics/?p=Lecture6_P4

Intralaminar and translaminar cracks

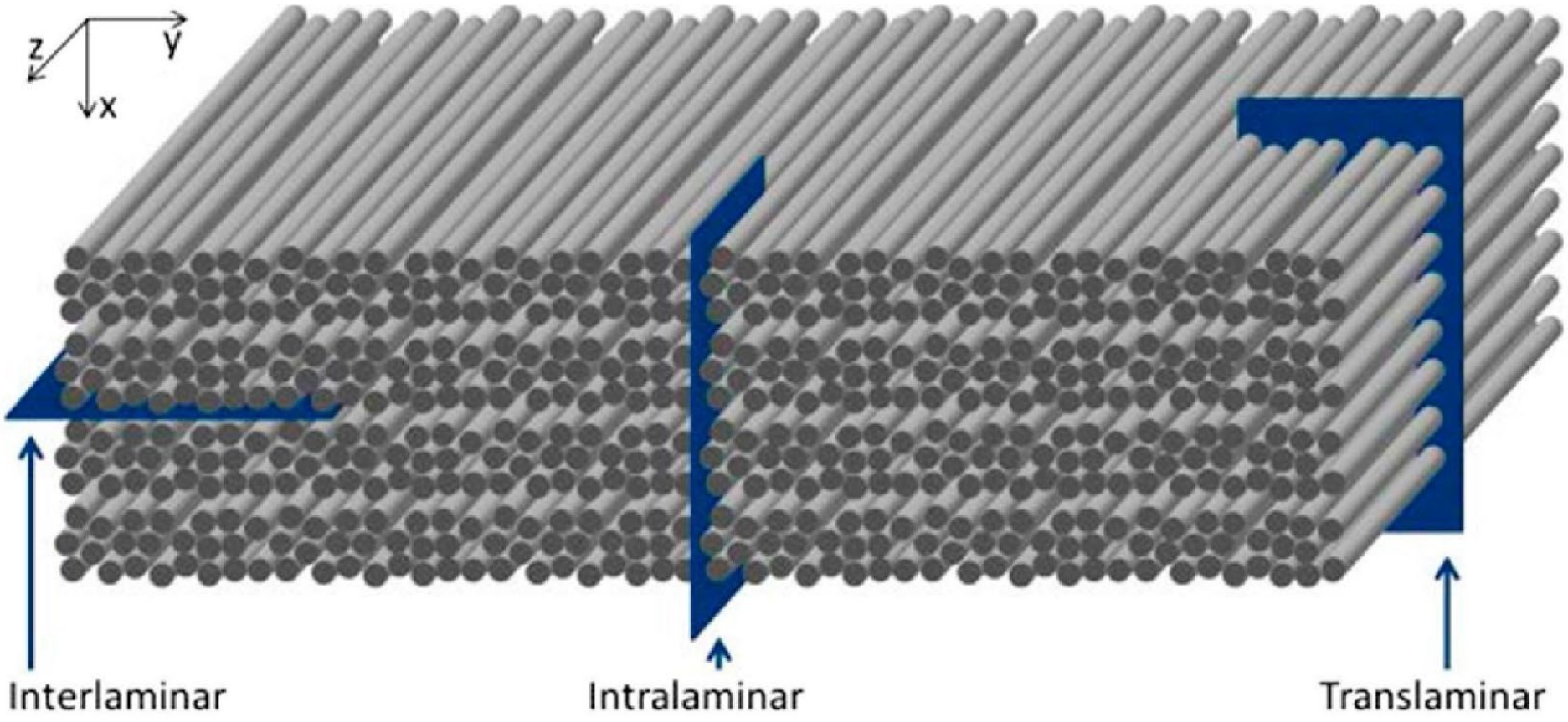

https://doi.org/10.1016/j.compositesa.2018.03.001

2D fracture

Traditional fracture analysis?

Delamination in real structures

- Two-dimensional (2D) crack propagation

Decomposition

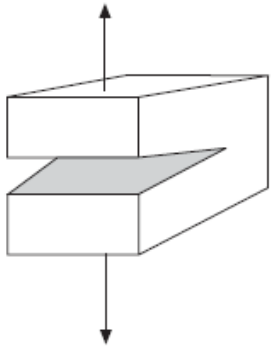

Mode I (opening)

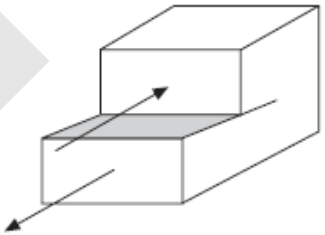

Mode II (sliding shear)

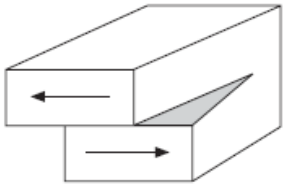

Mode III (tearing shear)

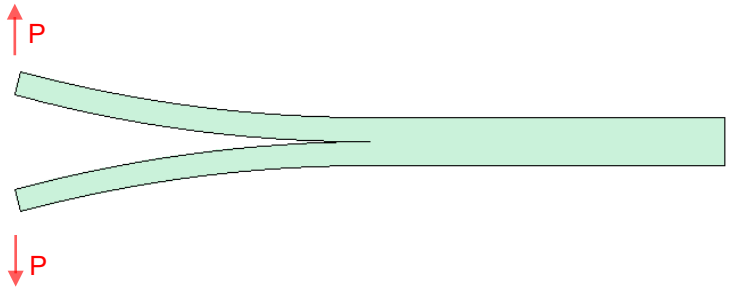

ISO 15024:2001 – Double cantilever beam (DCB) test

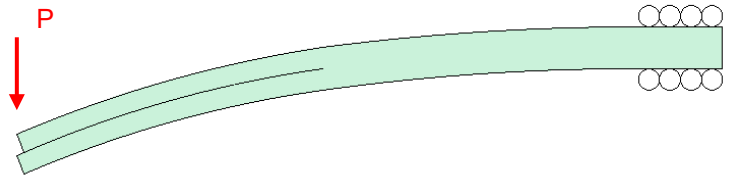

ISO 15114:2014 – End-loaded split (ELS) test

- One-dimensional (1D) crack propagation
- Constant crack width (beam width)
- Free boundary at cracked ends

?

From coupon to structure


Avançon bridge, Switzerland, 2012

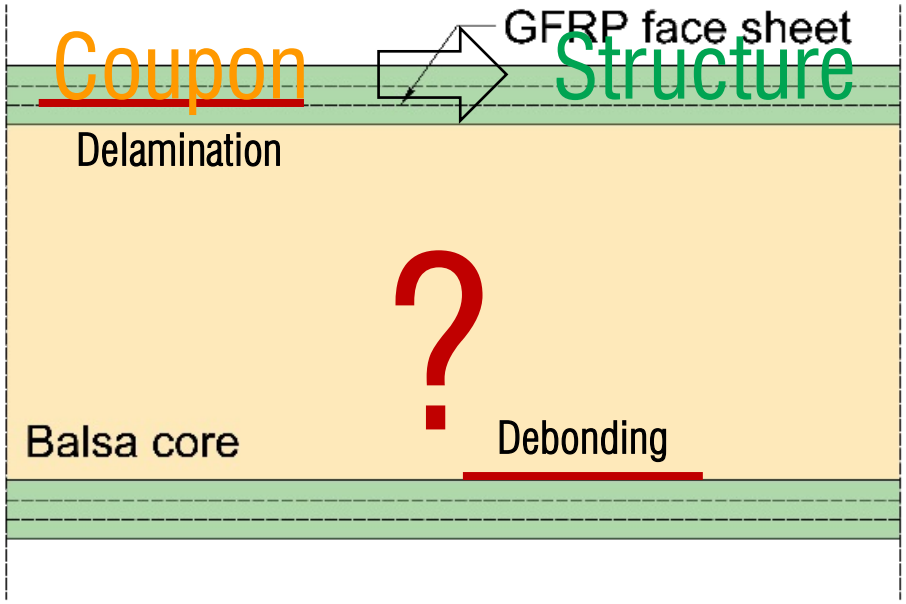

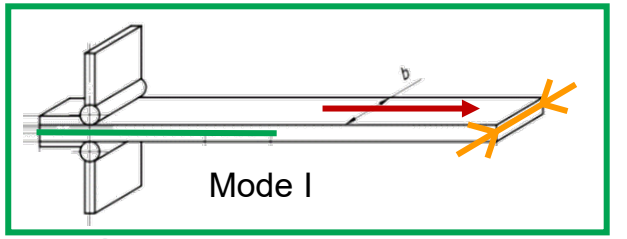

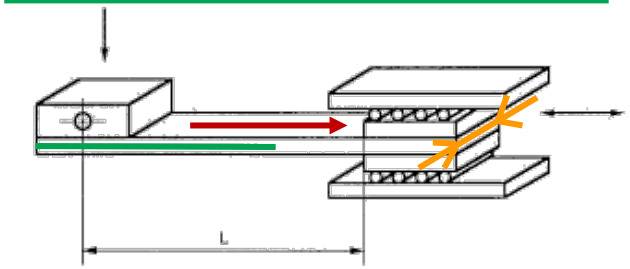

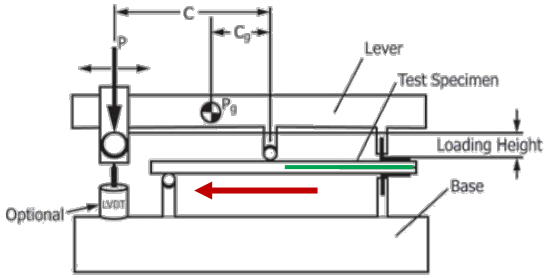

In the past...Mode I 2D opening

EXPERIMENTAL DETERMINATION OF INTERLAMINAR G_{Ic} USING A FULLY EMBEDDED CENTRE-CRACKED SPECIMEN

P. KUMAR† and S. R. REDDY

Engineering Fracture Mechanics Vol. 59, No. 2, pp. 183–189, 1998

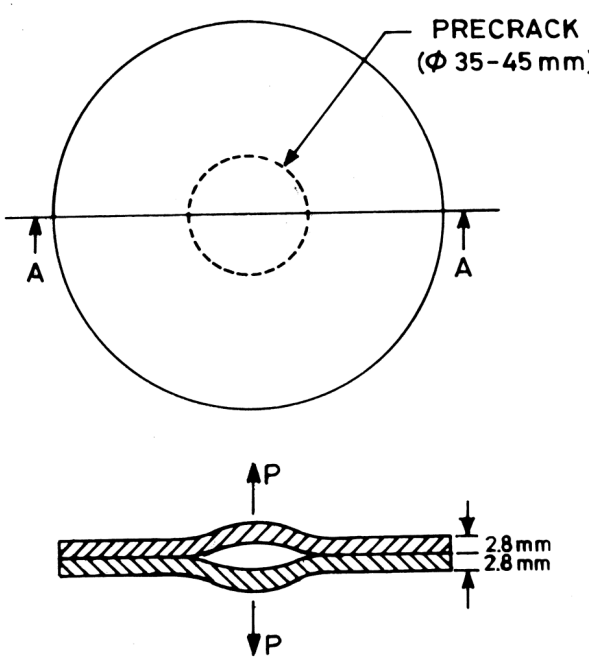

Fig. 1. Plate specimen with a circular crack.

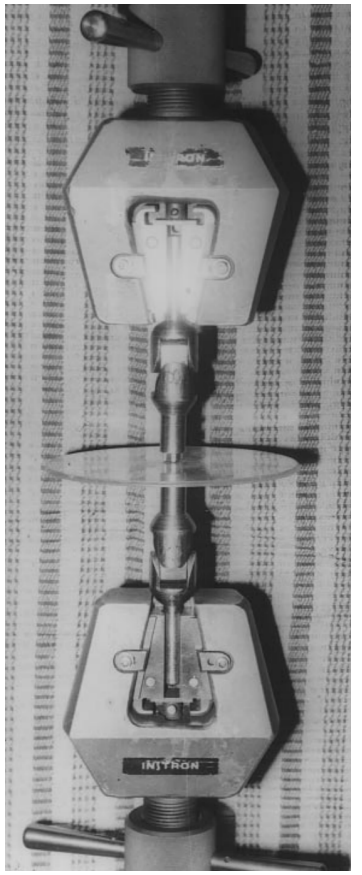

- Modeling of G: Theoretical formulation neglecting geometrical non-linearities
- G (2D) was estimated to be ~33% lower than that estimated from DCB (1D) tests

In the past... panels with central hole

A.T. Rhead et al. / Composite Structures 171 (2017) 326–334

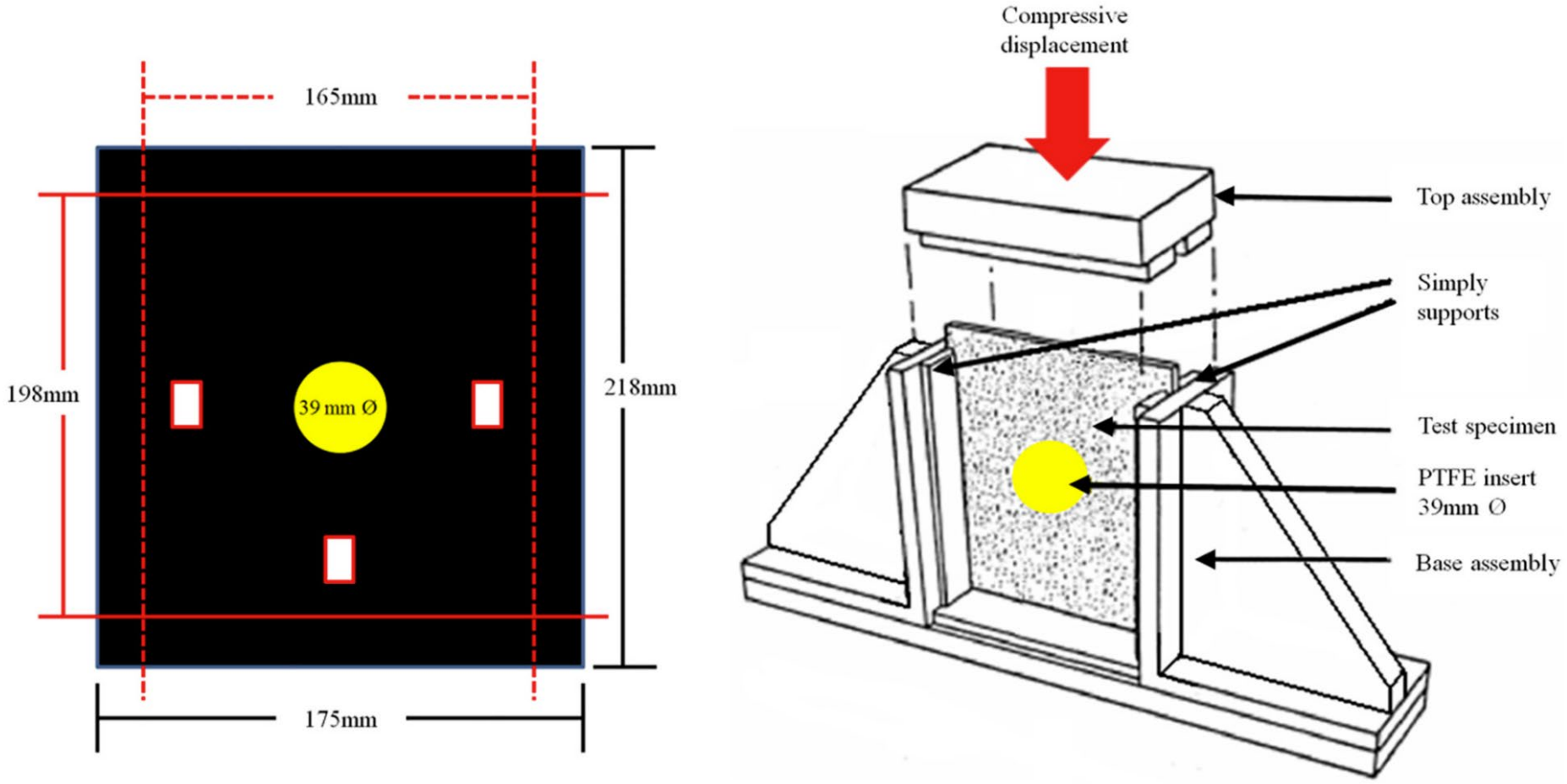

Fig. 1. Test fixture and panel dimensions for testing of laminates unrestrained against global buckling.

In the past...buckling/growth in stiffened panels

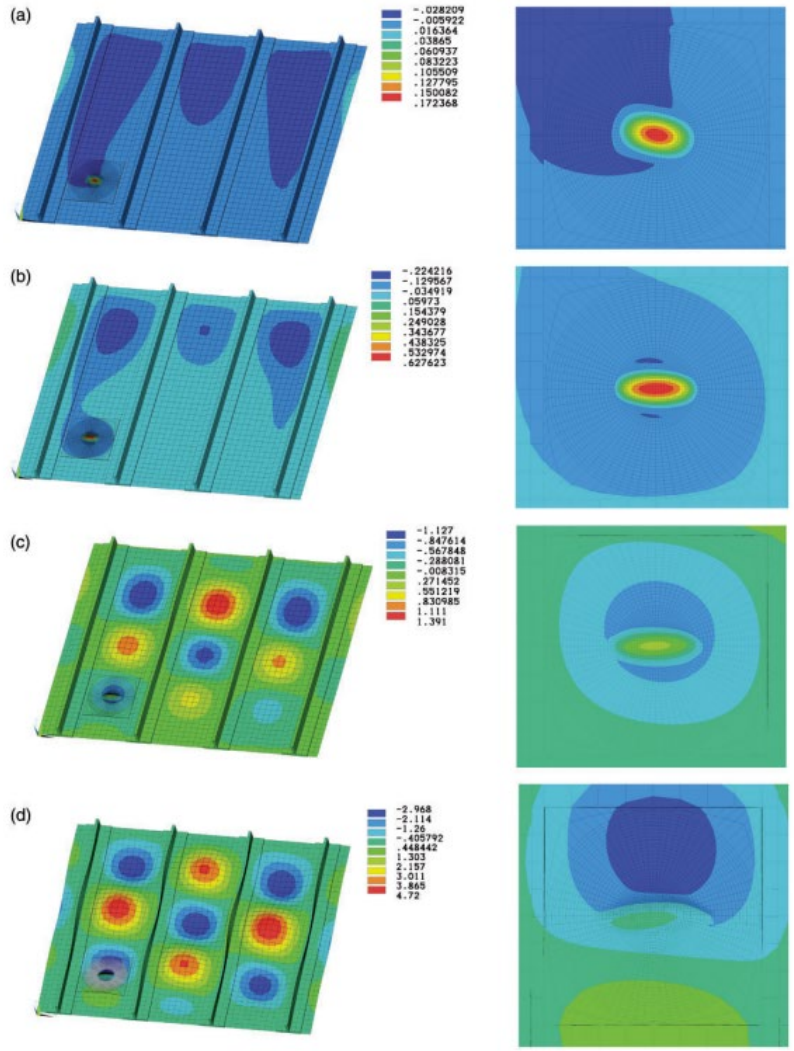

Figure 9. Deformed shapes at: (a) local delamination buckling (69 kN), (b) delamination growth initiation (279 kN), (c) global buckling (390 kN), (d) last available step (571 kN).

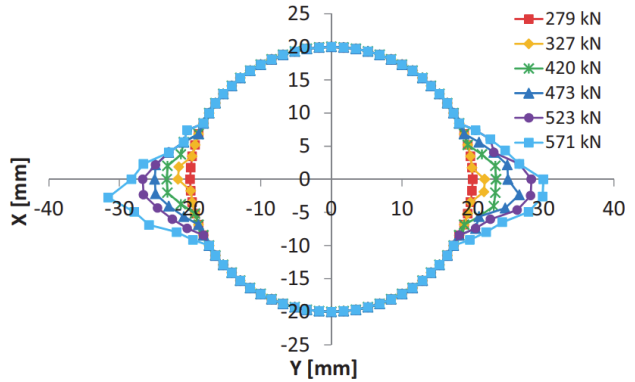

Figure 12. Delamination front shapes at different load steps.

Article

JOURNAL OF COMPOSITE MATERIALS

Journal of Composite Materials
2014, Vol. 48(23) 2857–2870

DOI: 10.1177/0021998313502742
jcm.sagepub.com
SAGE

Delaminations buckling and growth phenomena in stiffened composite panels under compression. Part II: a numerical study

A Riccio[1], A Raimondo[1], F Di Caprio[2] and F Scaramuzzino[1]

Wide single lap shear joints (WSLS)

Aircraft fuselage longitudinal joint

Low velocity impacted CFRP WSLS joint

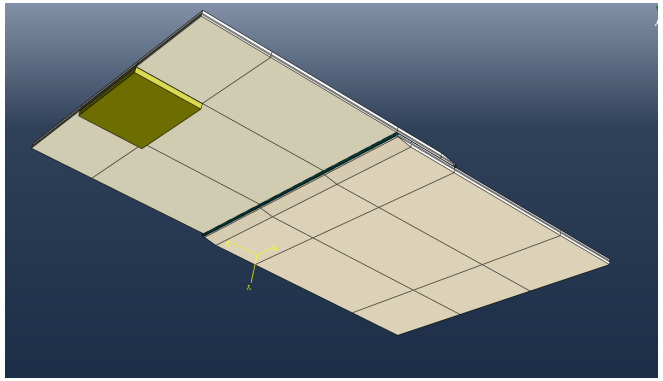

Modelling the joint in Abaqus®

Work with **ZHAW** and **Airbus, Germany.**
Wide single lap shear joints (WSLS): Element level testing of aircraft fuselage joints/ repairs
CFRP adhesive joints: Impacted, water and ice, under fatigue loading.

Two-dimensional delamination

Experimental investigation

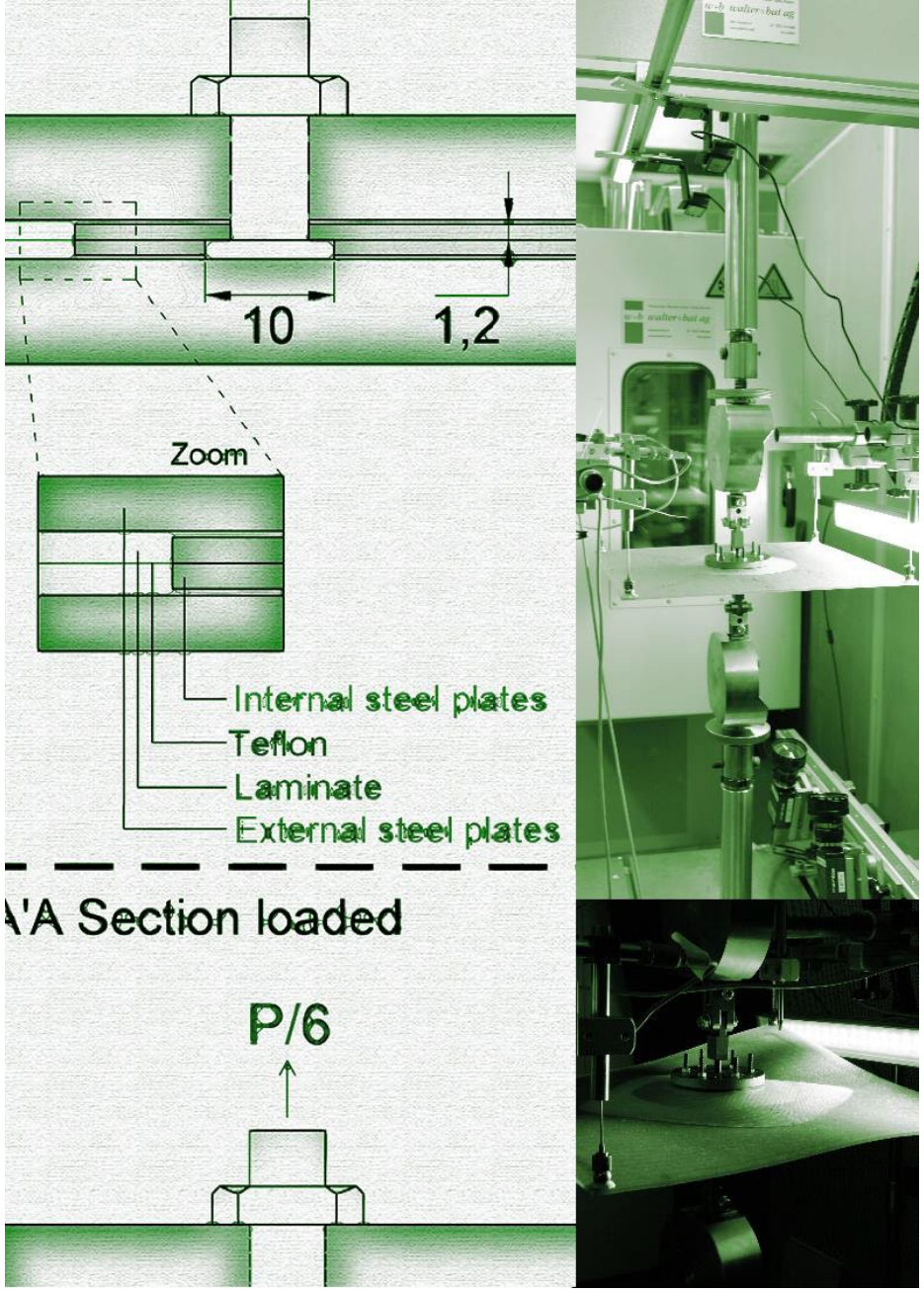

Two-dimensional crack growth in FRP structures, PhD Thesis, Aida Cameselle Molares, EPFL, 2019

Experimental investigation

Glass fiber and epoxy matrix
E-glass and E-CR glass

6 fiber architectures

12 laminated plates

Resin infusion method

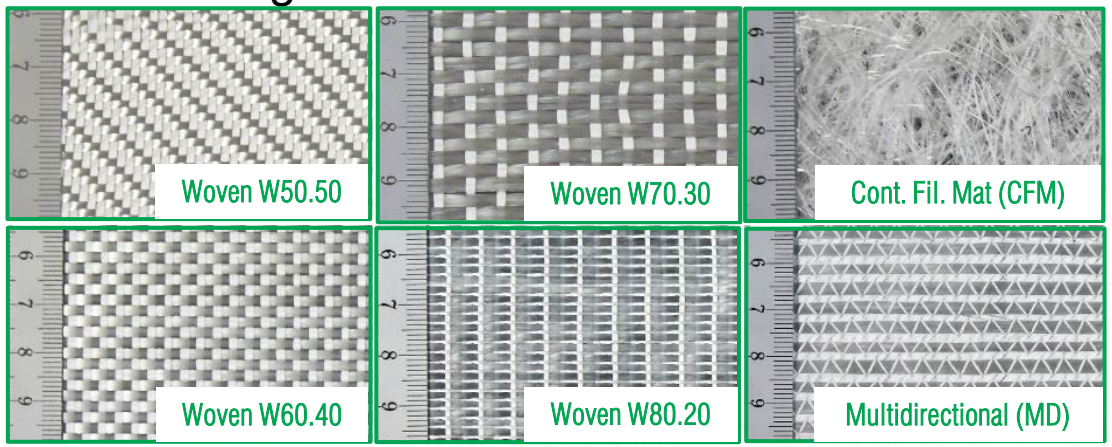

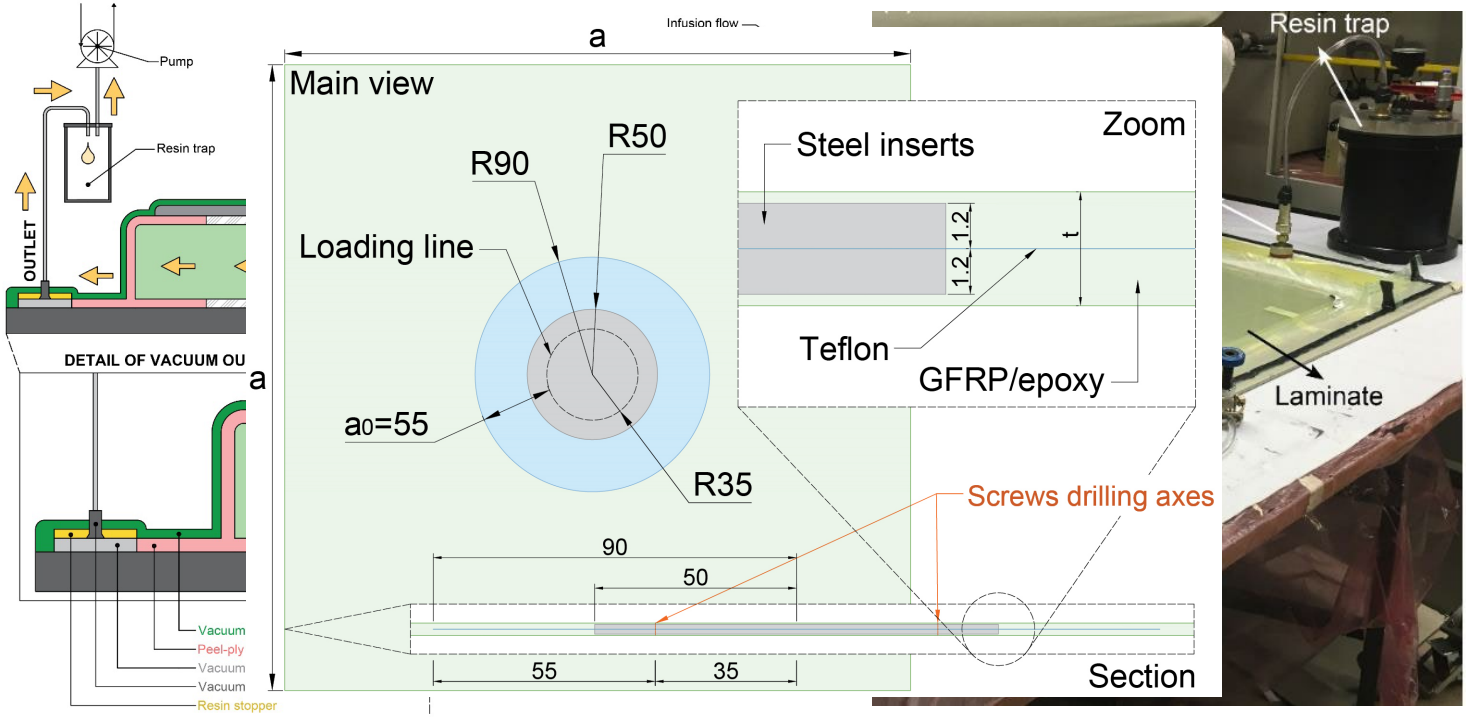

Experimental investigation

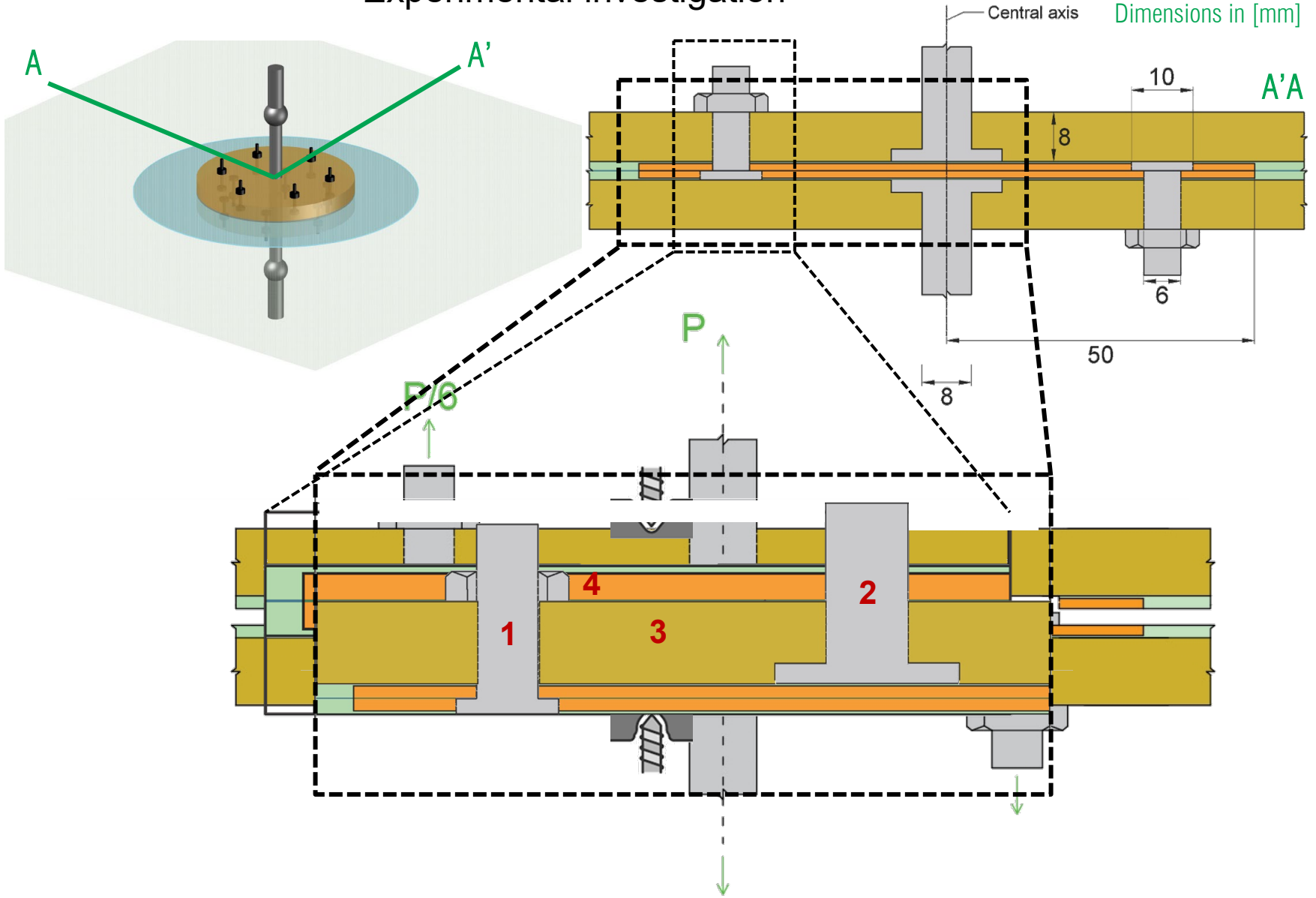

Experimental investigation

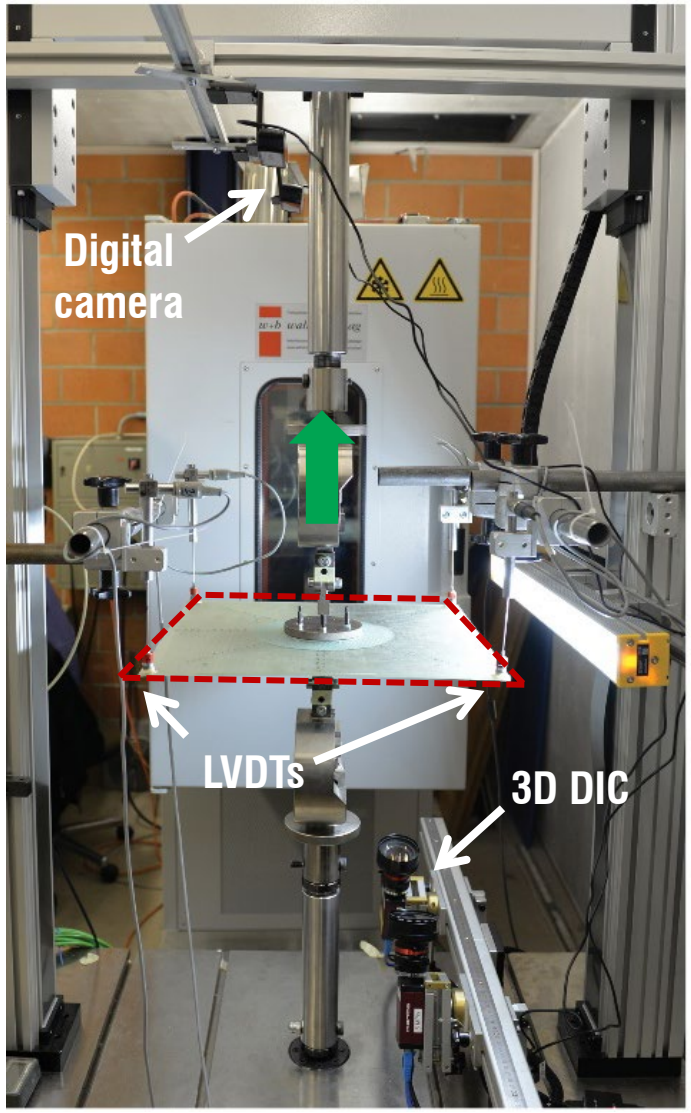

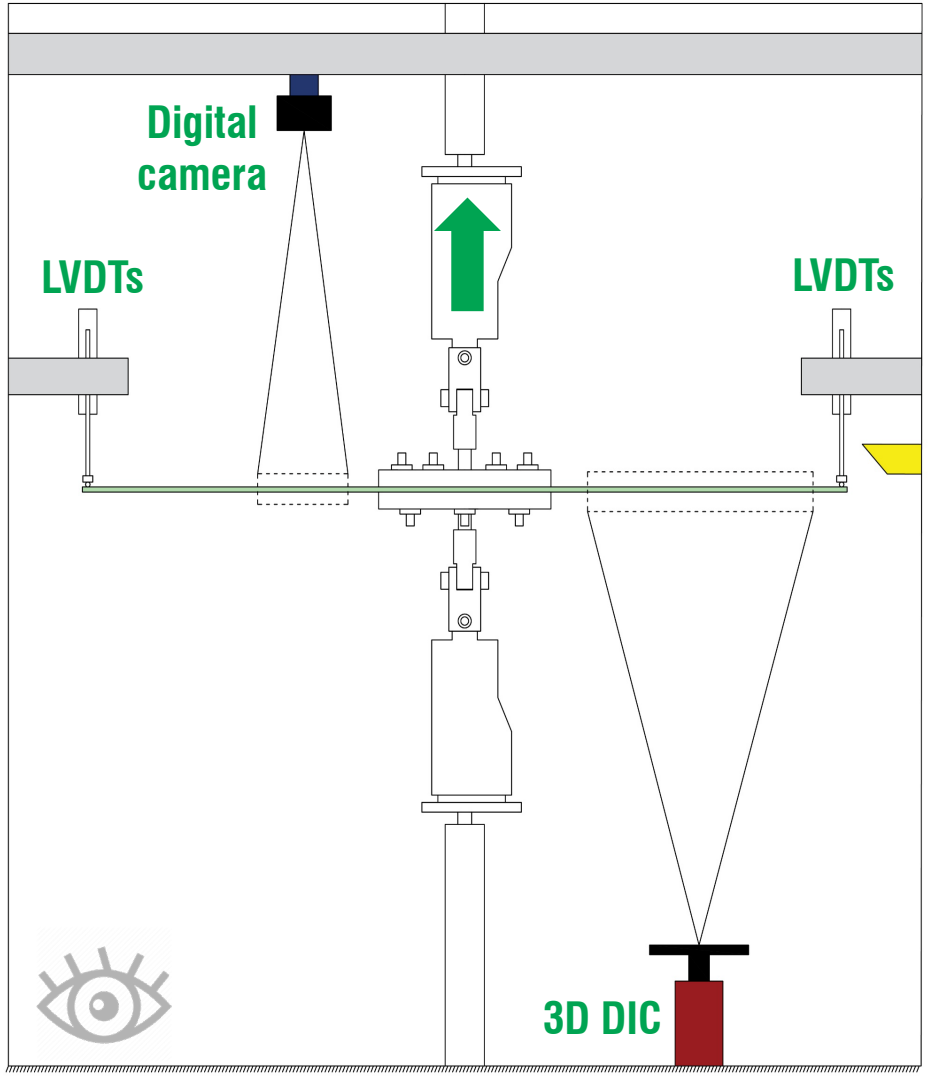

Load and crack-displacement responses and crack pattern

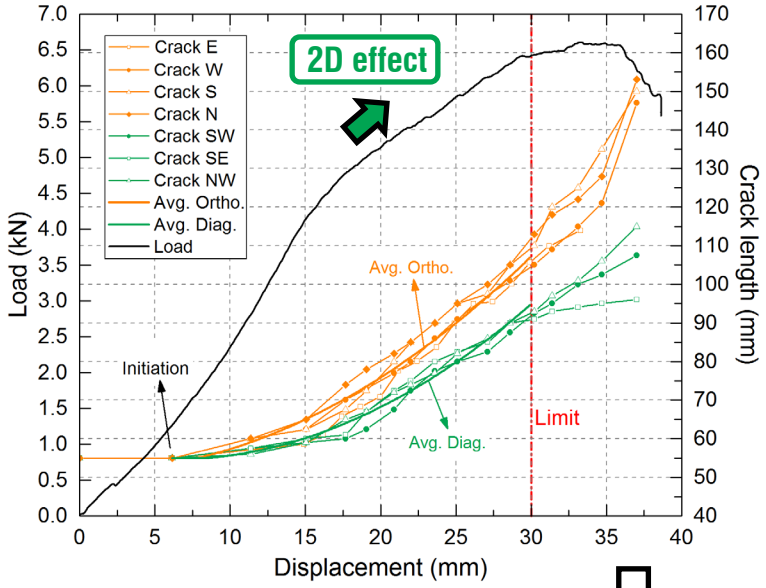

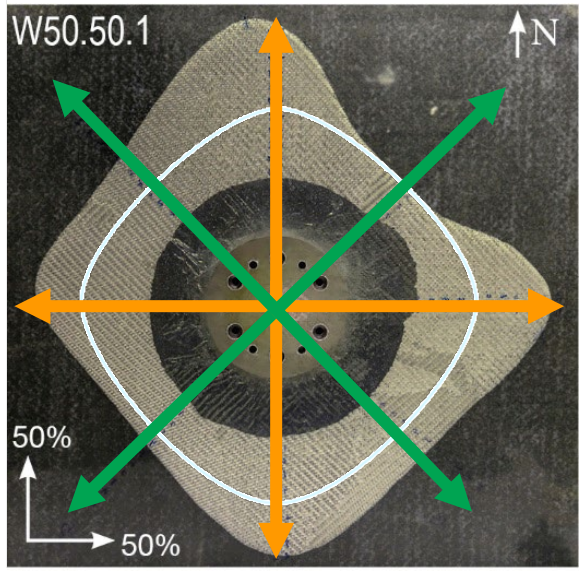

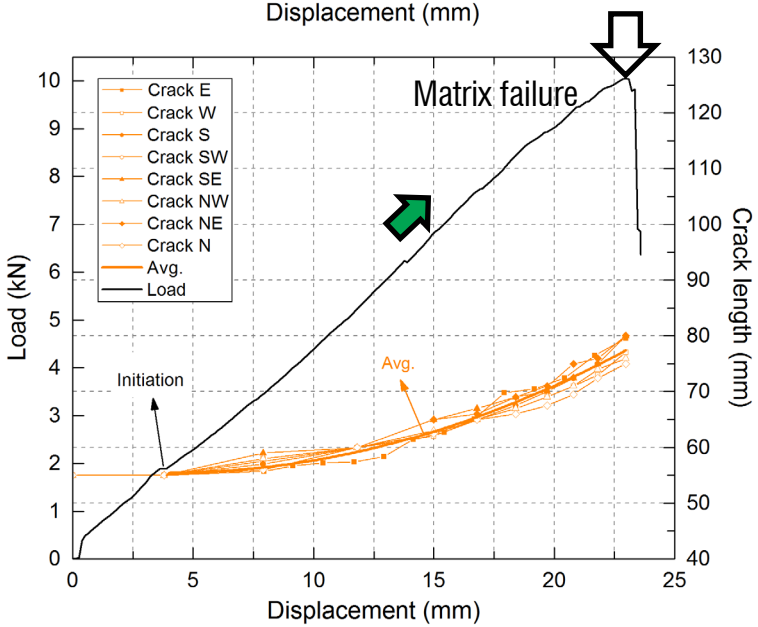

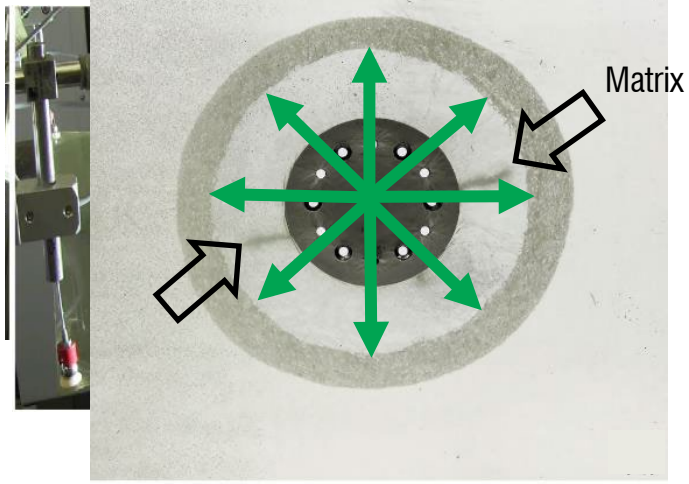

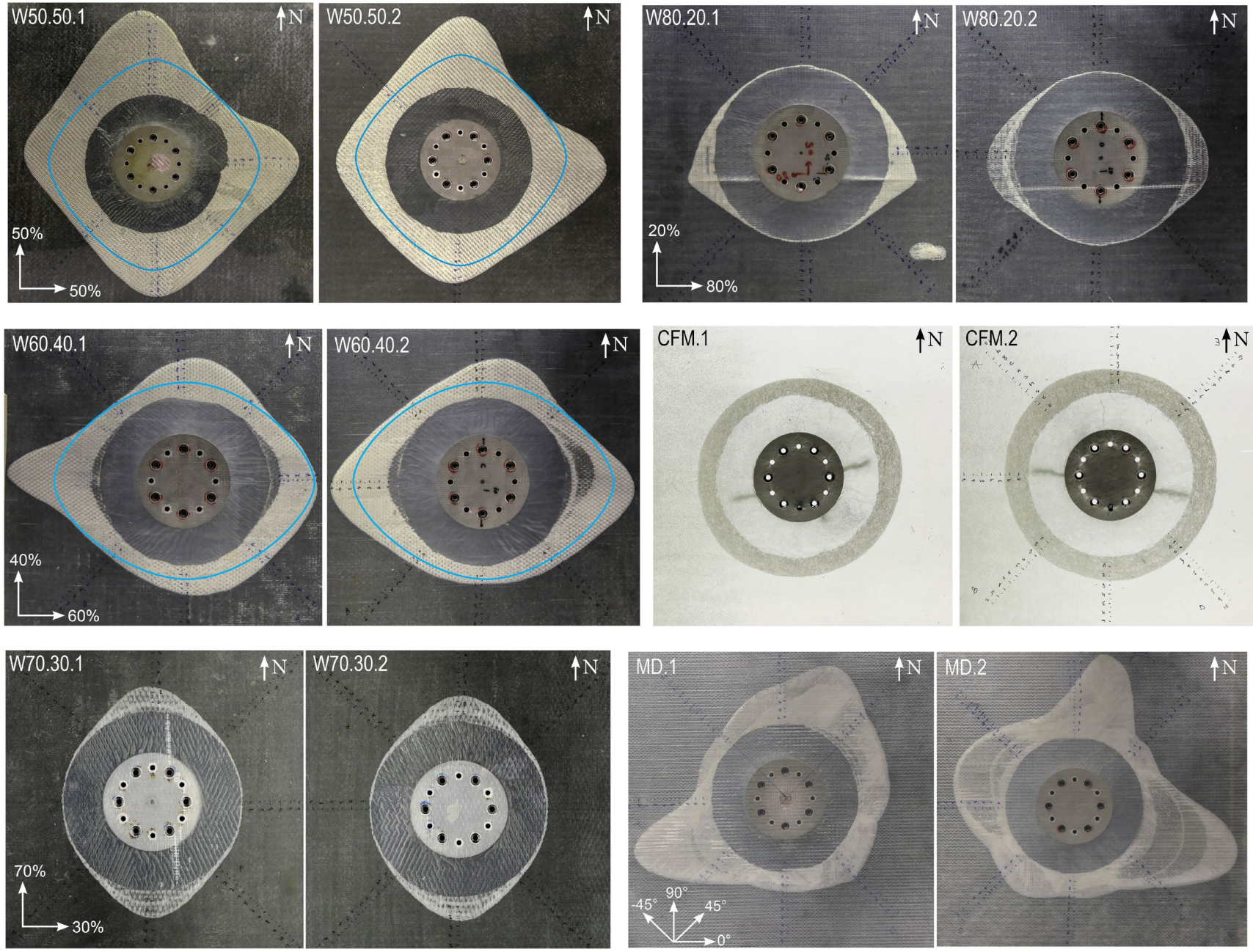
W50.50.1
N
50%
50%
W50.50.2
N
W80.20.1
N
20%
80%
W80.20.2
N
W60.40.1
N
40%
60%
W60.40.2
N
CFM.1
N
CFM.2
N
W70.30.1
N
70%
30%
W70.30.2
N
MD.1
N
90°
-45°
45°
0°
MD.2
N

Compliance-crack area responses

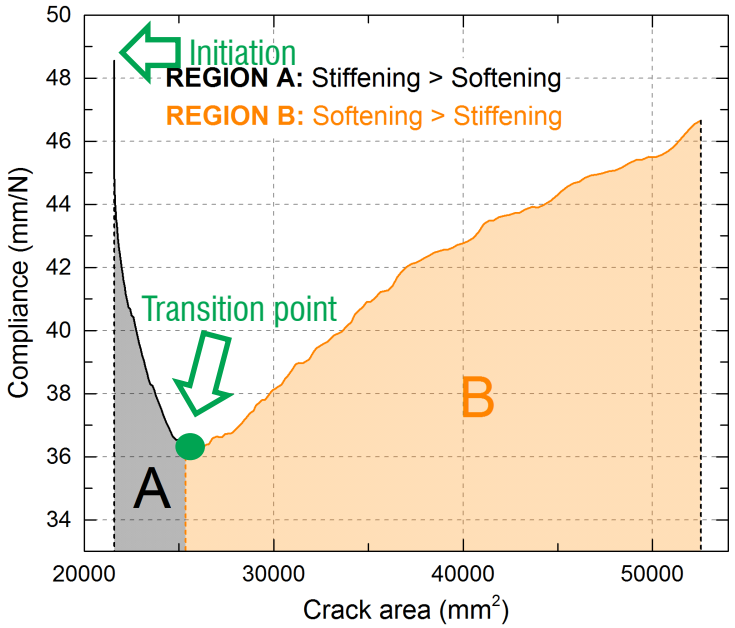

W50.50.1

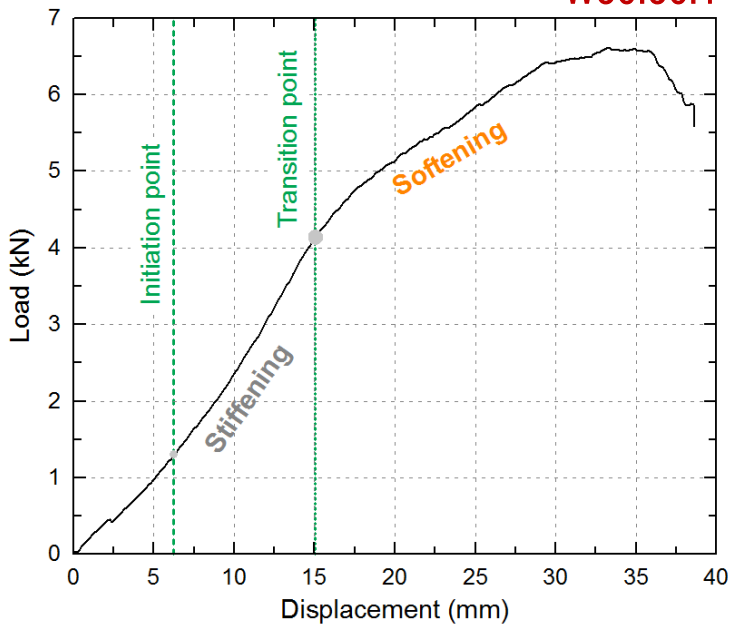

Stiffening mechanisms

Stretching → Stress stiffening

Fiber-bridging

→ **2D effect** not revealed in 1D fracture experiments

→ **Similar behavior in all plates**

✗ Compliance-based fracture data reduction methods

Two-dimensional Mode-I delamination

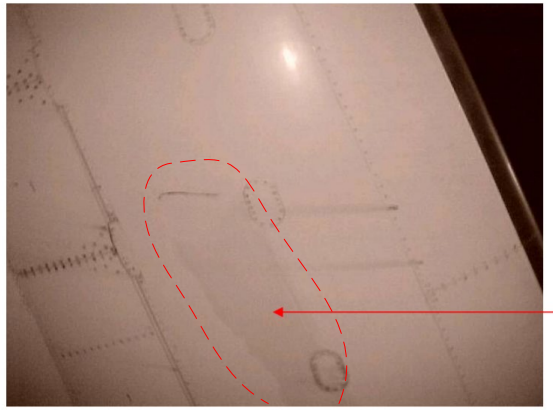

Example of impact damage on Airbus A330 after horizontal stabilizer accident

Background

- Fracture in composites in real scenarios is usually two-dimensional (2D)

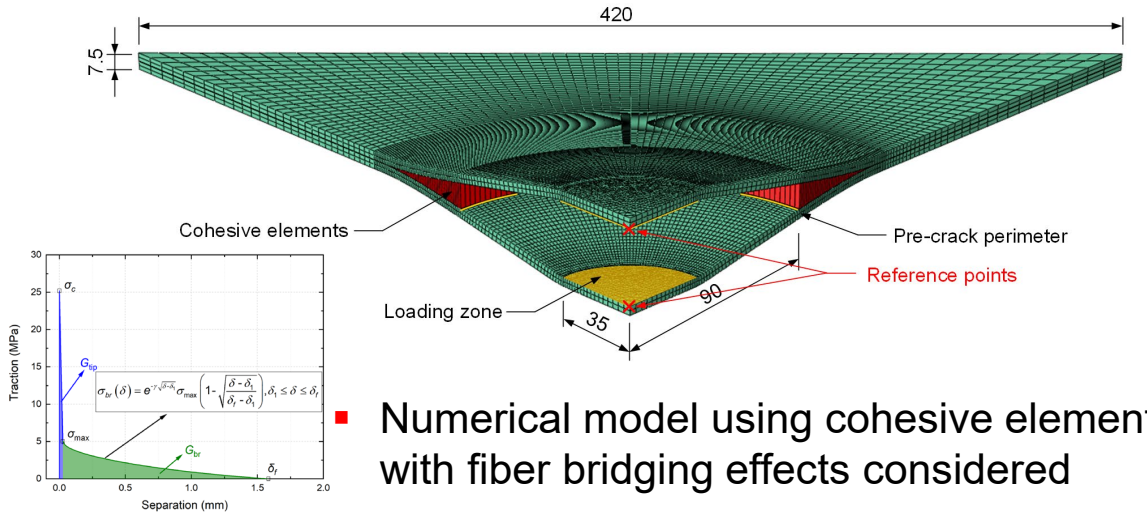

- Numerical model using cohesive elements with fiber bridging effects considered

Numerical investigation of 2D Mode-I delamination

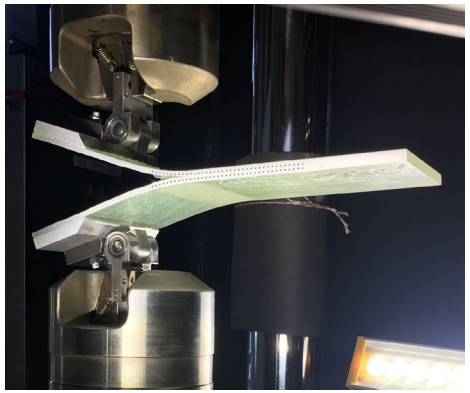

vs

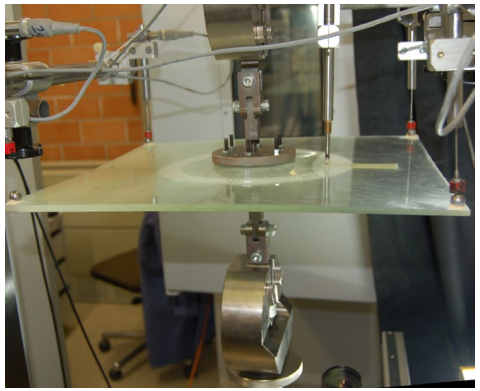

(a) DCB (Gtot=2.0 kJ/m2) (b) 2D (Gtot=2.8 kJ/m2)

Experimental investigation of 2D Mode-I delamination

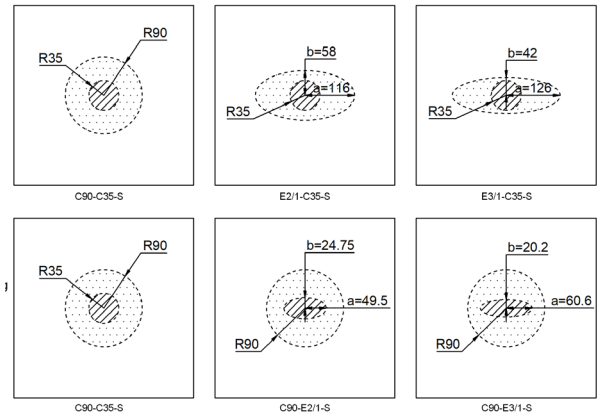

… …

Effects of:

- Pre-crack size
- Pre-crack shape
- Loading-zone size
- Loading-zone shape
- Fracture toughness
- Stiffness

Parametric study on 2D Mode-I delamination

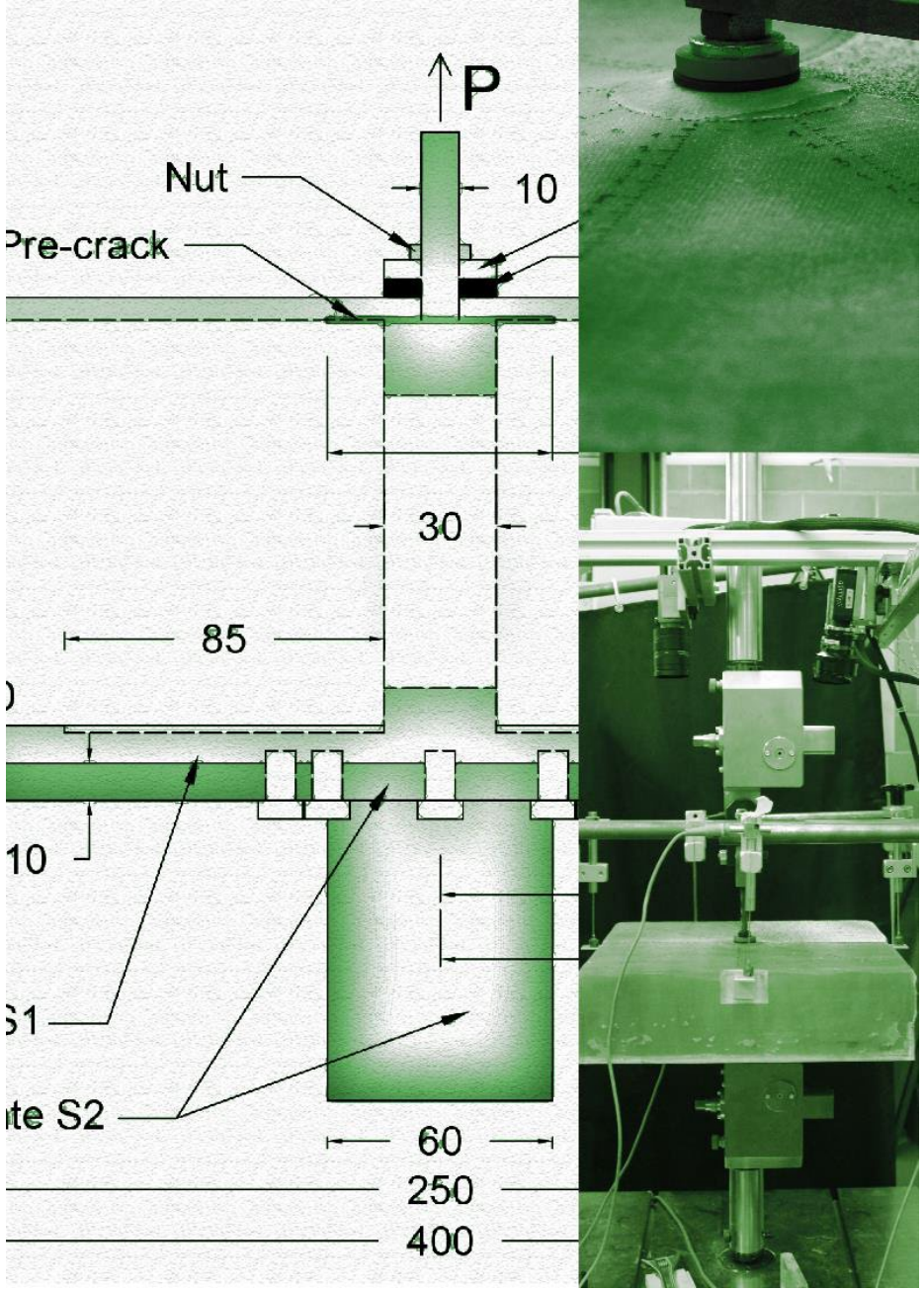

Two-dimensional debonding

Quasi-static experimental investigation

Experimental investigation

Face sheet

Glass fiber and epoxy matrix

Core

Balsa wood

2 face sheet configurations | SPA $(W)_{18}$ / SPB $(CFM)_2/(W)_9/(CFM)_2$

4 sandwich panels

Resin infusion method

≈ *bending stiffness*

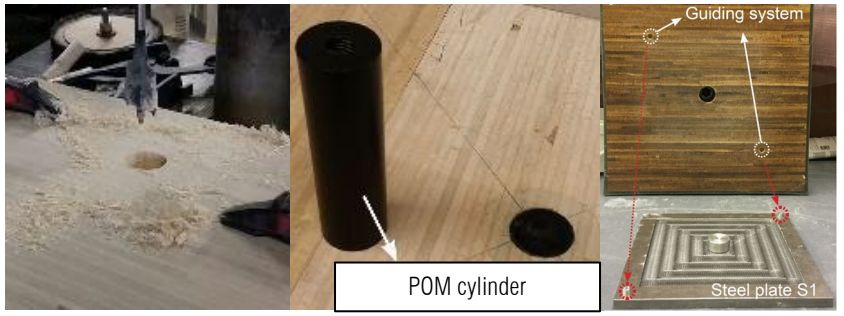

Top view

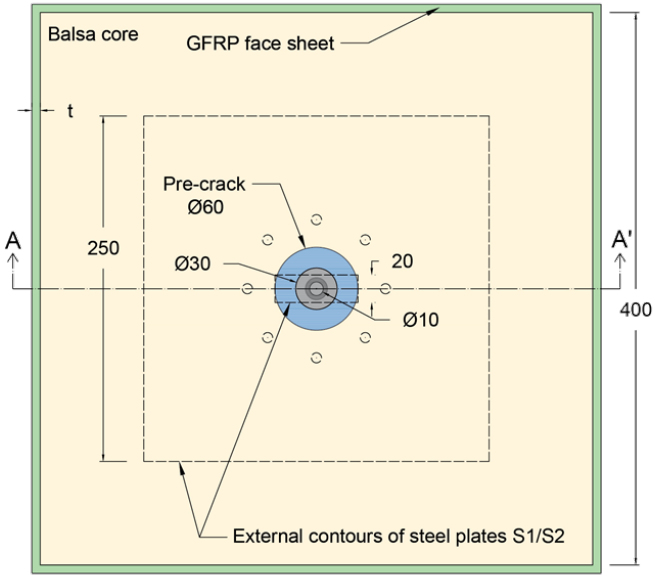

Side view AA'

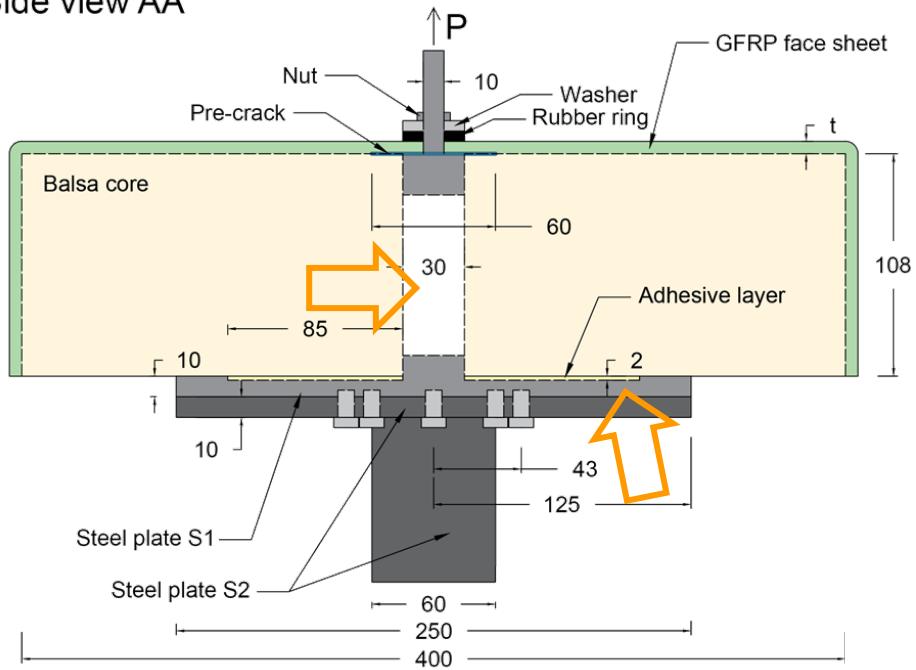

Experimental investigation

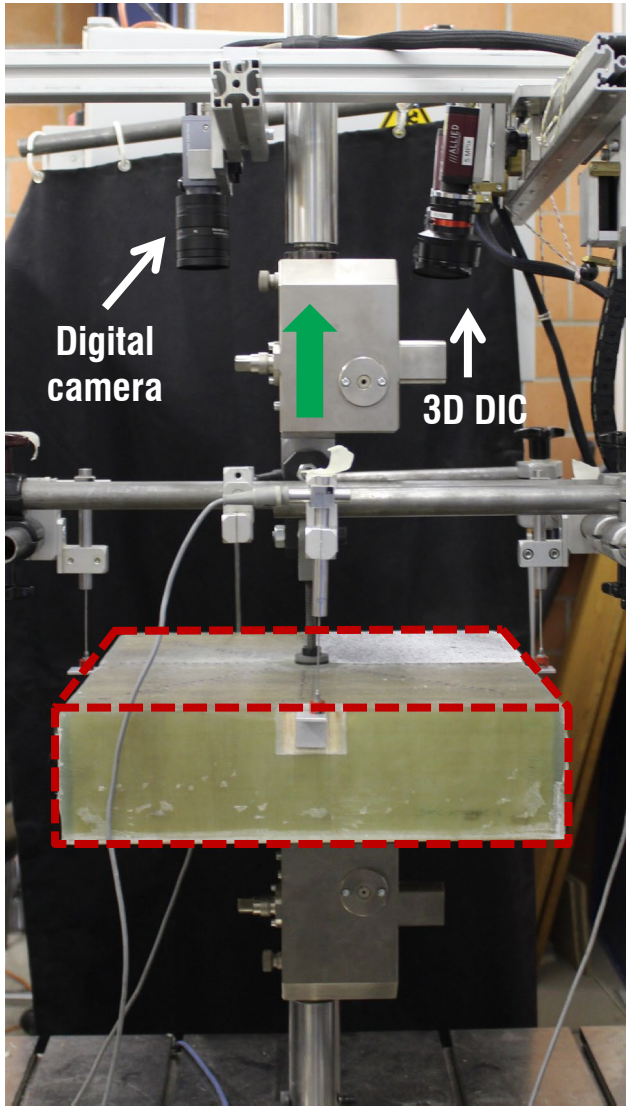

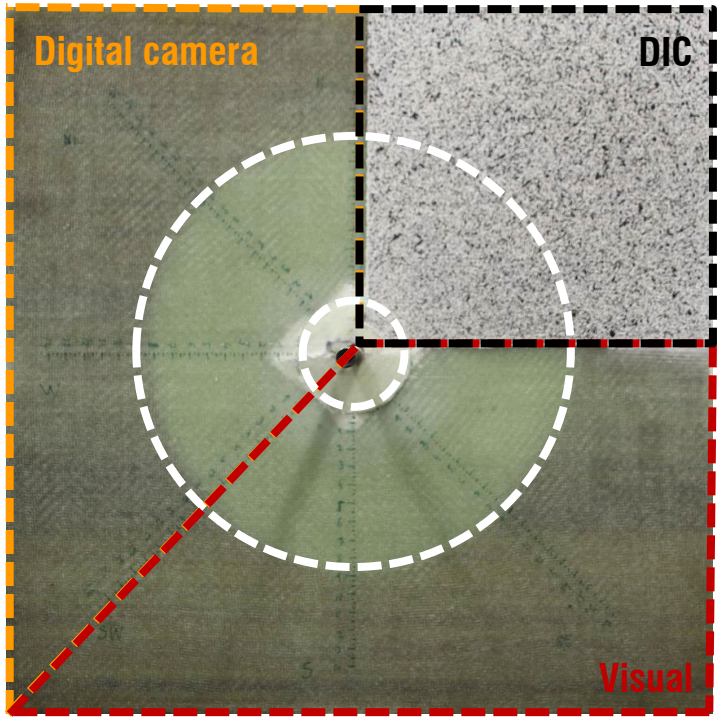

Load-displacement and crack propagation

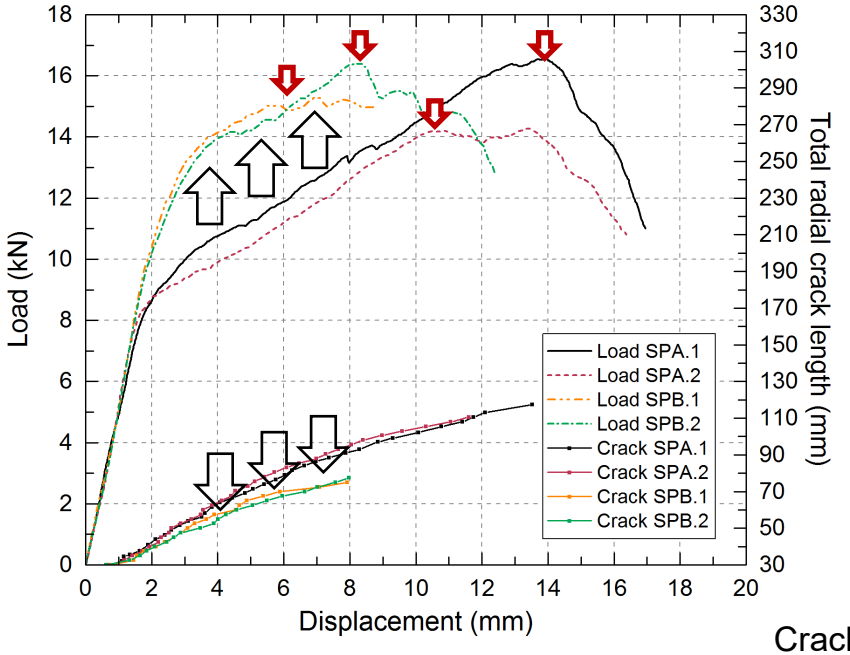

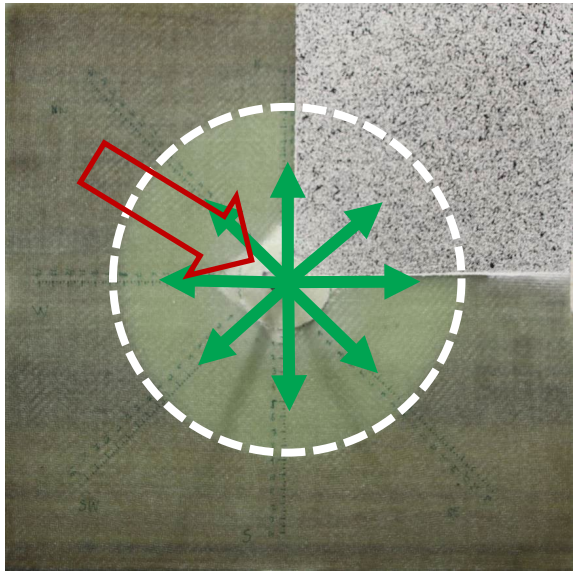

Crack migration

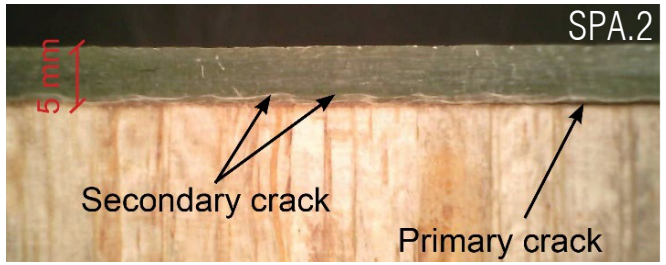

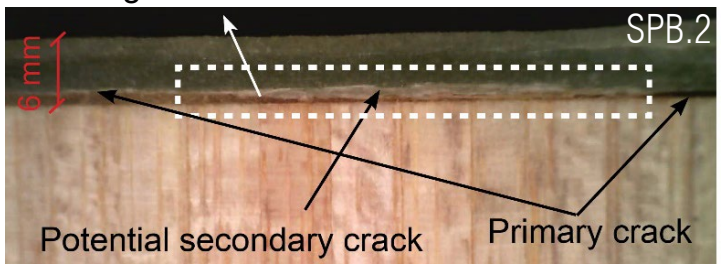

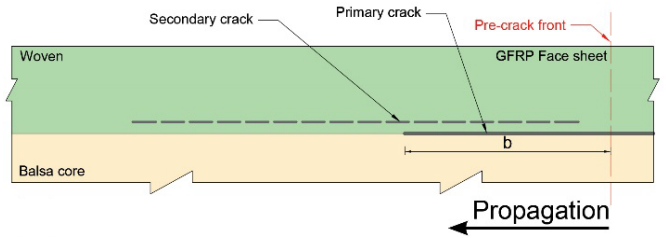

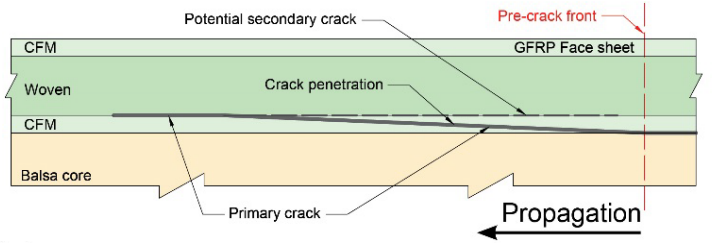

Stretching induced shear fracture modes

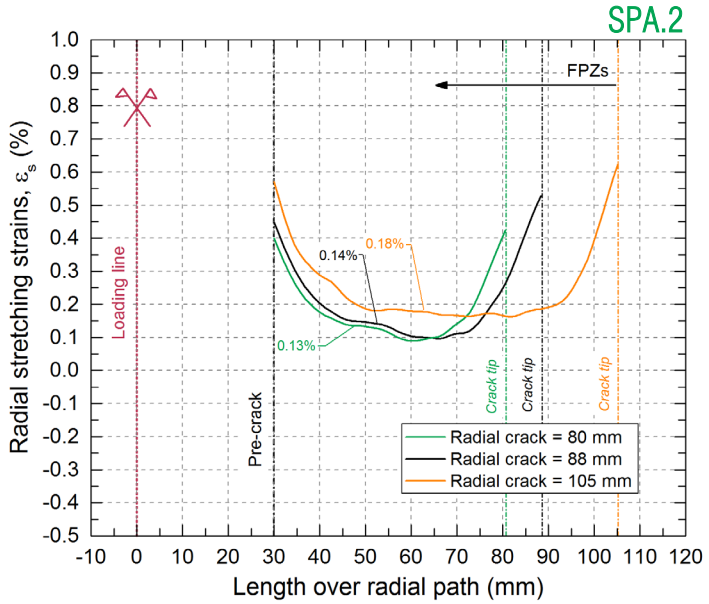

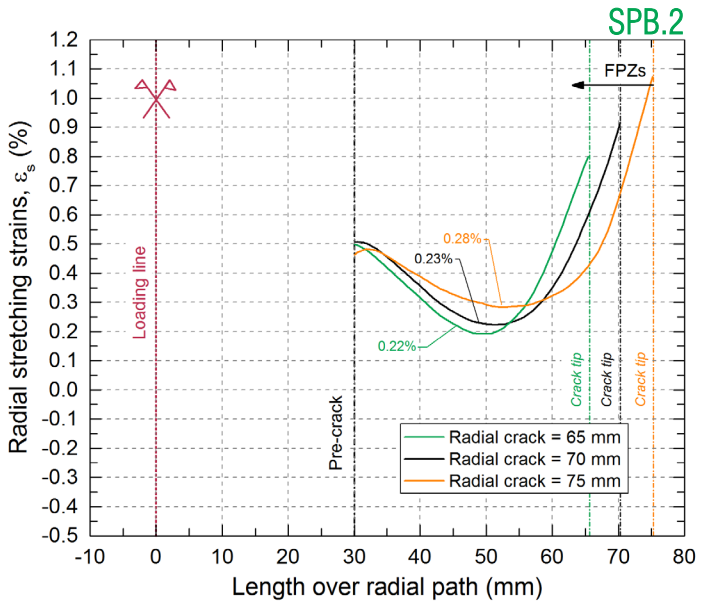

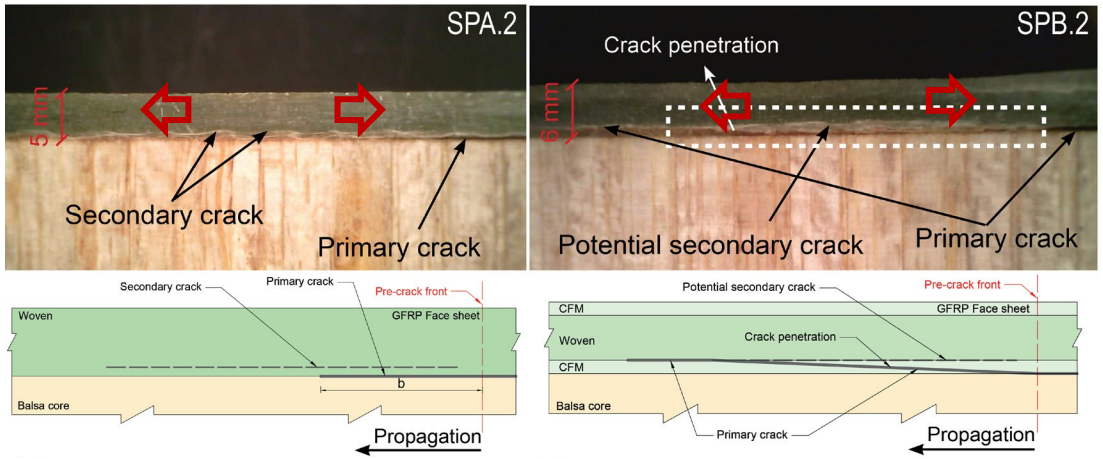

Stretching-induced shear fracture modes

Crack nucleation

Crack migration

2D effect

2D Mode-I experiments: What we learned?

Main differences from 1D tests

- Increasing crack-front length
- Constrained boundary at the crack wake
- Appearance of membrane stresses

Resulting 2D effects

- Increasing loads even after crack propagation
- Enhancement of fiber bridging
- Greater G_I

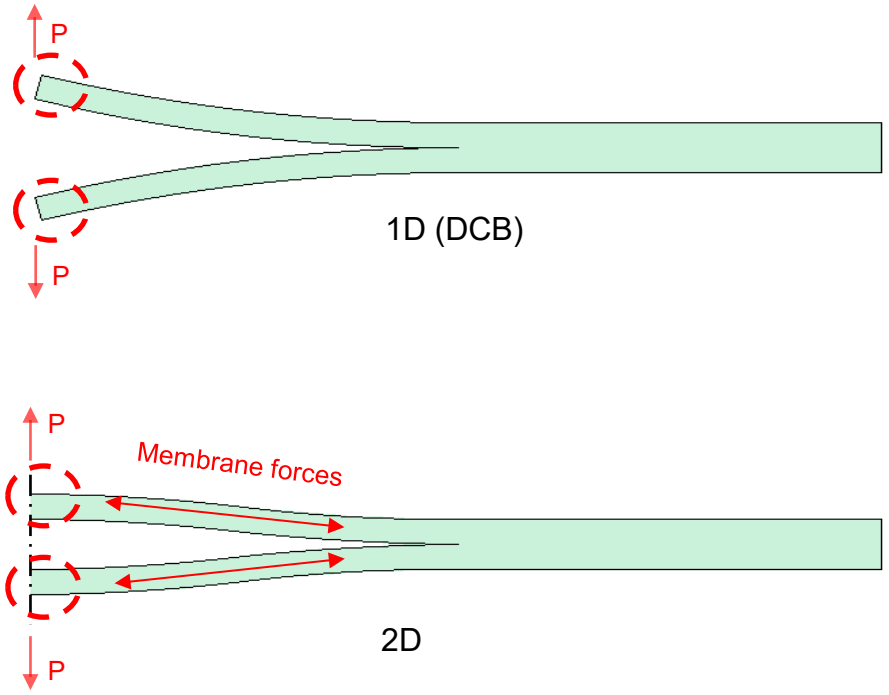

Schematic illustrations of 1D and 2D Mode-I delamination experiments

Parametric investigation

MODE-I DELAMINATION MODELS

Model description

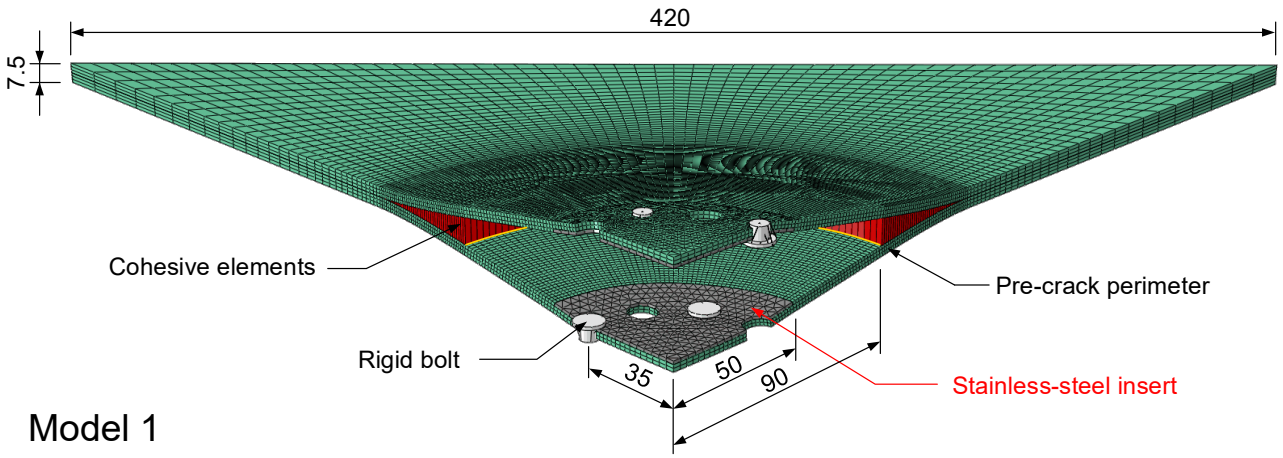

Model 1

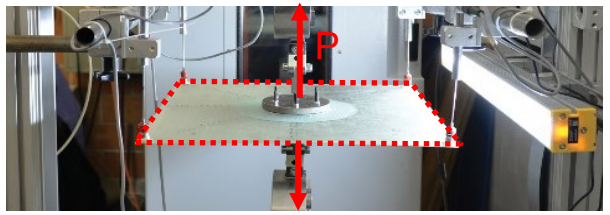

1. Detailed finite square plate

- Simulation of experiments (specimen CFM1)
- Detailed modeling
- Fitting the cohesive law

Simplification

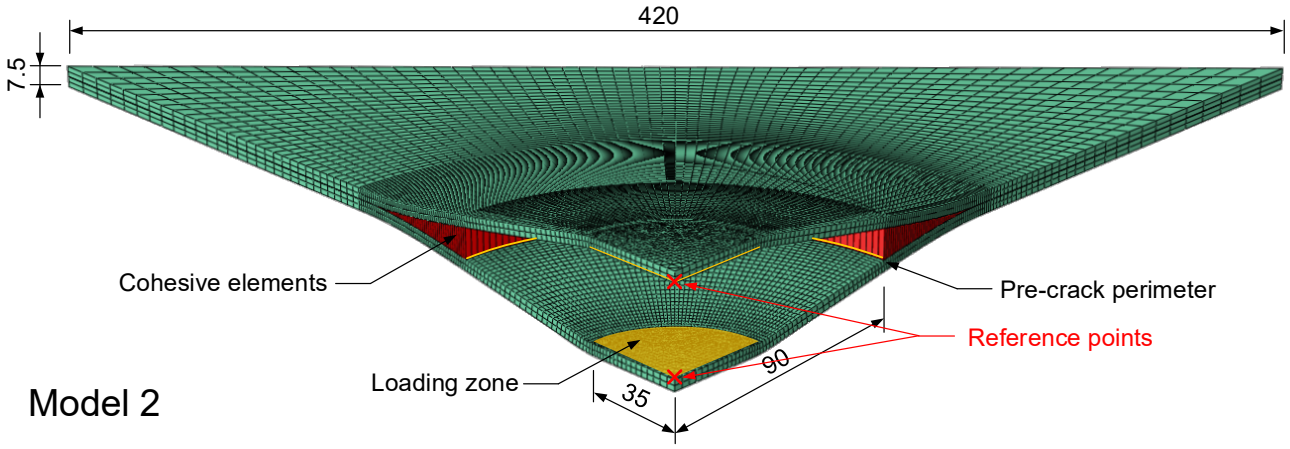

Model 2

2. Simplified finite square plate

- Same fitted cohesive law
- Simplification of the above model
- Parametric study focusing on early stages

Model description

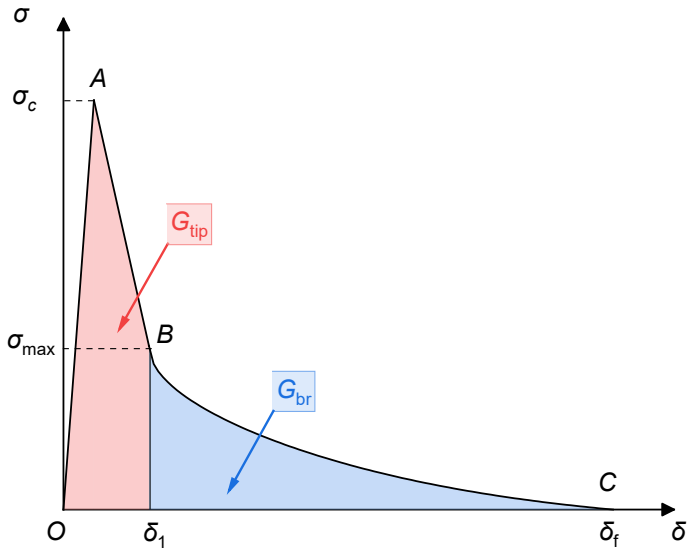

Cohesive model employed

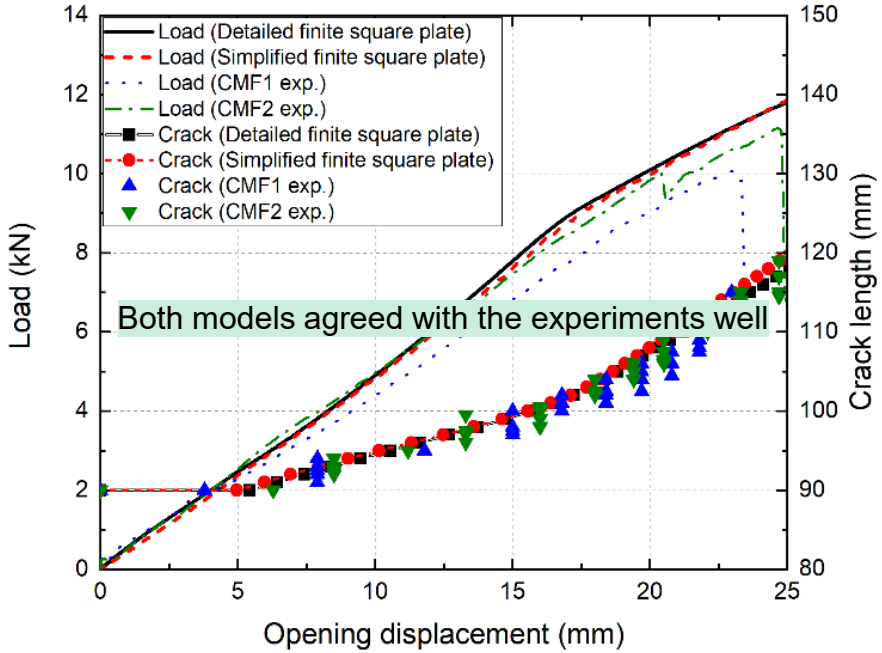

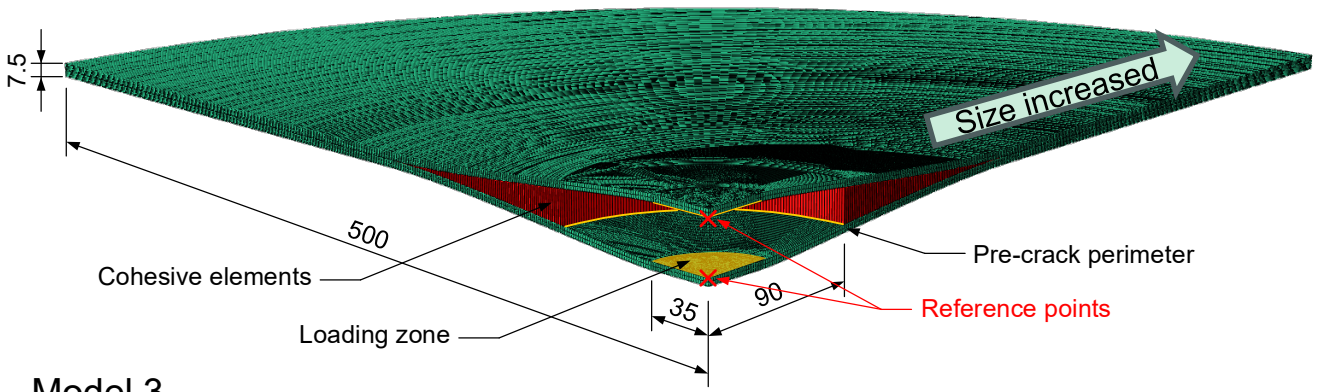

Model 3

3. Simplified semi-infinite circular plate

- Same simplified modeling strategy
- Artificially increased dimensions, stiffness and fracture resistance
- Parametric study focusing on late stages

Parameters description (simplified square plates)

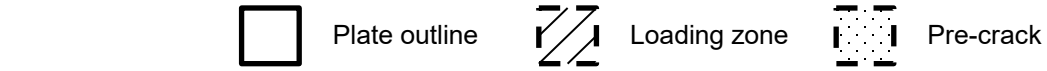

Different pre-crack shapes
(same circumference)

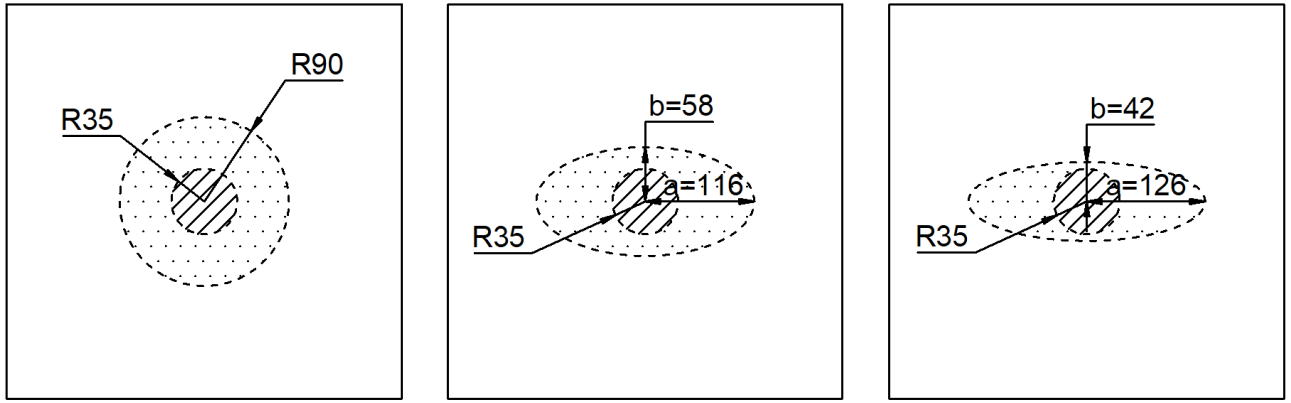

C90-C35-S E2/1-C35-S E3/1-C35-S

Different loading-zone shapes
(same area)

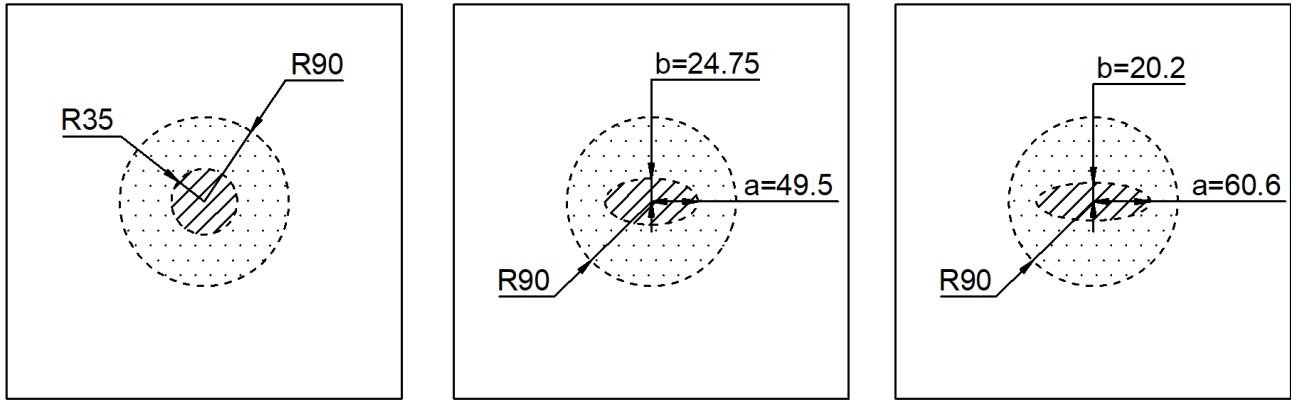

C90-C35-S C90-E2/1-S C90-E3/1-S

Parameters description (simplified square plates)


Pre-crack


Loading zone

Different pre-crack shapes

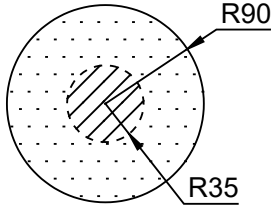

C90-C35-1.0G

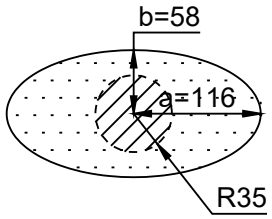

E2/1-C35-1.0G

(same circumference)

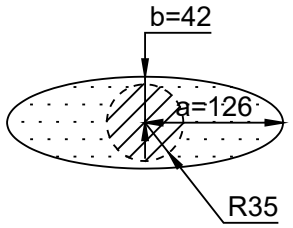

E3/1-C35-1.0G

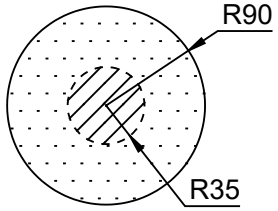

C90-C35-1.0G

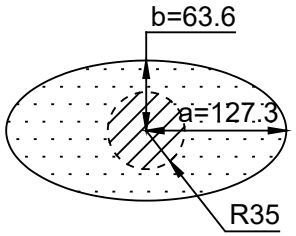

E'2/1-C35-1.0G

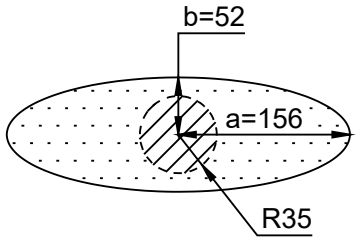

E'3/1-C35-1.0G

(same area)

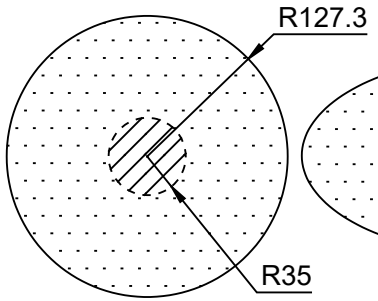

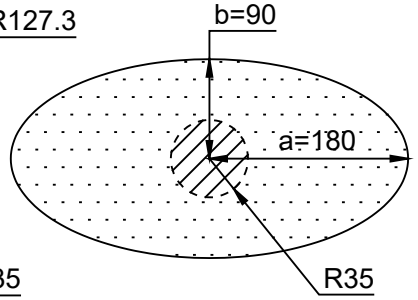

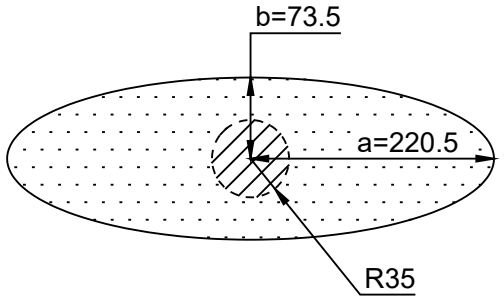

(same area, doubled)

Different loading-zone shapes

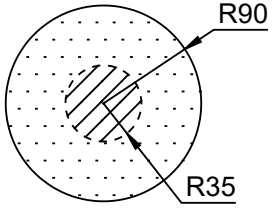

C90-C35-1.0G

- -0.5G
- -1.0G
- -1.5G

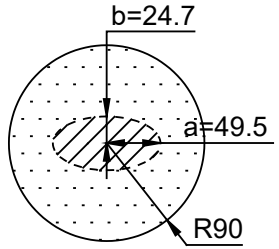

C90-E2/1-1.0G

- -0.5G
- -1.0G
- -1.5G

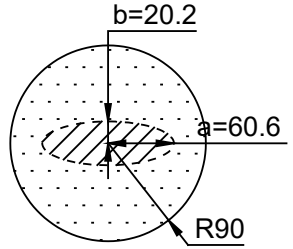

C90-E3/1-1.0G

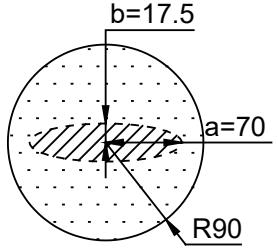

C90-E4/1-1.0G

(same area)

- -0.14G
- -0.25G
- -0.5G
- -1.0G
- -1.5G
- -2.0G

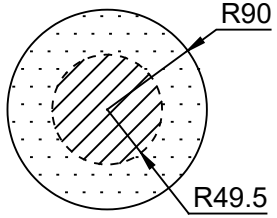

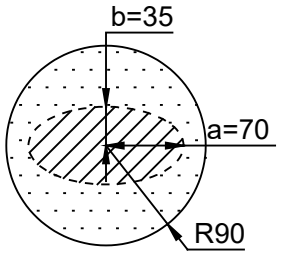

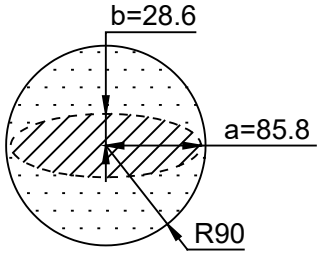

(same area, doubled)

2D Mode II delamination – experimental

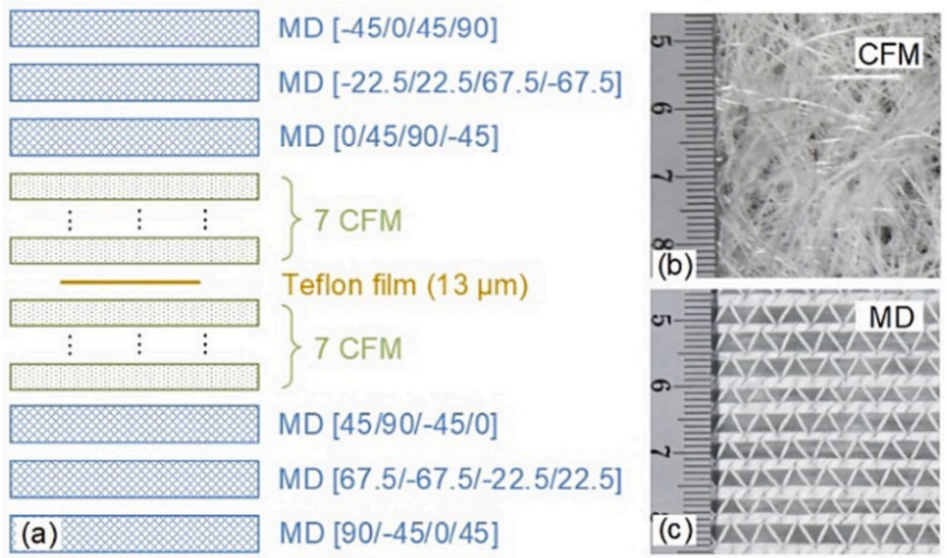

Fig. 2. Material description: (a) laminate layup; (b) continuous filament mat and (c) multidirectional sewed fabric. (For interpretation of the references to colour in this figure legend, the reader is referred to the web version of this article.)

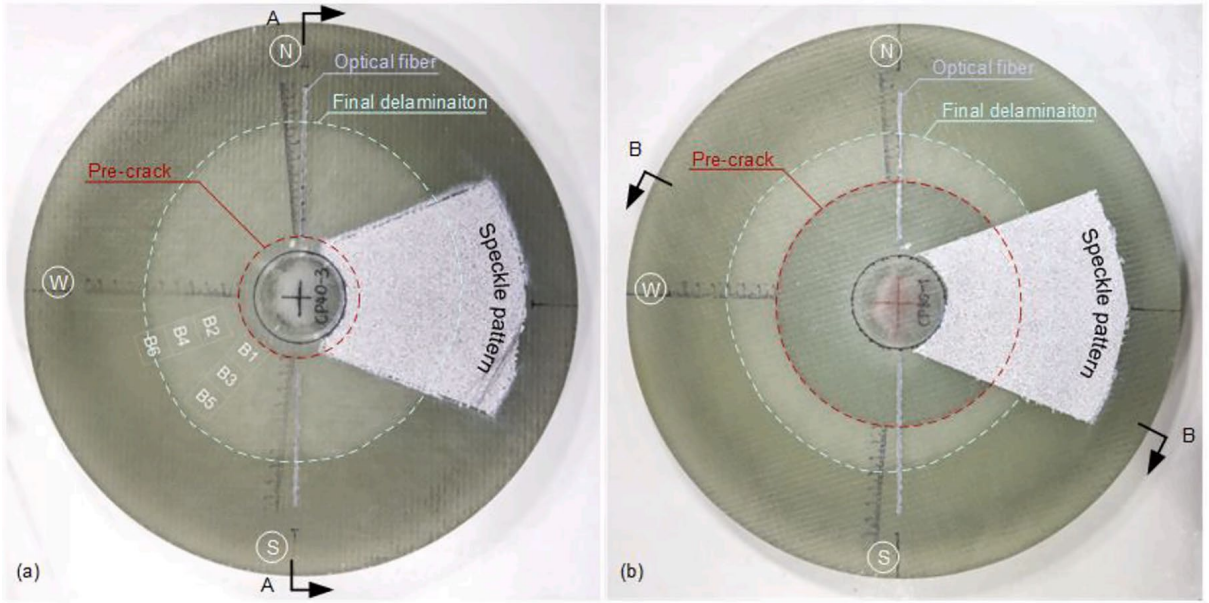

Fig. 2. 2D specimen description and final delamination patterns of specimens (a) CP40-3 and (b) CP80-1.

1D Mode and 2D Mode II delamination

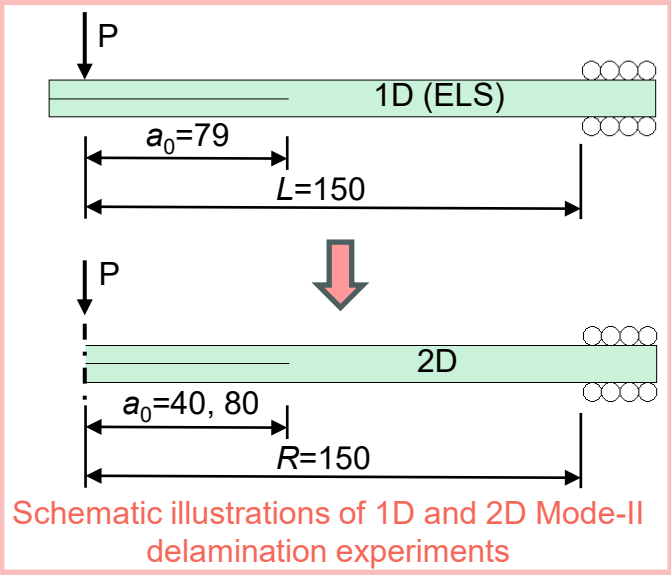

Schematic illustrations of 1D and 2D Mode-II delamination experiments

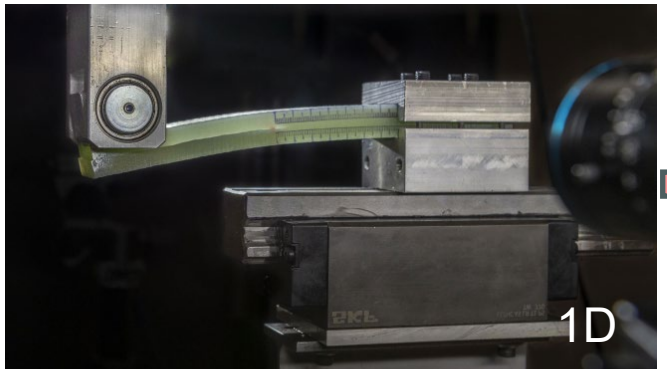

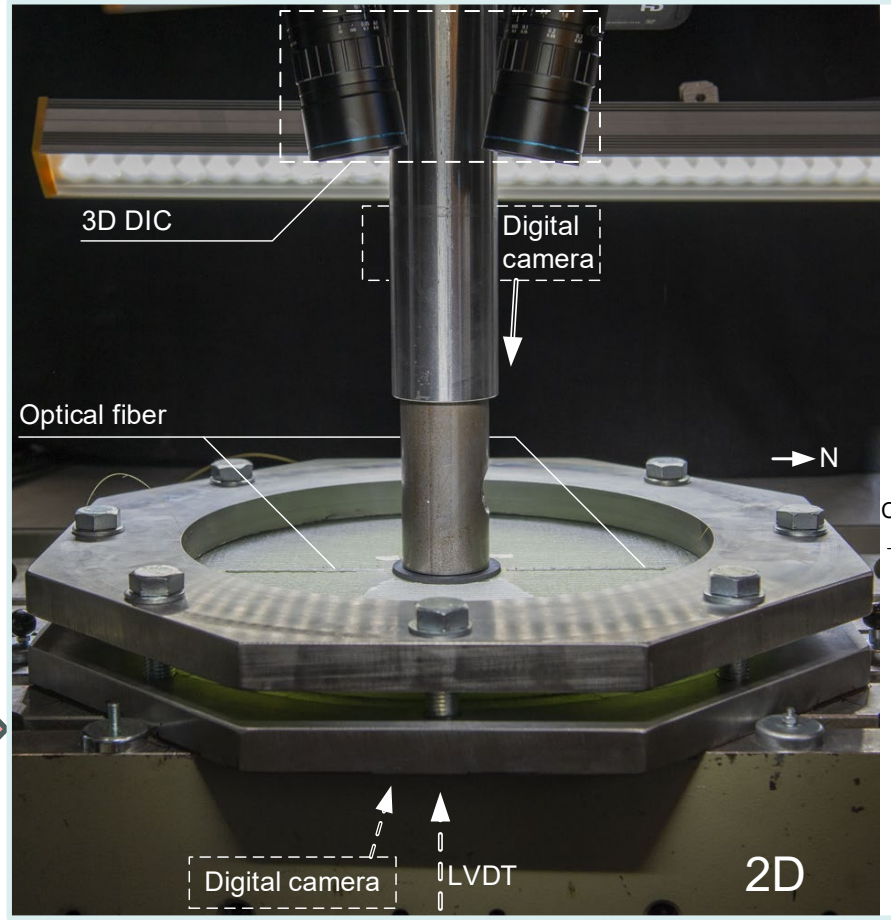

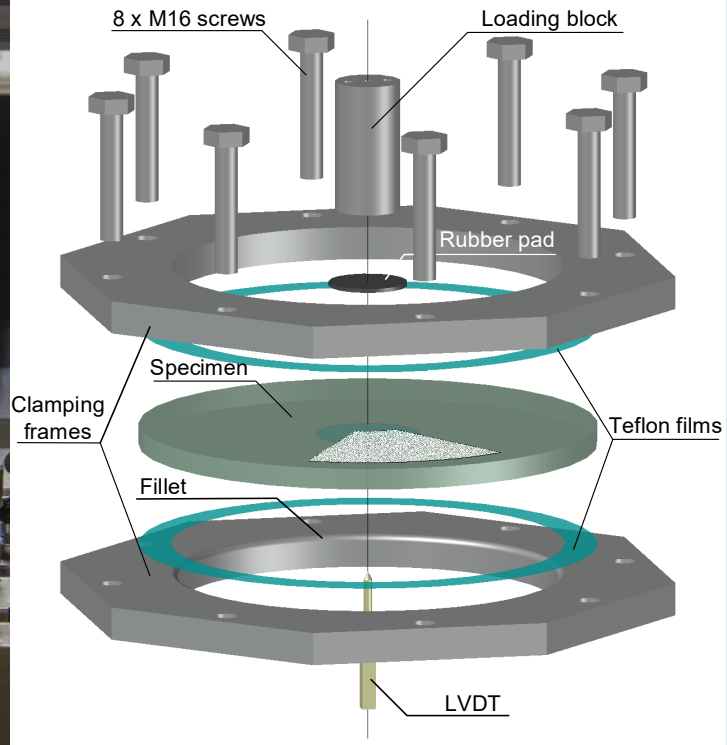

Fixture assembly

2D Mode II delamination – experimental

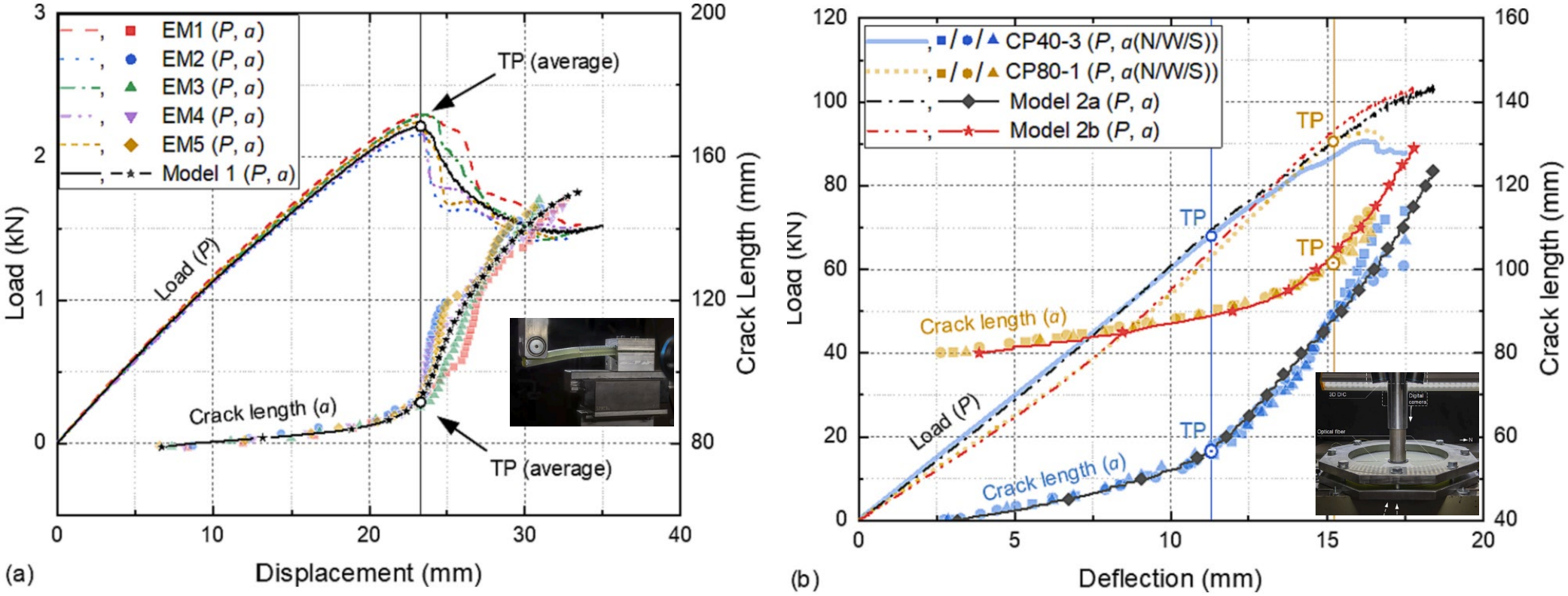

Experimental results (a) 1D ELS, (b) 2D plate testing

Experimental analysis (2D)

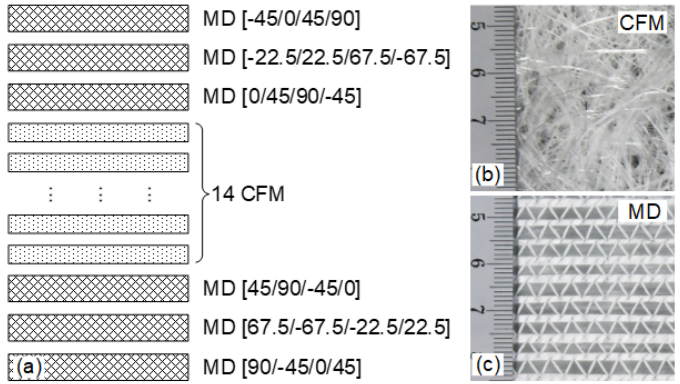

Laminate lay-up (in-plane quasi-isotropic)

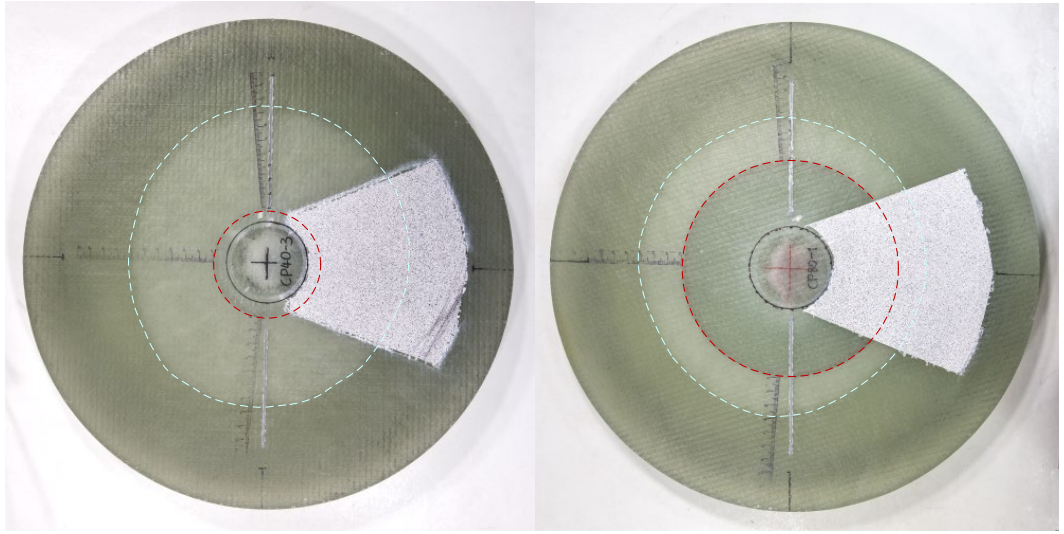

CP40-3

(CP40-1~5, 5 specimens)

CP80-1

(CP80-1~3, 3 specimens)

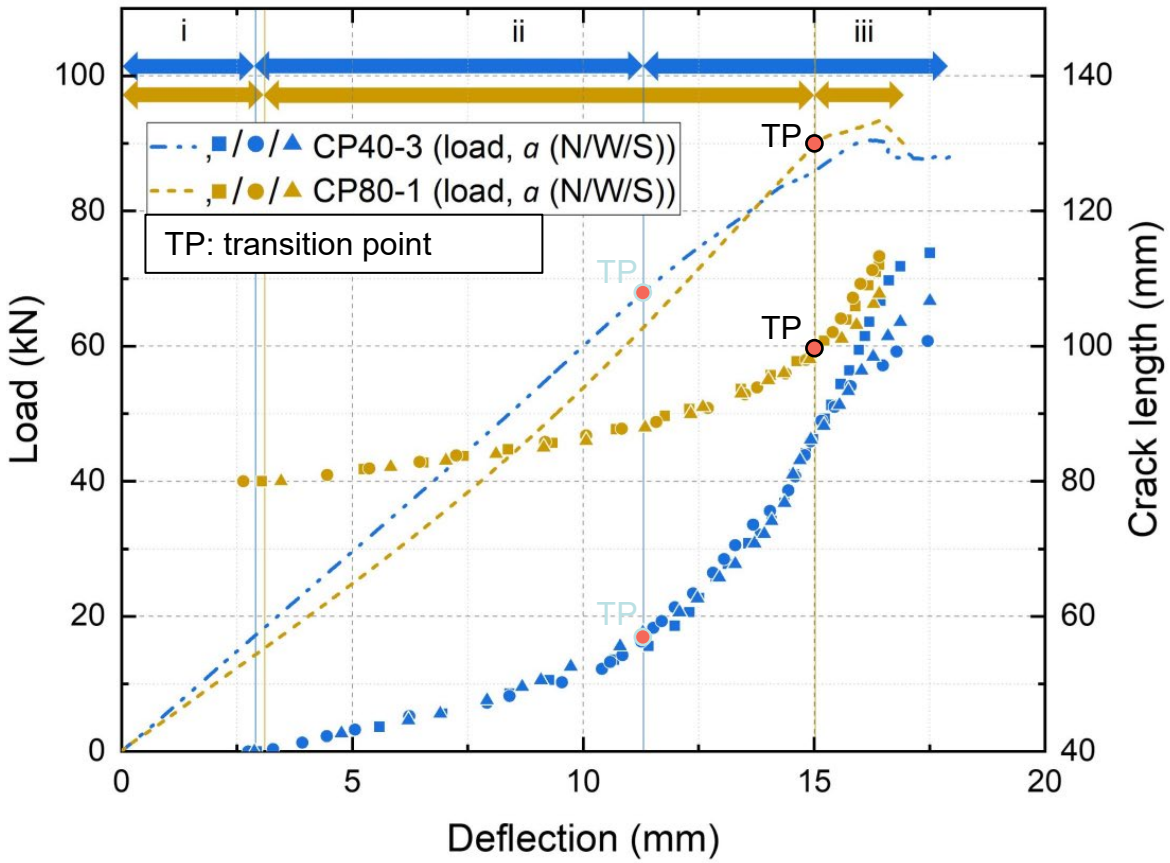

Three stages:

(i) crack initiation → (ii) slow propagation → (iii) rapid propagation

Experimental analysis (2D)

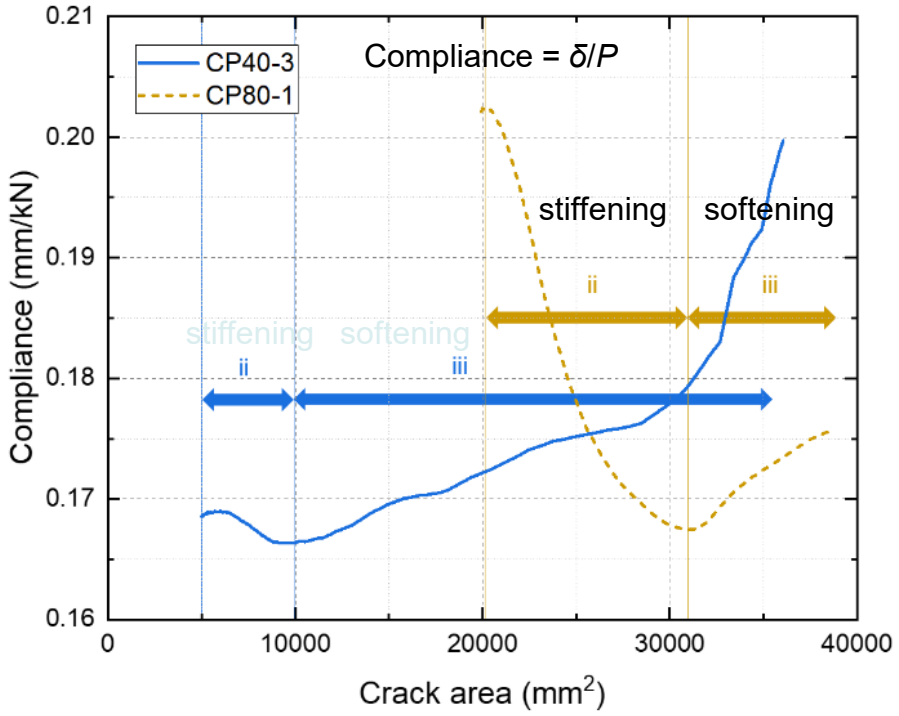

- Stiffening mechanism: membrane effect
- Softening mechanism: delamination growth (resisted by microcracking and fiber bridging)

a_0=40

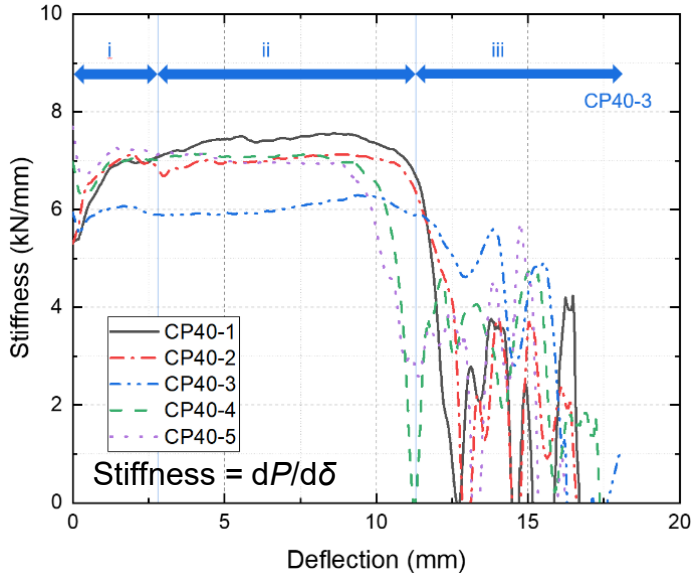

a_0=80

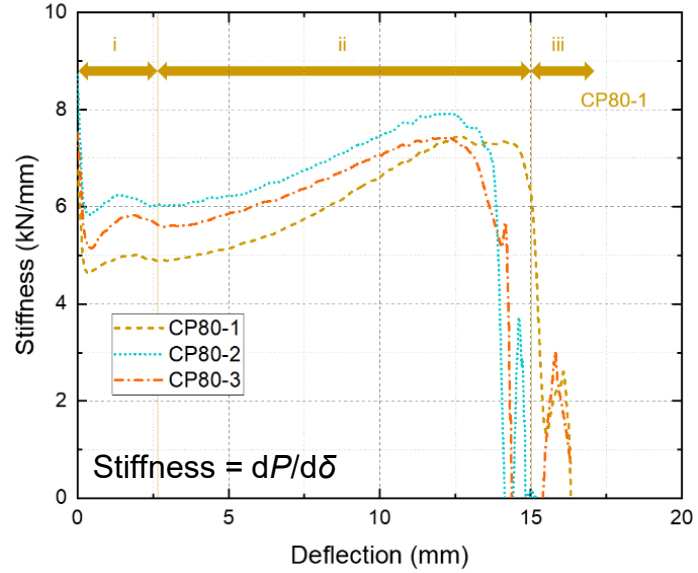

Experimental analysis (2D)

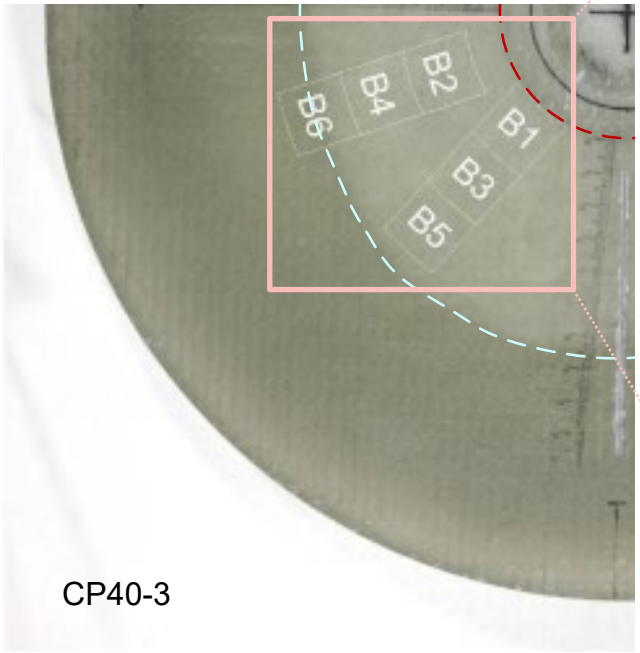

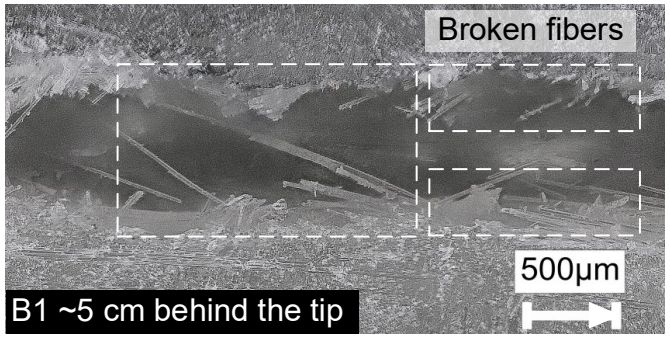

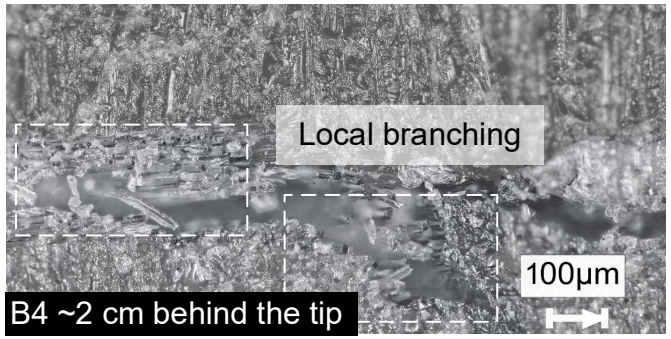

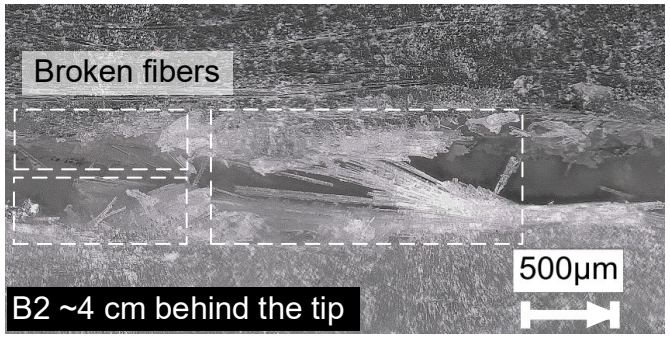

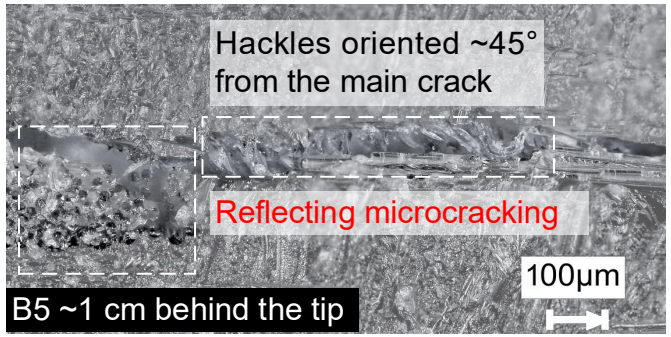

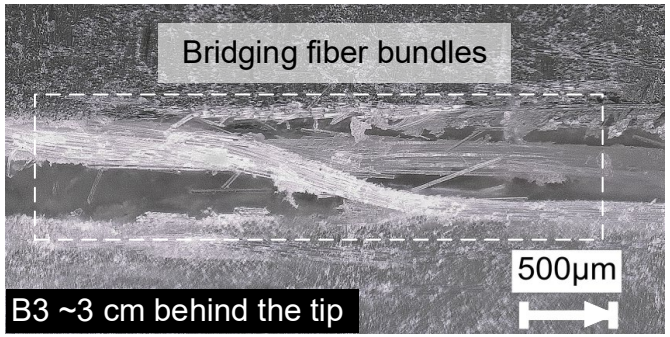

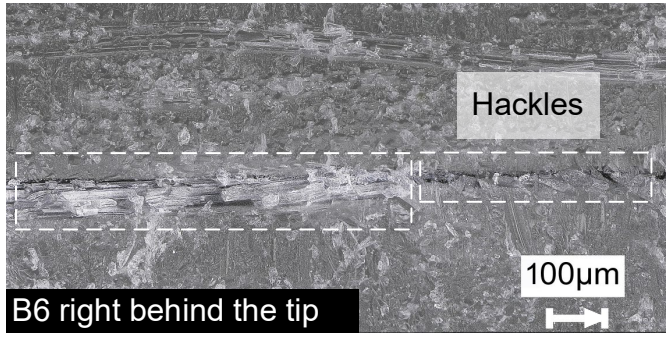

B1 – B3, manually opened

B4 – B6, original position

Post-inspection of delamination path

Experimental analysis (2D)

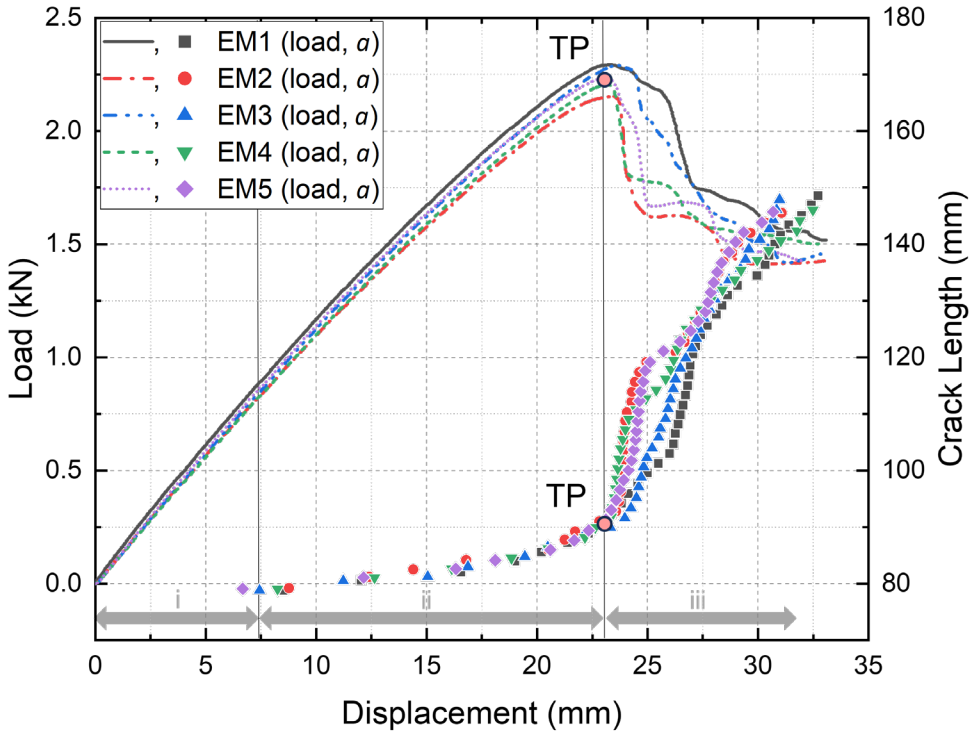

Load and crack length vs displacement

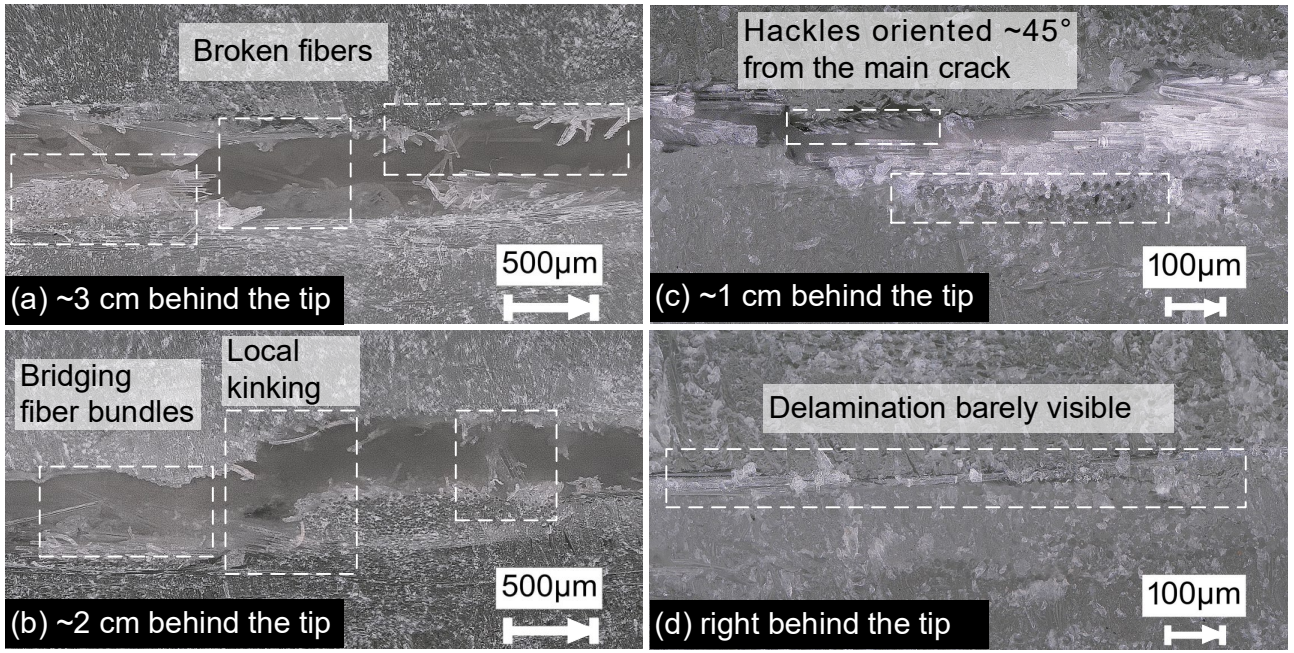

(a) – (b) manually opened

(c) – (d), original position

Post-inspection of delamination path

2D Mode II delamination – numerical modeling

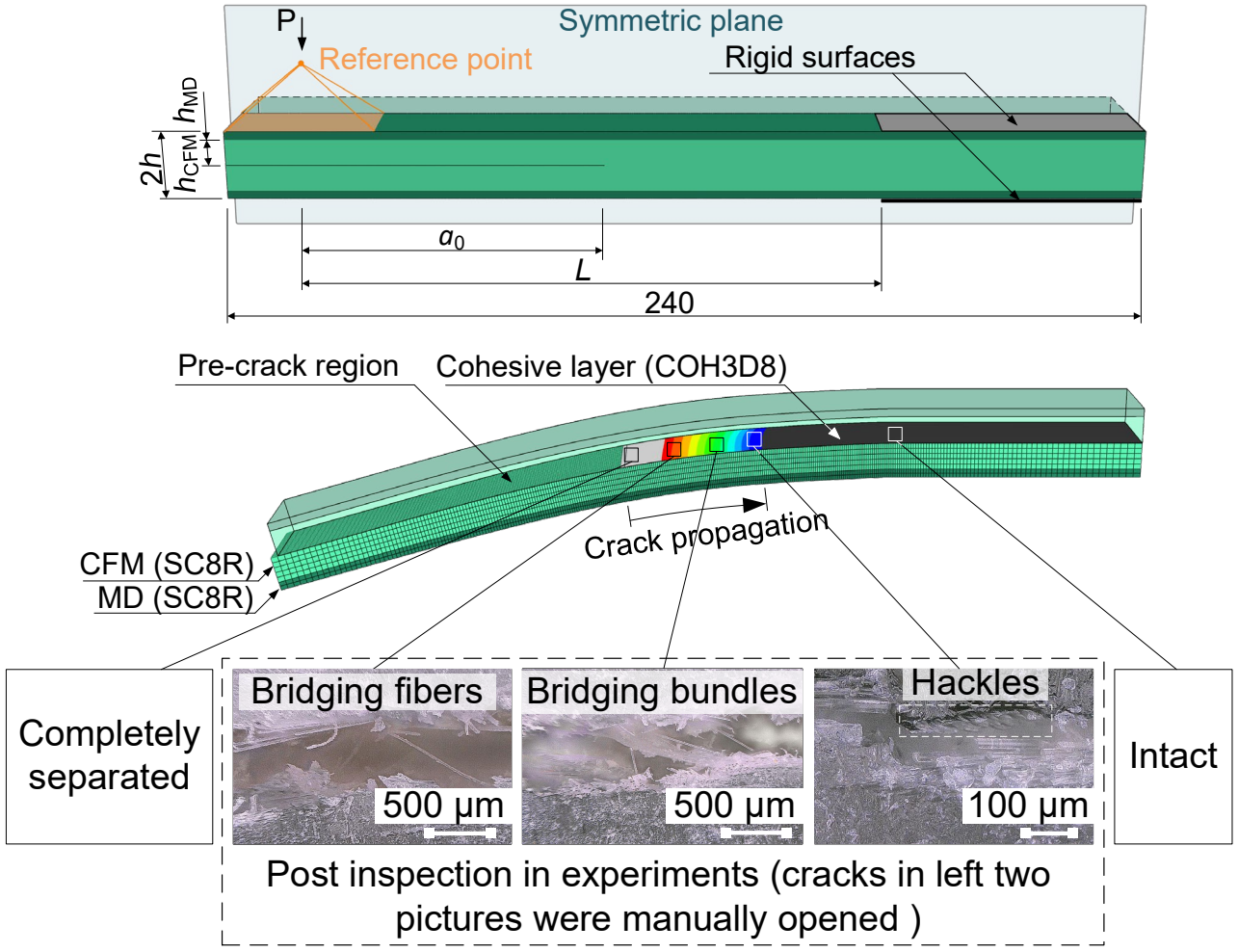

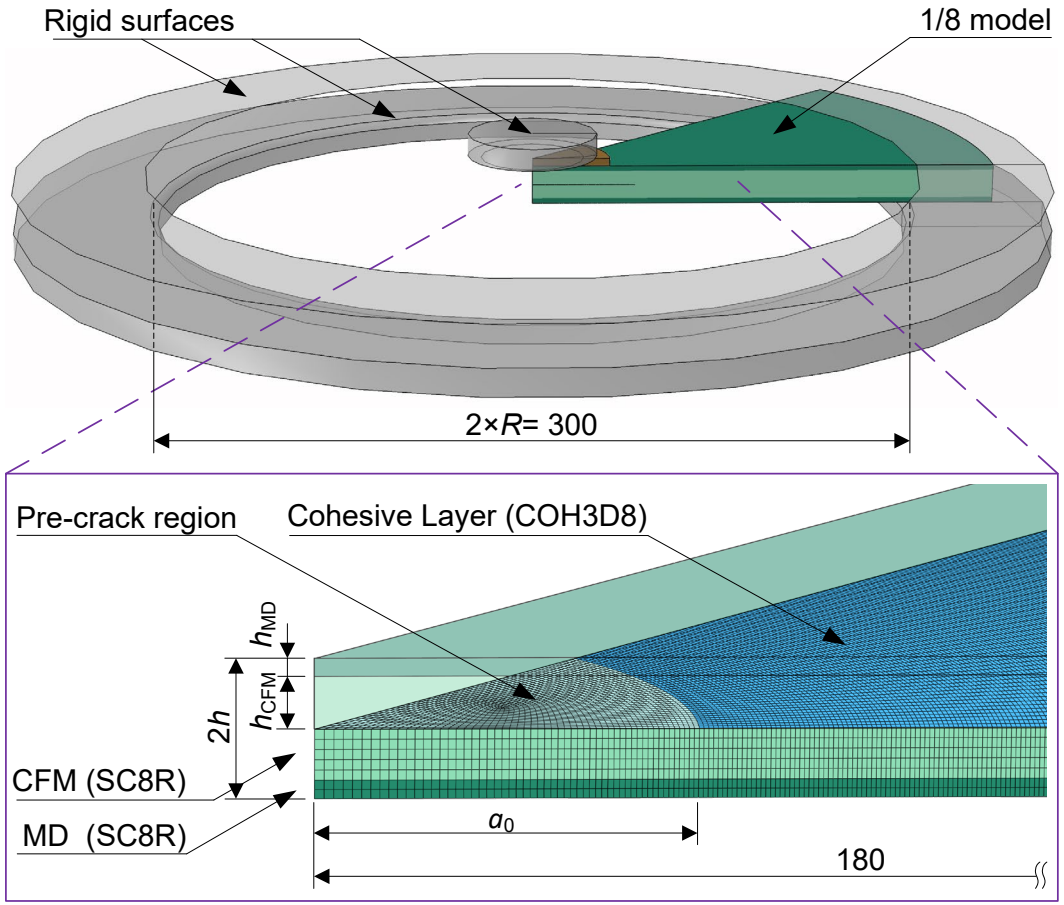

2D Mode II delamination – 1D numerical modeling

Crack sliding at the insert tip in 1D (ELS) experiments

$$G = \int_0^{\delta^*} \sigma(\delta) d\delta \quad \Rightarrow \quad \sigma(\delta^*) = \frac{\partial G_{II}}{\partial \delta^*}$$

A semi-experimental method was developed to derive the softening traction-separation law based on video extensometer measurements.

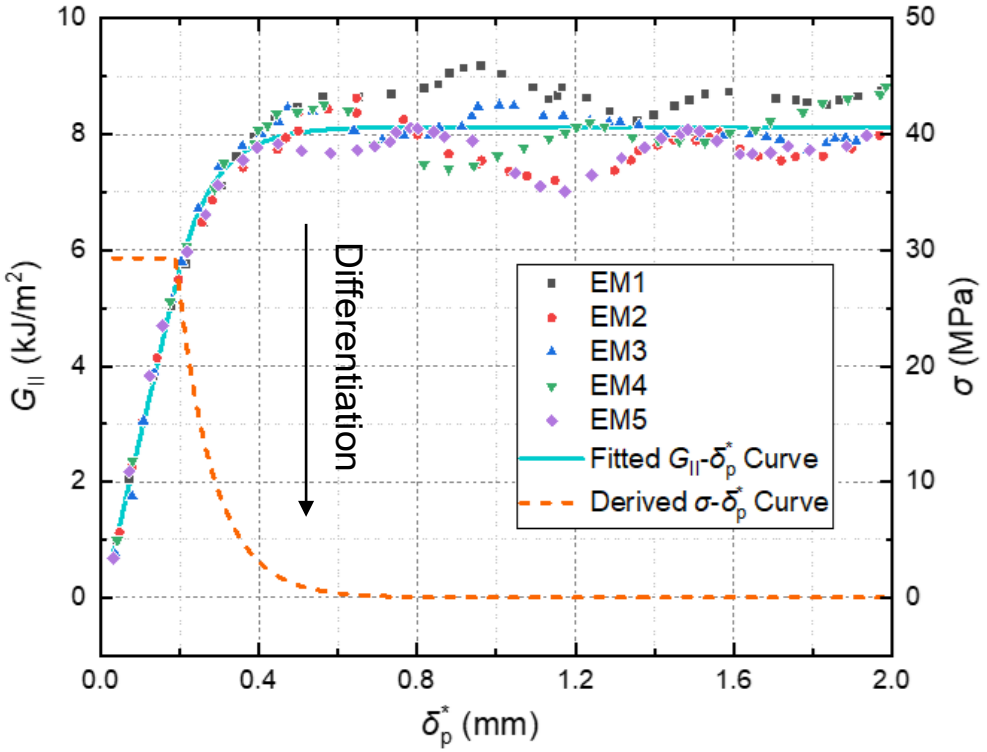

G_{II} vs crack sliding at the insert tip and the derivative curves

Derivation of cohesive law

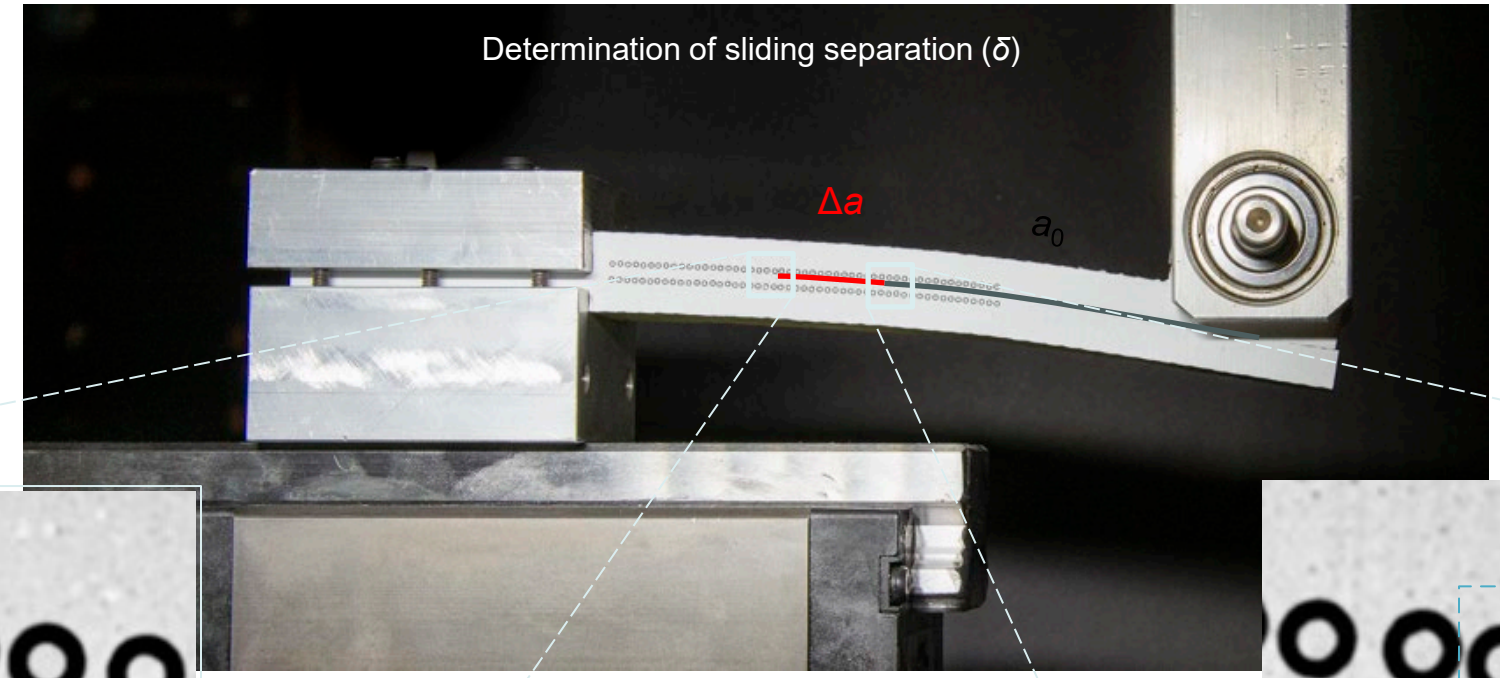

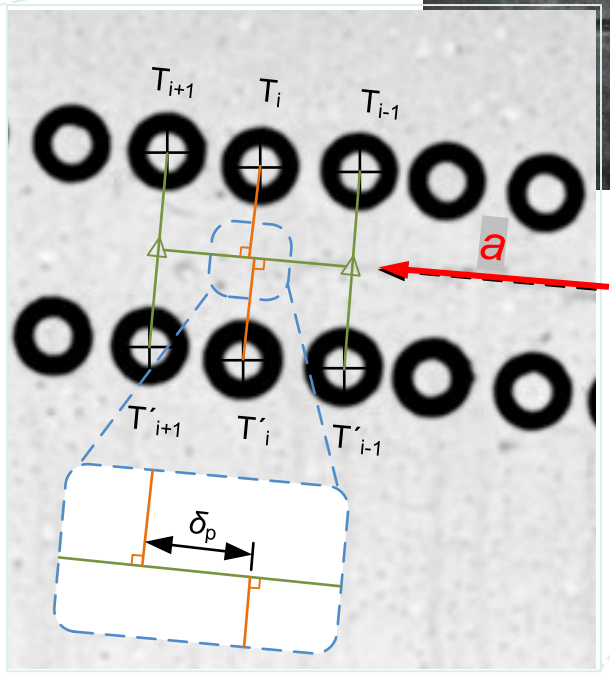

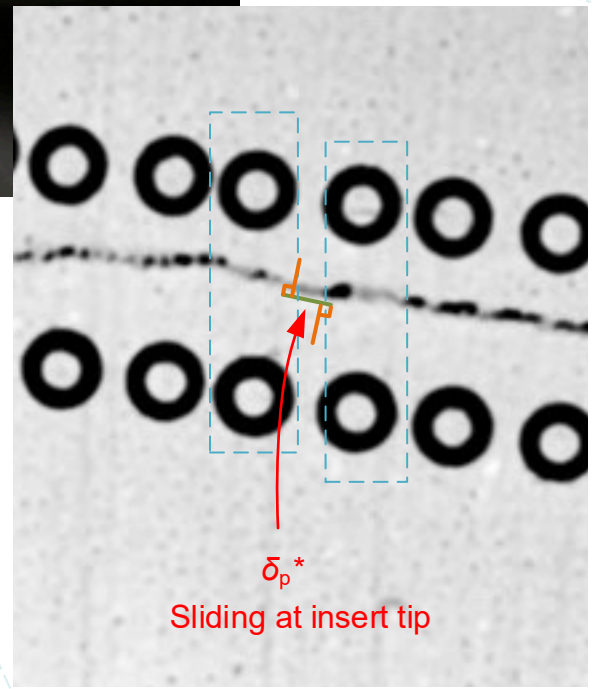

Derivation of cohesive law

Traction-separation law

Sliding separation at insert tip

$$\sigma\left(\delta_p^*\right) = \frac{\partial G_{II}}{\partial \delta_p^*}$$

R-curve

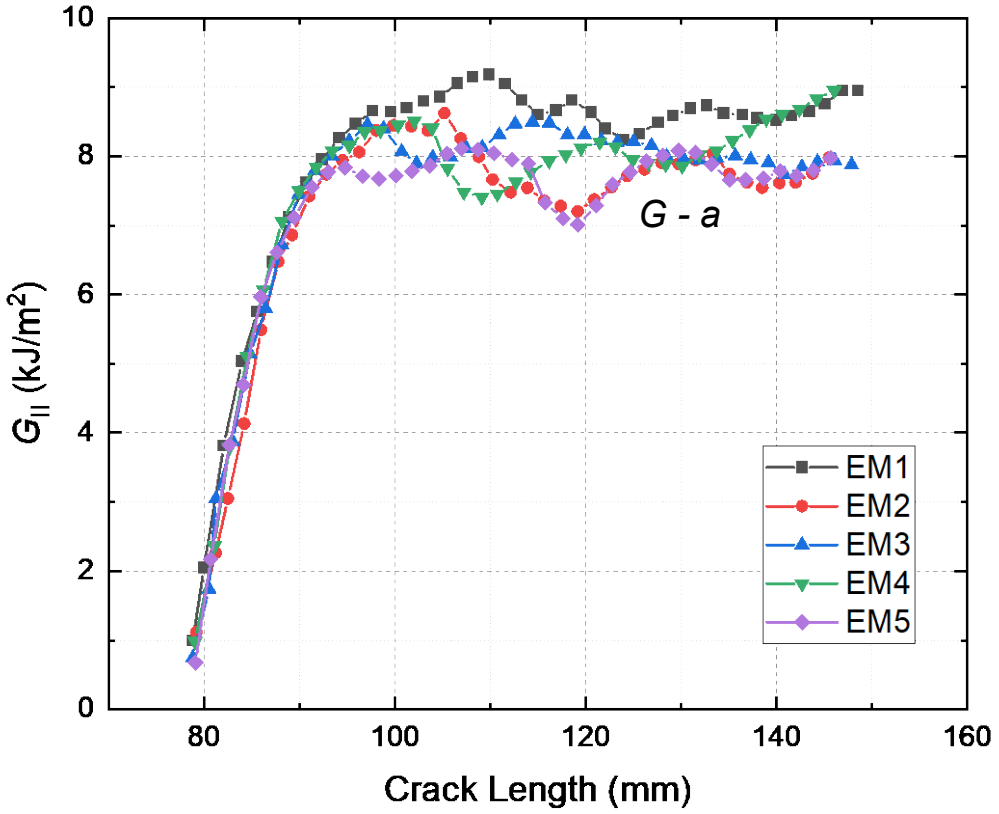

G and *σ* vs *δ**

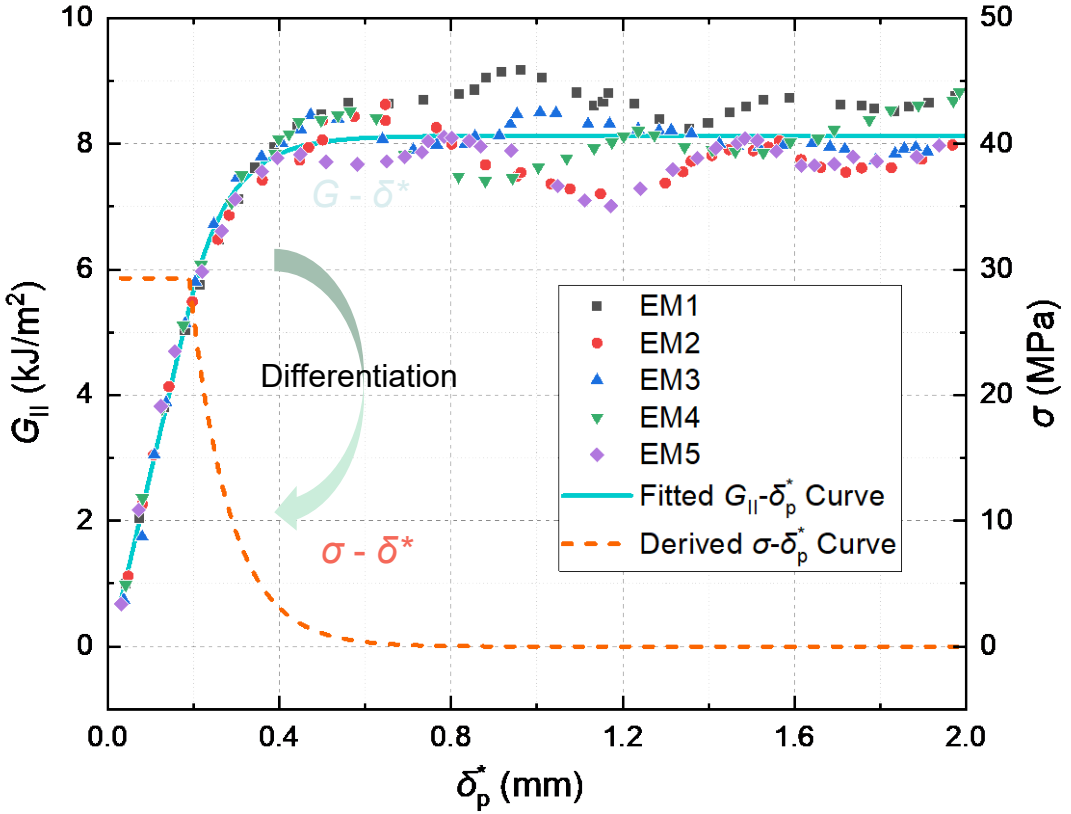

Derivation of cohesive law

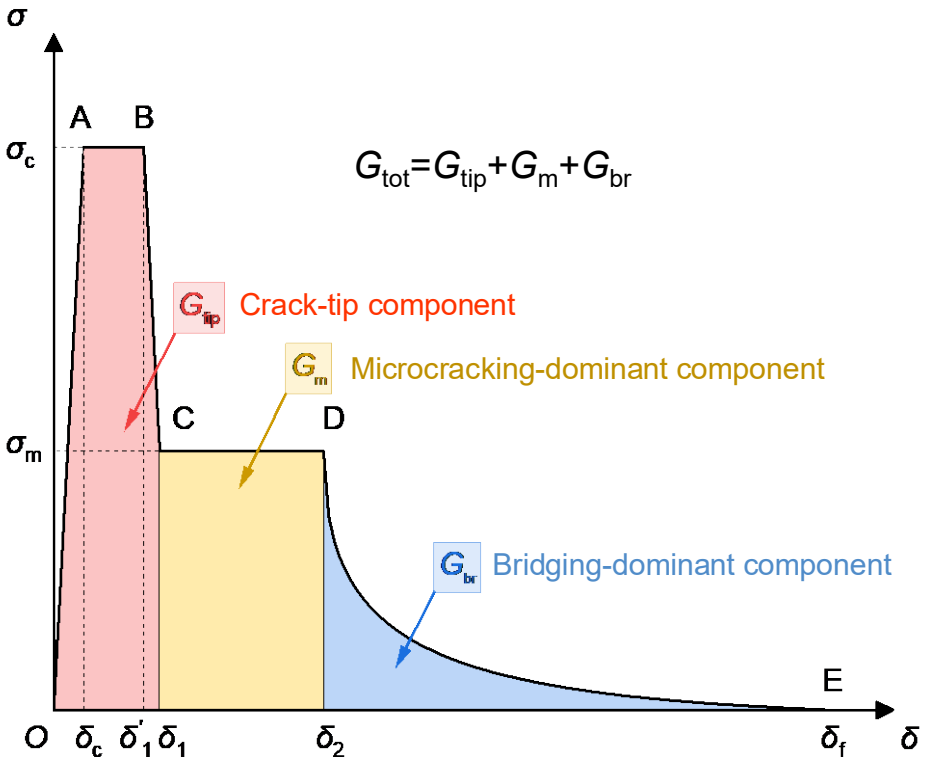

Independent variables: {G_{tip}, G_{IIc}, K_0, σ_c, σ_m, δ_2, δ_f}

Iterative fitting for Models 1, 2a and 2b

1D 2D

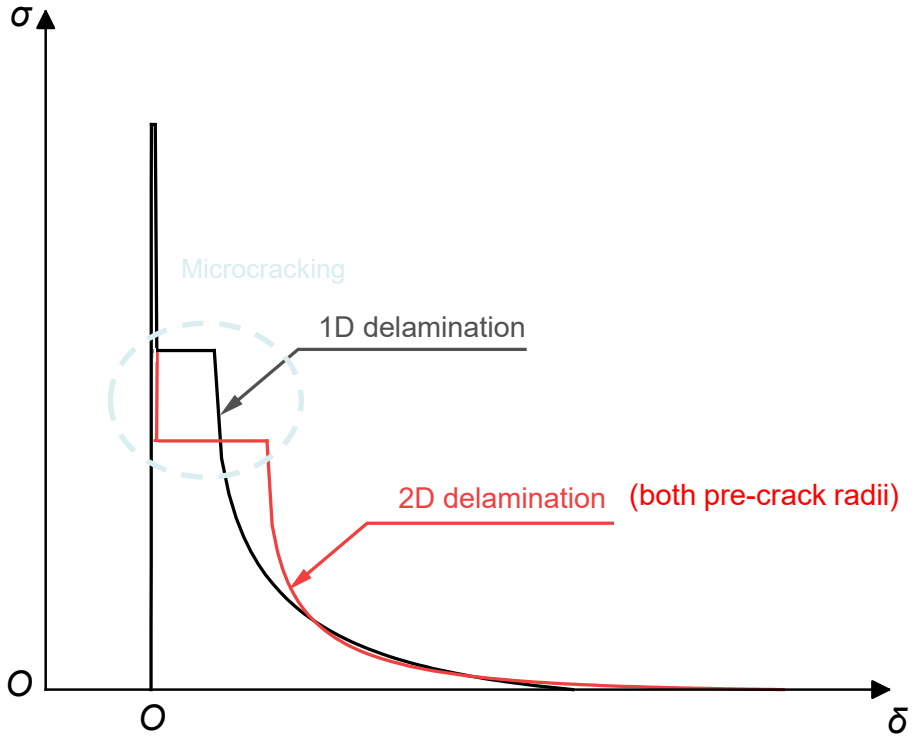

Comparison of 1D and 2D cohesive laws

2D Mode II delamination – numerical analysis

A **new Mode-II cohesive law** considering microcracking and fiber bridging was developed using a semi-experimental approach.

The analysis resulted in **two** distinct cohesive laws, one for the 1D case and another for the 2D cases.

The assumption of equal G_{tip} in 1D and 2D Mode-I and Mode II delamination was validated by comparisons between the numerical and experimental results regarding the crack initiation displacement (deflection).

G_{IIc} value was similar for 1D and 2D regardless of the difference in the traction-separation response. This contradicts the results in Mode-I (1D, 2D) delamination and raises more questions for future investigations.

2D Mode II delamination – publications

Composites: Part A 173 (2023) 107666

Contents lists available at ScienceDirect

Composites Part A

journal homepage: www.elsevier.com/locate/compositesa

Experimental investigation of two-dimensional Mode-II delamination in composite laminates

Congzhe Wang, Anastasios P. Vassilopoulos, Thomas Keller *

Composite Construction Laboratory (CCLab), Ecole Polytechnique Fédérale de Lausanne (EPFL), Station 16, Bâtiment BP, CH-1015 Lausanne, Switzerland

Composites: Part A 179 (2024) 108012

Contents lists available at ScienceDirect

Composites Part A

journal homepage: www.elsevier.com/locate/compositesa

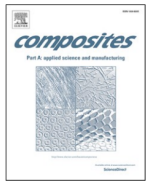

Numerical investigation of two-dimensional Mode-II delamination in composite laminates

Congzhe Wang, Anastasios P. Vassilopoulos, Thomas Keller *

Composite Construction Laboratory (CCLab), Ecole Polytechnique Fédérale de Lausanne (EPFL), Station 16, Bâtiment BP, CH-1015 Lausanne, Switzerland